Spectrum and Energy Efficient Medium Access Control for Wireless Ad Hoc Networks

by

Kamal Rahimi Malekshan

A thesis
presented to the University of Waterloo
in fulfillment of the
thesis requirement for the degree of
Doctor of Philosophy
in
Electrical and Computer Engineering

Waterloo, Ontario, Canada, 2016

I hereby declare that I am the sole author of this thesis. This is a true copy of the thesis, including any required final revisions, as accepted by my examiners.

I understand that my thesis may be made electronically available to the public.

Abstract

The increasingly growing number of mobile devices and volume of mobile data traffic necessitate establishing an effective self-organizing wireless ad hoc network to efficiently utilize radio spectrum and energy. The transmissions time and bandwidth should be dynamically coordinated based on instantaneous traffic load of the links in the network. Energy consumption in a mobile device can be reduced by putting the radio interface into a sleep mode. However, the mobile device cannot receive incoming data packets in the sleep mode. Thus, awake and sleep times of radio interfaces should be carefully planned to avoid missing incoming packets. In a wireless network, links that are far apart in distance can simultaneously transmit using the same bandwidth without interfering reception at destination nodes. Concurrent transmissions should be properly scheduled to maximize spatial spectrum utilization. Also, the transmission power level of each link should be optimized to enhance spectrum and energy efficiencies.

First, we present a new energy-efficient medium access control (MAC) scheme for a fully connected wireless ad hoc network. Energy consumption is reduced by periodically putting radio interfaces in the sleep mode and by reducing transmission collisions. The network throughput and average packet transmission delay are also improved because of lower collision and contention overhead. The proposed MAC scheme can achieve energy saving for realtime traffic which requires a low packet transmission delay. An analytical model is established to evaluate the performance of the proposed MAC scheme. Analytical and simulation results demonstrate that the proposed scheme has a significantly lower energy consumption, achieves higher throughput, and has a lower packet transmission delay in comparison with existing power saving MAC protocols.

Second, we present a novel distributed MAC scheme based on dynamic space-reservation

to effectively coordinate transmissions in a wireless ad hoc network. A set of coordinator nodes distributed over the network area are employed to collect and exchange local network information and to periodically schedule links for transmission in a distributed manner. For each scheduled transmission, a proper space area around the receiver node is reserved to enhance spatial spectrum reuse. Also, the data transmission times are deterministic to minimize idle-listening radio interface energy consumption. Simulation results demonstrate that the proposed scheme achieves substantially higher throughput and has significantly lower energy consumption in comparison with existing schemes.

We study joint scheduling and transmission power control in a wireless ad hoc network. We analyze the asymptotic joint optimal scheduling and transmission power control, and determine the maximum spectrum and energy efficiencies in a wireless network. Based on the asymptotic analysis, we propose a novel scheduling and transmission power control scheme to approach the maximum spectrum efficiency, subject to an energy consumption constraint. Simulation results show that the proposed distributed scheme achieves 40% higher throughput than existing schemes. Indeed, the scheduling efficiency of our proposed scheme is about 70% of the asymptotic optimal scheduling and transmission power control. Also, the energy consumption of the proposed scheme is about 20% of the energy consumed using existing MAC protocols.

The proposed MAC, scheduling and transmission power control schemes provide effective spectrum sharing and energy management for future wireless hotspot and peer-to-peer communication networks. The presented asymptotic analysis determines the maximum spectrum and energy efficiencies in a wireless network and provides an effective means to efficiently utilize spectrum and energy resources based on network traffic load and energy consumption constrains.

Acknowledgements

I would like to express my deepest gratitude to my supervisor Professor Weihua Zhuang for her great support, valuable advice and enthusiastic encouragement during my PhD program.

I sincerely would like to thank Professor Sherman (Xuemin) Shen for his valuable insights and great support and also all my colleagues in Broad Band Communications Research (BBCR) group for their kind support and beneficial discussions.

I gratefully acknowledge my PhD committee members, Professor Liang-liang Xie, Professor Zhou Wang, Professor Carolyn Ren and Professor Jian Tang for their comments and suggestions that have greatly improved the thesis. I also acknowledge Professor Patrick Mitran for accepting to serve as a delegate in my PhD thesis defense.

Table of Contents

List of Tables **ix**

List of Figures **xi**

List of Abbreviations **xv**

List of Symbols **xvii**

1 Introduction **1**

1.1 Wireless Ad Hoc Networks 2

1.2 Medium Access Control 3

1.3 Thesis Objective and Contributions 7

1.4 Overview of The Thesis 10

2 Related Research Works **11**

2.1 Medium Access Control Protocols 11

2.2 Power Saving MAC Protocols 13

2.2.1 Power saving MAC for wireless ad hoc networks 14
2.2.2 Power saving MAC for networks with APs 16
2.3 Radio Access Control in Cellular Networks 18
2.4 Transmission Power Control 19
2.5 Summary 22

3 MAC for a Fully Connected Network 23

3.1 System Model 24
3.2 The MAC Protocol 24
3.3 Performance Analysis for Realtime Traffic 31
3.3.1 Markov modeling of the system 32
3.3.2 Steady state probability of system states 35
3.3.3 Minimum frame duration to guarantee the required QoS of realtime traffic 36
3.4 Numerical Results and Discussions 37
3.4.1 Non-realtime traffic 38
3.4.2 Realtime traffic 44
3.4.3 Mixed realtime and non-realtime traffic 45
3.5 Summary 48

4 MAC for Exploiting Spatial Spectrum Reuse 49

4.1 System Model 50

4.2 Medium Access Control 51
4.2.1 Transmission policies in the different time slots 55
4.2.2 Operation of the MAC protocol 57
4.3 Numerical Results 63
4.4 Summary 74

5 Joint Scheduling and Transmission Power Control 76

5.1 System Model 77
5.2 Asymptotic Joint Optimal Scheduling and Transmission Power Control . . 80
5.3 Scheduling and Transmission Power Control 86
5.3.1 Transmission power and target interference power 88
5.3.2 Link scheduling 92
5.4 Distributed Scheduling and Transmission Power Control 96
5.5 Numerical Results 101
5.6 Summary 112

6 Conclusions and Future Work 114

6.1 Conclusions 114
6.2 Future Research Directions 117

A Derivation of Conditional Probabilities 118

B Determining the Number of Contention Slots and Contention Window Size **122**

Bibliography **128**

List of Tables

3.1 Simulation Parameters 39

3.2 EDCA-W Parameters 44

4.1 Simulation Parameters 64

5.1 Simulation Parameters 102

List of Figures

1.1 The hidden node and exposed node problems in a CSMA based MAC . . . 6

3.1 Structure of one beacon interval of the proposed scheme for $\beta = 2$. 25

3.2 The flowchart operation of a node in the proposed MAC. 30

3.3 Sender node states of a realtime call. 33

3.4 Aggregate throughput of the proposed scheme, PSM, and DCF-W 41

3.5 Energy consumption per packet of the proposed scheme, PSM, and DCF-W 42

3.6 Average packet transmission delay of the proposed scheme, PSM, and DCF-W 43

3.7 Packet loss rate of realtime traffic 45

3.8 Minimum required realtime frame duration to guarantee packet loss rate no larger than 1% 46

3.9 Performance of the proposed scheme, and EDCA-W for mixed realtime and non-realtime traffic (K=20 nodes) 47

4.1 Partitioning the network area into hexagonal cells, where C_i, $i \in \{1, 2, ..., m\}$, denotes the coordinator of cell i, the dotted circle centred at C_i shows the area that C_i broadcasts all scheduled transmissions/receptions, and the shaded area shows the space reserved for transmission from node f to node e. 52

4.2 Structure of one frame of the proposed scheme. 53

4.3 Assignment of scheduling time slots to coordinators, in which a scheduling time slot is assigned to all the coordinators of cells of a same group/color. . 54

4.4 The area centred at coordinator C_0 in which the coordinator obtains the information of scheduled transmissions by overhearing scheduling packets of adjacent coordinators, where a circular area centred at each coordinator denotes the area that the coordinator broadcasts the information of scheduled transmissions. 60

4.5 The flowchart operation of a non-coordinator node in each time slot. 62

4.6 The flowchart operation of a coordinator node in each time slot. 63

4.7 Throughput of the IEEE 802.11 DCF MAC vs traffic load for different carrier sensing ranges (N=100, $\eta_s = 6$ dB). 67

4.8 Throughput of the IEEE 802.11 DCF MAC in power saving mode (PSM) vs traffic load for different ATIM sizes when the carrier sensing range is set for highest throughput (N=100, $\eta_s = 6$ dB). 68

4.9 Throughput of the proposed MAC (PMAC), best-DCF, and best-PSM (N=100, $\eta_s = 6$ dB and $\eta_d = 9$ dB). 69

4.10 Energy consumption of the proposed MAC (PMAC), best-DCF, and best-PSM (N=100, $\eta_s = 6$ dB and $\eta_d = 9$ dB). 70

4.11 Collision rate of the proposed MAC (PMAC), best-DCF, and best-PSM (N=100, $\eta_s = 6$ dB and $\eta_d = 9$ dB). 71

4.12 Performance of the proposed MAC (PMAC), best-DCF, and best-PSM versus node density (Traffic load=8000 p/s, $\eta_s = 6$ dB and $\eta_d = 9$, 17 dB). . . 73

5.1 Symmetric scheduling paradigm 81

5.2 Plot of function $G(\cdot)$ for different path loss exponent values 84

5.3 Data rate per unit of network area versus energy consumption per transmitted bit as $\hat{E}$ in the network objective function varies ($\Gamma_c = 1.25$ mW, $\gamma \in [1, 100]$ mW, $g_a = 10$, $\alpha = 3.5$, $d = 1$, $r_g \in [d, 4d]$.) 85

5.4 A two-link network 89

5.5 Weak link scheduling plan versus good link scheduling plan 93

5.6 Partitioning the network area into hexagonal cells, where C_i, $i \in \{0, 1, 2, ...\}$, denotes the coordinator of cell i. A circular area centred at each coordinator denotes the location area of the nodes that their scheduling information is broadcasted by the coordinator ($r_a = 1.5r_g$). 98

5.7 Structure of one frame of the proposed MAC framework. 99

5.8 The optimal transmission power as energy consumption constraints vary ($\hat{E}_l = \theta \times \min E_l$). 103

5.9 The optimal target interference power as energy consumption constraints vary ($\hat{E}_l = \theta \times \min E_l$). 103

5.10 The optimal SINR as energy consumption constraints vary ($\hat{E}_l = \theta \times \min E_l$). 104

5.11 The asymptotic spectrum efficiency as energy consumption constraints vary ($\hat{E}_l = \theta \times \min E_l$). 104

5.12 The energy consumption per bit as energy consumption constraints vary ($\hat{E}_l = \theta \times \min E_l$). 105

5.13 Throughput and energy consumption of proposed scheme as θ varies with saturated data traffic at all nodes ($N = 400$). 107

5.14 Throughput and energy consumption of different schemes as network traffic load varies ($N = 400$, $\theta = \infty$). 109

5.15 Throughput and energy consumption of different schemes as number of nodes varies with saturated data traffic at all nodes ($\theta = \infty$). 110

5.16 Energy consumption of proposed scheme and best-PSM as network traffic load varies ($N = 400$, θ is adjusted such that the proposed scheme provides the same throughput as best-PSM). 111

5.17 Data transmission rate of the nodes using different schemes with saturated data traffic at all nodes ($N = 400$, $\theta = \infty$). 111

5.18 Scheduling efficiency of different schemes as number of nodes varies with saturated data traffic at all nodes ($\theta = \infty$). 112

B.1 The number of successful transmission requests in 1 ms. 126

B.2 The expected number of successful transmission requests in one frame (with the optimal contention window size). 126

B.3 The average delay to initiate a new transmission normalized to frame duration (with the optimal contention window size). 127

List of Abbreviations

AP	Access point.
ACK	Acknowledgement.
ATIM	Ad hoc traffic indication message.
BS	Base station.
CDMA	Code division multiple access.
CSMA	Carrier sense multiple access.
CSMA/CA	Carrier sense multiple access with collision avoidance.
DCF	Distributed coordination function.
D2D	Device-to-device.
EDCA	Enhanced distributed channel access.
HCCA	Hybrid controlled channel access.
IoT	Internet of Things.
MAC	Medium access control.
M2M	Machine-to-machine.
PCF	Point coordination function.
pmf	Probability mass function.
QoS	Quality of service.
RTS/CTS	Request-to-send/clear-to-send.

TCP	Transmission control protocol.
TDMA	Time division multiple access.
TIM	Traffic indication message.
VoIP	Voice over IP.
WLAN	Wireless local area network.

List of Symbols

C_i	Coordinator node i.
c	Path-loss constant factor.
B	Channel bandwidth in hertz.
D_l	Destination node of link l.
D_{max}	Maximum tolerable delay of a realtime packet.
d_{lk}	The distance between the source node of link l and the destination node of link k.
d_{max}	The maximum distance between single-hop source and destination nodes.
E	Energy consumption per transmitted data bit (Joule/(bit/Hz)).
E_l	Energy consumption per transmitted data bit (Joule/(bit/Hz)) at link l.
$\hat{E}$	The maximum energy consumption per bit threshold.
$\hat{E}_l$	The maximum energy consumption per bit threshold at link l.
g_a	The inverse of the power efficiency of radio interface amplifier.
h_{lk}	The channel gain between the source node of link l and the destination node of link k.
I	The interference power level.
I_l	The interference power level at link l.
I_{lt}	The interference power level at link l at time slot t.

$\tilde{I}$ Target interference power.

$\tilde{I}_l$ Target interference power of link l.

K Number of the nodes (with non-realtime traffic).

L Number of links.

M Maximum number of sender nodes with realtime traffic that can be scheduled for transmission in one realtime beacon interval.

$m(s)$ Number of nodes with realtime traffic scheduled for transmission when the system state is s.

N Number of the nodes (with realtime traffic).

N_i Number of sender nodes with realtime traffic that are in state i at the beginning of each beacon interval.

N_0 Thermal noise power.

R Transmission data rate.

R_l Transmission data rate of link l.

R_{lt} Transmission data rate of link l at time slot t.

$\tilde{R}$ Total data transmission rate per unit network area.

$\hat{R}$ The maximum required data rate.

$\hat{R}_l$ The maximum required data rate of link l.

R_s Transmission data rate of signaling packets.

r_a The range around a coordinator that it announces all the scheduled transmision/reception in that area.

r_g The distance between the center and a vertex of a hexagonal cell.

r_n The range around a coordinator that it acquires the information of scheduled trasnmssions/receptions.

S	System state at each beacon interval.
S_l	Source node of link l.
T	Number of time slots in a frame.
$T_{cf}(s)$	Duration of contention-free period when the system state is s.
$T_{cp}(s)$	Duration of contention period when the system state is s.
T_{nb}	Beacon interval for non-realtime traffic.
T_{rb}	Beacon interval for realtime traffic.
T_{rf}	Realtime traffic frame duration in a realtime beacon interval.
t_a	Inter-arrival time of packets in the *on* mode of a realtime call.
t_{off}	Average duration of *off* period of a realtime call.
t_{on}	Average duration of *on* period of a realtime call.
$\bar{\boldsymbol{u}}$	Scheduling matrix.
W	Contention window size.
X_i	Number of nodes that have transition i in a realtime beacon interval.
α	path loss exponent.
δ^*	Maximum tolerable packet loss rate of each realtime call.
δ_{ch}	Packet error rate due to channel impairments.
δ_{mac}	Packet error rate due to MAC contention.
η	Signal to noise plus interference ratio.
η_l	Signal to noise plus interference ratio of link l.
η_{lt}	Signal to noise plus interference ratio of link l at time slot t.
Γ_c	The power consumption in the radio interface circuit.

Γ_0 The power consumption in the radio interface at the sleep mode.

γ Transmission power level.

γ_l Transmission power level of link l.

γ_{lt} Transmission power level of link l at time slot t.

ρ Payload of an aggregated realtime packet.

τ_q Duration of one transmission request packet.

τ_v Duration of one aggregated realtime packet.

Chapter 1

Introduction

The number of mobile devices and the volume of mobile data traffic have been constantly increasing. It is forecasted that there will be over 10 billion interconnected mobile devices, including machine-to-machine (M2M) modules, by 2018 [1]. Overall, mobile data traffic is expected to grow nearly 11-fold by 2018 from that in 2013 [1]. To meet the increasing growth of mobile data traffic, it is essential to efficiently utilize network resources in the next generation wireless communication networks. A short communication range in small cells (or WiFi) for hotspot mobile communications is a key to increase network capacity via spatial radio spectrum reuse. Such a dense network of mobile nodes and access points (APs), and the emerging device-to-device (D2D), M2M and Internet of Things (IoT) communications necessitate establishing effective self-organizing ad hoc networks to efficiently leverage radio spectrum. Yet, energy consumption by radio interfaces should be minimized, because of limited battery capacity of mobile devices.

1.1 Wireless Ad Hoc Networks

A wireless ad hoc network is a collection of stationary and/or mobile nodes that communicate through a shared radio channel without requiring a pre-established infrastructure. Nodes are free to move and can join or leave the network anytime anywhere, which facilitates establishing dynamic and flexible wireless networks. The communication links are arbitrary and can be single-hop or multi-hop (with the aid of intermediate nodes). In ad hoc networks, network management and transmission medium control are performed in a distributed manner without a central control unit. The distributed operation of ad hoc networks allows establishing scalable networks. However, due to the lack of a central controller and high network dynamics, efficient utilization of the radio spectrum and energy resources is a challenging issue.

The increasing number of mobile devices and volume of mobile Internet traffic necessitate dense deployment of Internet APs in an ad hoc manner to increase network capacity via shorter communication links [2]. Thus, a centralized network management is impractical due to high complexity, signaling overhead and latency. The self-organizing and distributed characteristics of ad hoc networks provide effective and timely network management and transmission medium control for the future dense hotspot communication networks.

Direct D2D communications [3] among nearby devices in WiFi and cellular networks are emerging to increase spectrum and energy efficiencies (as a result of shorter communication links) and to enable peer-to-peer and location-based applications and services. Also, the emerging IoT requires M2M communications [4] to interconnect several billion physical objects and integrate them into the existing networks. Self-organizing ad hoc networks provide effective and scalable network and transmission medium control to organize and optimize diverse peer-to-peer communications in future wireless networks.

1.2 Medium Access Control

The medium access control (MAC) determines how nodes share the transmission medium. It also directly controls the operations of node radio interfaces. Thus, MAC plays an important role in the throughput, latency, and energy consumption of wireless networks.

Radio access mechanism

Existing MAC protocols for wireless networks can be classified into contention-free and contention-based schemes. The former uses pre-defined assignments to allow nodes to transmit without contention, which includes time-division, polling, and token-based MAC protocols. For instance, time division multiple access (TDMA) assigns fixed transmission time for each node. In contention-based MAC, a node dynamically contends with other nodes to access the channel. For instance, in carrier sense multiple access with collision avoidance (CSMA/CA), a node starts transmitting its packet after a random waiting time if it does not sense any ongoing transmission. Contention-based schemes are more flexible and efficient in managing the medium in a distributed way. However, as the data traffic load and/or the number of contending nodes increase, there are high chances for packet transmission collisions. The collisions cannot be detected quickly at the transmitting nodes, and the lack of an acknowledgment message is often the only way for the sender to detect collisions. As a result, whenever a transmission collision happens, the radio bandwidth and power for transmitting and receiving a packet are wasted. Hence, an efficient MAC scheme should minimize the chances of transmission collisions to reduce channel time and energy wastage in a wireless network.

Transceiver sleep scheduling

The radio interface is a main source of energy consumption of mobile devices such as laptops and smartphones, which can quickly drain the device's limited battery capacity [5–8]. For instance, a WiFi radio consumes more than 70% of total energy in a smartphone when the screen is off [7], which is reduced to 44.5% and 50% in the power saving mode when the screen is on and off respectively [8]. A radio interface can be in one of the following modes: transmit, receive, idle, and sleep. It has maximum power consumption in the transmit mode and minimum power consumption in the sleep mode. In the idle mode, a node needs to sense the medium and, hence, consumes a similar amount of power as when it is in the receive mode. For instance, a *Cisco Aironet 350 series* wireless local area network (WLAN) adapter [9] consumes 2.25W, 1.25W, 1.25W and 0.075W in transmit (transmit power level equal to 30mW), receive, idle, and sleep modes respectively. Clearly, a significant amount of energy is consumed even in the idle mode. This occurs in the CSMA/CA mechanism in IEEE 802.11 [10], where each node in the network has to continuously listen to the channel. To conserve energy, power saving mechanisms [10–13] allow a node to enter the sleep mode by powering off its radio interface when the node is not involved in transmission or reception. Although existing power saving MAC mechanisms reduce energy consumption by periodically putting the wireless interface into a sleep mode, the wireless interface still consumes a large amount of energy because of long idle-listening periods in mobile devices. Also, the existing MAC schemes have high collision rate and contention overhead, which degrade the performance of wireless ad hoc networks. Moreover, existing power saving MAC schemes cannot guarantee that the packet transmission delay is not larger than the maximum tolerable packet delay of realtime traffic.

Spatial spectrum reuse

In a wireless ad hoc network, nodes that are not in the communication range of each other cannot hear each others' transmissions. However their transmission may interfere each other at the receiver nodes. On the other hand, nodes that are far enough apart in space can transmit simultaneously without a collision (spatial frequency reuse). Thus, an effective MAC scheme for a wireless ad hoc network should have the following features:

1. It should prevent simultaneous transmission of interfering links. Otherwise, one or more of the transmissions will fail because of transmission collision, which results in wastage of bandwidth and energy;

2. It should allow simultaneous transmissions of non-interfering links for spatial reuse of the radio channel, because preventing non-interfering links from simultaneous transmission will unnecessarily degrade throughput of the network.

When a MAC scheme fails to accomplish the first feature, the *hidden node* problem arises. On the other hand, when a MAC scheme does not have the second feature, the *exposed node* problem occurs. A TDMA MAC scheme can potentially solve both the hidden node and exposed node problems in a wireless ad hoc network. However, finding an efficient time schedule requires a central controller and the optimal solution is NP-hard [14, 15]. Moreover, in a wireless ad hoc network, the traffic load and network topology change with time, which makes the static TDMA very inefficient. In addition, reassignment of channel time imposes a large overhead and requires global changes. The CSMA/CA MAC is commonly used in wireless ad hoc (and wireless local area) networks because of its flexibility and simplicity. However, it suffers from transmission collision and contention overhead, and cannot resolve the hidden and exposed node problems in a wireless ad hoc

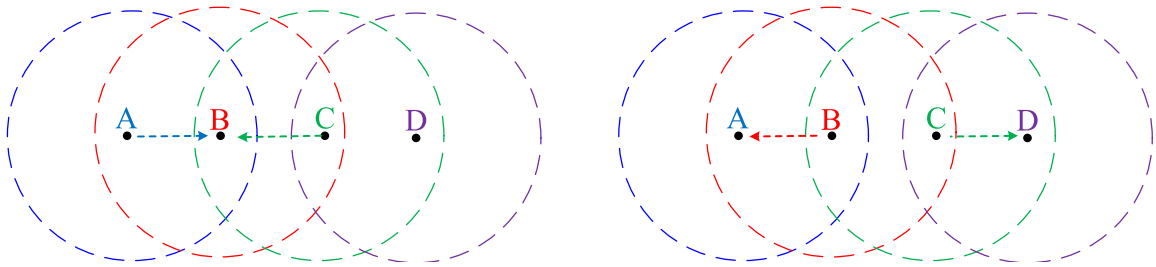

(a) Hidden node problem (b) Exposed node problem

Figure 1.1: The hidden node and exposed node problems in a CSMA based MAC

network. To illustrate the hidden and exposed node problems in a CSMA based MAC scheme, consider the network illustrated in Figure 1.1, where the dashed circles show the carrier sensing range of each node. When node A transmits to B, since node C is not in the carrier sense range of A, node C may start transmission that causes collision at node B. This phenomenon is known as the hidden node problem. Also, when B transmits to A, node C has to defer its transmission to D. However, both transmissions can be performed simultaneously. This phenomenon is known as the exposed node problem. The hidden node problem can be avoided by increasing the carrier sensing range [16], which however aggravates the exposed node problem and results in wastage of radio bandwidth. The request-to-send/clear-to-send (RTS/CTS) mechanism is used in [10, 17–20] to mitigate the hidden node problem. However, this mechanism imposes a significant amount of overhead in bandwidth and energy.

Transmission power control

Transmission power level significantly affect the performance and the energy consumption of wireless networks [21–24]. It determines the signal quality at the receiver, the amount of

interference on other concurrent transmissions, and the energy consumption at the transmitter node. A higher transmission power level increases the signal strength at the target receiver, but also negatively affects the other simultaneous transmissions by increasing the amount of interference. To enhance the overall network performance and reduce the energy consumption, the transmission power level of each node should be carefully adjusted based on network conditions. The optimal transmission power level to maximize the network throughput or minimize the energy consumption depends on network conditions and varies for different links in the network [21,25,26]. When nodes transmit at different power levels using a CSMA based MAC protocol, the interference levels at the receivers cannot be predicted. Therefore, when the data rates are adjusted for the worst case of interference, network throughput is reduced and energy consumption is increased. On the other hand, using the RTS/CTS control packets to avoid transmission collision (as in [27–30]) imposes overhead which causes throughput reduction and energy consumption.

1.3 Thesis Objective and Contributions

The objective of this research is to develop a spectrum and energy efficient MAC scheme for wireless ad hoc networks. In order to achieve this objective, the following fundamental issues have been investigated:

- How to dynamically coordinate access to the shared channel with low MAC overhead;
- How to efficiently schedule the sleep and awake times of the radio interfaces to reduce energy consumption, while avoiding large packet transmission queuing delay and signaling overhead for energy saving;

- How to efficiently schedule concurrent transmissions for efficient spatial spectrum utilization;
- How to adjust the transmission power level of each link to maximize spectrum and energy efficiencies.

We have taken the following steps to develop a spectrum and energy efficient MAC scheme for wireless ad hoc networks.

1. **MAC for a Fully-connected Network:** As a first step, we consider effective channel access coordination and transceiver sleep scheduling in a fully connected wireless network, in which every node can hear transmissions of all other nodes and only one node can transmit at each time instance over the radio channel. We propose an energy efficient MAC scheme with high throughput and low packet transmission delay for a fully connected wireless network using coordination among nodes. Using a temporary coordinator node, the proposed MAC effectively schedules data transmissions in a distributed way and with low signaling overhead. The idle-listening energy consumption and transmission collisions are minimized by dynamic assignment of contention-free transmission times. The proposed MAC scheme can address the energy saving in realtime traffic which require very low packet transmission delay. An analytical model is established to effectively allocate channel time to realtime and non-realtime traffic, such that the realtime traffic quality of service (QoS) constraints can be satisfied and the non-realtime traffic throughput is maximized. Analytical and simulation results demonstrate that the proposed MAC scheme has a significantly lower energy consumption, achieves higher throughput, and has lower packet transmission delay in comparison with existing MAC protocols.

2. **MAC for Exploiting Spatial Spectrum Reuse:** In the second step, we study effective channel access coordination with consideration of spatial spectrum reuse and effective radio transceiver sleep scheduling. We propose a novel MAC scheme that employs a set of coordinator nodes distributed over the network coverage area to effectively coordinate all nodes transmissions. In the proposed MAC, a coordinator node monitors transmission requests from source nodes in its vicinity, actively exchanges scheduling information with its adjacent coordinators, and periodically schedules transmissions for nodes inside its coverage area. For each scheduled transmission, an adequate space area around receiver node is reserved to guarantee the required link signal to noise plus interference ratio (SINR) and maximize spatial spectrum reuse. The data transmission times are deterministic. It allows nodes to stay awake only when they are transmitting/receving a packet, in order to minimize idle-listening energy consumption. Simulation results show that the proposed MAC achieves substantially higher throughput and has a significantly lower energy consumption in comparison with existing schemes.

3. **Joint Scheduling and Transmission Power Control:** In the third step, we study how to determine concurrent transmissions and the transmission power level of each link to maximize spectrum efficiency and minimize energy consumption. We show that the optimal joint scheduling and transmission power control can be determined when the node density goes to infinity and the network area is unbounded. Based on the asymptotic analysis, we determine the fundamental capacity limits of a wireless network, subject to an energy consumption constraint. We propose a scheduling and transmission power control mechanism to approach the optimal solution to maximize spectrum and energy efficiencies in a practical wireless ad hoc network. We present a distributed implementation of the proposed scheduling and transmission power con-

trol scheme based on our proposed MAC framework in the previous step. Simulation results demonstrate that the proposed scheme achieves 78% of the asymptotic network capacity, and the distributed scheme (with consideration of the MAC signaling overhead) achieves 70% of the asymptotic network capacity. The achieved throughput is about 35% higher than the throughput obtained using existing schemes. Also, the energy consumption using the proposed scheme is about 20% of the energy consumed using existing power saving MAC protocols.

1.4 Overview of The Thesis

The rest of the thesis is organized as follows: Chapter 2 reviews related research works. Thesis contributions are presented in Chapters 3, 4 and 5 respectively [31–34]. Finally, Chapter 6 provides conclusions and future work.

Chapter 2

Related Research Works

2.1 Medium Access Control Protocols

The distributed coordination function (DCF) is the basic medium access defined in the IEEE 802.11 standard [10] known as WiFi[1]. The DCF is based on CSMA/CA, which uses carrier sensing with exponential back-off to avoid collision. Each node randomly chooses a back-off time between zero and its contention window size; Nodes decrease their back-off by one after each idle mini-slot of channel time. The back-off is frozen while the channel is sensed busy. Once the back-off of a node reaches zero, it starts transmission. If an acknowledgement packet is not received from the receiver, the transmission is considered as a collision. After each collision, the nodes involving in the collision double their contention window size (until it reaches the maximum contention window size) to avoid future collisions, and starts the back-off again. A node restores its back-off to the minimum value after it successfully transmits a packet.

[1]The WiFi stand for Wireless Fidelity.

The DCF provides an optional RTS/CTS handshake before transmitting a data packet. When a transmitter has a data packet for transmission, it sends an RTS packet to the receiver. The nodes in the transmission range of the sender (that overhear the RTS packet) defer their transmissions. If the receiver node successfully receives the RTS packet, it will reply with a CTS packet. The nodes in the transmission range of the receiver (that overhear the CTS packet) also defer their transmissions. Once the medium around the transmitter and receiver is reserved for the data packet transmission, the sender transmits the data packet. The RTS/CTS mechanism can prevent transmissions collisions caused by hidden nodes. However, it also imposes a significant amount of signaling overhead that reduces network throughput.

The IEEE 802.11 has also defined a point coordination function (PCF) MAC protocol which is only available in networks with a central controller or AP. In PCF, the AP sends beacon frames at regular intervals (e.g., 100 ms) and each beacon interval is divided into two parts: contention period and contention-free period. The DCF MAC protocol is used in the contention period. But in the contention-free period, the AP sends a contention-free-poll packet to each node to allow the node transmit without contention. The DCF and PCF are enhanced in the IEEE 802.11e [10] to support QoS. The IEEE 802.11e defines two medium access schemes: enhanced distributed channel access (EDCA) and hybrid controlled channel access (HCCA). The EDCA defines different traffic categories with different priorities. The EDCA is based on the CSMA/CA MAC protocol and the priory associated to each traffic category is obtained by varying inter-frame spaces, the contention window size, and the maximum transmission duration. The performance of EDCA is evaluated in [35–43]. The HCCA is available only for networks with a central controller or AP. In HCCA, similar to PCF, the AP sends beacons at regular intervals and each beacon interval consists of several contention periods and contention-free periods. The medium

access in the contention periods, is similar to EDCA. However, in the contention-free periods, the AP sends the contention-free-poll packets to give contention-free transmission time to each node.

A dynamic TDMA MAC scheme is proposed in [44, 45]. Time is partitioned into frames that are consisting of a fixed number of slots. Every node acquires a transmission slot in each frame, in which it transmits a packet to inform the other nodes of the time slots that it will transmit/receive data packets (frame information). A node can reserve additional transmission slots using ALOHA and/or via broadcasting its frame information. A node can reserve a new time slot only if none of the neighboring nodes has announced a transmission in that time slot in the previous frame. This mechanism can mitigate the hidden node problem; however the imposed overhead of transmitting frame information by every node in each frame reduces network throughput and increases energy consumption. A hybrid TDMA-CSMA MAC scheme is proposed in [46] using CSMA as the baseline MAC scheme. A transmission time slot is assigned to each node such that none of the interfering nodes are assigned a same transmission slot. At each time slot, the owner has a higher priority to transmit a packet. If a node experiences successive collisions because of hidden nodes, it will transmit a request packet to prevent the interfering nodes from transmission in its assigned transmission slot for a requested period of time.

2.2 Power Saving MAC Protocols

To conserve energy, power saving mechanisms allow a node to enter the sleep mode by powering off its radio interface when the node is not involved in transmission. In the following, we review existing power saving MAC protocols proposed for wireless ad hoc networks and for networks with AP support.

2.2.1 Power saving MAC for wireless ad hoc networks

The IEEE 802.11 standard [10] provides a power saving mechanism for wireless ad hoc networks (here referred to as PSM). In the PSM, time is partitioned into fixed size beacon intervals, and nodes in the network are synchronized using distributed beacon transmission. There is an ad hoc traffic indication message (ATIM) window at the beginning of each beacon interval, in which all the nodes stay awake. During the ATIM window, every node (that has data packets for transmission) informs its destination node by transmitting an ATIM packet. If the targeted node of an ATIM packet successfully receives the packet, it will reply with an acknowledgement (ACK) packet and both nodes stay awake for the rest of the beacon interval (the communication period) to transmit packets. After the ATIM window, the nodes (that are not involved in transmission or reception) turn their radio interfaces into the sleep mode for the rest of that beacon interval to save energy. The DCF or EDCA MAC protocol is used to access the channel during the ATIM window and the communication period.

The performance of PSM depends on the ATIM window size [47]. If the ATIM window size is too small, nodes do not have enough time to declare their buffered packets. On the other hand, a large ATIM window size decreases the actual packet transmission time during the communication period of a beacon interval. Generally, the ATIM window size should be adjusted based on the number of source nodes and network traffic load. How to adjust the size of ATIM window is a challenging issue in the existing power saving schemes. In the DPSM [13], each node independently varies its ATIM window size based on network conditions. Since in the DPSM nodes may have different ATIM window sizes, the ATIM packet of a sender node may not be heard by its intended receiver with a smaller ATIM window size. This problem causes the wastage of radio bandwidth and energy, and

increases packet transmission delay.

In the PSM, a node (that transmits or receives ATIM during the ATIM window) should stay awake for the rest of the beacon interval, i.e., the whole communication period of that beacon interval. While this approach has the advantage that one ATIM packet can be followed by multiple data packets in one beacon interval, it results in high energy consumption because of the long awake period. The DPSM [13] reduces the awake time of nodes by allowing a node to switch its radio interface into the sleep mode once it finished transmitting/receiving data packets. This approach reduces the awake period of nodes in the communication period. However, sender nodes have to contend with each other to transmit packets. Thus, nodes still have to stay awake for a long period until they finish transmission/reception of all the packets. The TMMAC [48] employs a contention-free MAC protocol in the communication period of a beacon interval to reduce the awake period of nodes. In TMMAC, during the ATIM window, nodes reserve time slots for transmission in the communication period of that beacon interval. In this way, nodes stay awake in the communication period only for their packet transmision/reception time. However, it cannot fully utilize the channel transmission time during the communication period because nodes reserve time slots without coordination among them, which degrades channel utilization.

In the existing power saving MAC protocols, all the sender nodes that have data packets for transmission need to contend with each other to send a request packet to their destination nodes during the ATIM window of a beacon interval. This approach not only imposes overhead and reduces the communication period in each beacon interval, but also consumes a significant amount of energy, because every node has to stay awake during the ATIM window to send/receive the ATIM packets.

In PSM and DPSM, the contention and collision overhead in the communication period

further reduces the network throughput and increases the average packet transmission delay. Although the TMMAC uses a contention-free MAC during the communication period to reduce energy consumption, as discussed, it cannot fully utilize the available transmission time during the communication period.

In the existing power saving MAC protocols proposed for ad hoc networks, another serious problem is that they cannot address power saving for realtime traffic which requires a very low packet transmission delay. In the PSM, DPSM and TMMAC, each packet has to wait at least one beacon interval before transmission. However, the beacon interval cannot be chosen to be too short, because a short beacon interval leads to high energy consumption and low network throughput due to more frequent ATIM windows.

2.2.2 Power saving MAC for networks with APs

The PSM for a network with AP support [10] is similar to that in an ad hoc network. Time is partitioned into beacon intervals and, at beginning of each beacon interval, the AP broadcasts a traffic indication message (TIM) to inform the power saving nodes that it has packets to deliver. The nodes that are included in the TIM stay awake during the communication period and poll the AP to receive the packets. Also, if a node has packets for transmission to the AP, it stays awake and sends the packets to the AP during the communication period.

The PSM performance is improved in energy saving by separating the delay sensitive traffic and delay tolerant traffic [49], giving priority to the power saving nodes [50], and distributing TIM of different APs to avoid traffic burst [51]. Dogar *et al.* in [49] suggest to separate the delay sensitive traffic (e.g., telnet) and delay tolerant traffic (e.g., ftp) at the mobile devices to batch the packets of data tolerant traffic and send them at bursts in

order to increase the sleep time of the nodes. Doser *et al.* in [50] propose to separate the traffic of power saving nodes from the traffic of constantly awake nodes in the APs and give higher service priority to power saving nodes in order to decrease the waiting time of power saving nodes for getting service, which reduces their energy consumption. The TIM times of different APs are distributed over time in [51] to avoid traffic bursts. In this way, the clients of different APs are active during non-overlapping time windows, which decreases the contention among clients of different APs. It reduces the awake time and saves energy of mobile devices in the PSM mode. A traffic scheduler is proposed in [52] where the AP delivers packets to the clients in an order that reduces sum of energy consumption in the network.

The PSM performance for delay sensitive applications is investigated and active/sleep schedules that guarantee delay requirements are proposed in [53–56]. Anand *et al.* in [53] propose a self-tuning power management scheme for networks with AP support in which nodes switch to the PSM mode when it is beneficial, taking account of the pattern and intent of applications, characteristics of the network interface, and the energy usage of the platform. The SPSM proposed in [54] is a variation of the PSM, which schedules the nodes wake-up patterns at the ATIM window of beacon intervals based on the user required delay performance. An algorithm is proposed in [55] to derive an active/sleep schedule to save energy during voice over IP (VoIP) calls in networks with AP support, while ensuring that the application QoS is preserved. The authors in [56] investigate the interaction between PSM and the transmission control protocol (TCP) for web-like transfers. It is shown that the PSM increases the round trip times and, under a low traffic load, the PSM unnecessarily spends energy waking up nodes in long idle periods. Taking into account the TCP operation, a dynamic protocol for WLANs with AP is proposed to guarantee a required delay. The mobile devices after sending a request decrease the frequency of

waking up at the ATIM windows based on the response time from the AP. This scheme is applicable to only the requests initiated by mobile devices.

Other power saving protocols have been proposed in literature which require another low power interface (e.g., ZigBee) along a WiFi interface (e.g., [7, 8, 57, 58]) or require physical layer modifications (e.g. [59, 60]).

The power saving MAC protocols for networks with AP support can provide high performance and low energy consumption when there is only one AP in the network. However, in WLANs, several APs are usually located in the same area and have to contend with each other to access the shared channels, which degrades the network throughput and increases the energy consumption. In fact, the set of APs and nodes connected to APs form a wireless ad hoc network.

2.3 Radio Access Control in Cellular Networks

In a cellular network, network area is partitioned into cells and nodes inside a cell only communicate with the cell base station (BS) at the cell center. The BS schedules all transmissions to and from nodes (downlink and uplink) inside its cell. Therefore, transmission collisions are prevented among nodes in the cell and idle listening energy consumption of mobile nodes is minimized, because of deterministic transmission time which is assigned by the BS. In the conventional cellular networks, each cell is assigned a fraction of total available radio spectrum to avoid inter-cell interference. For instance, in GSM a cell commonly uses one-fourth of total available radio spectrum (frequency reuse factor 4) to prevent inter-cell interference. Several inter-cell interference coordination techniques are proposed to improve the performance of cellular systems using *fractional frequency reuse* [61, 62]. In fractional frequency reuse, the total available radio spectrum is used for transmissions to

and from the nodes close to the BS at the central region of a cell, but a fraction of spectrum is used for transmissions to and from nodes that are outside the central region of the cell, in order to reduce inter-cell interference [61–64]. The dense deployment of small cells in the next generation of wireless networks and the direct D2D and M2M communications form communication links in an ad hoc manner, which require a new MAC mechanism to efficiently utilize the shared radio spectrum and minimize energy consumption.

2.4 Transmission Power Control

In a CSMA based MAC protocol, spatial frequency reuse can be increased by either lowering the transmission power level or increasing carrier sensing threshold, both increasing the number of concurrent transmissions. Transmission at the minimum power level is proposed in [24, 29, 30] to maximize the spatial reuse. In [29], an access window is used to exchange multiple RTS/CTS control packets in order to perform multiple concurrent transmissions, each at the minimum transmission power level. In [30], each node maintains a table that contains the minimum required power level for transmission to any of its neighbors and the maximum power level that it can transmit when the neighboring nodes are transmitting/receiving packets. At any instant, a node may start a transmission only if the minimum required power level to deliver the packets to the destination is less than the maximum power level that it is allowed to transmit.

Although increasing spatial reuse allows more concurrent transmissions, it also decreases the SINR at the receivers (because of lower signal power strength and/or higher interference power level at the receivers). Therefore, the data rate of each transmission decreases as a result of a lower SINR. The trade-off between the increased spatial reuse and the decreased data rate when using a CSMA/CA MAC protocol has been studied in [25,26].

For a CSMA/CA MAC protocol, it is shown that the network capacity depends only on the ratio of the transmission power level to the carrier sensing threshold (i.e., carrier sensing range). The optimal ratio to maximize the network throughput depends on the distance between source-destination pairs. It is proposed that all nodes use a same carrier sensing threshold and each source node adjusts its transmission power level iteratively based on its distance from the destination, the interference feedback from the destination, and its required transmission rate.

The interference at a receiver node depends on the transmitting power levels of the interfering nodes. The set of interfering nodes for a transmission/reception may change over time. When the sender nodes transmit at different power levels, the interference at a receiver node varies over time. Therefore, when only carrier sensing is used, the transmission rates must be adjusted for the worst interference case to ensure successful reception of packets at the receiver. As a result, the transmission power level control schemes (in which only carrier sensing is used and nodes independently choose their transmission power levels) cannot fully utilize the network capacity. Also, the CSMA based MAC protocols provide poor spatial spectrum reuse due to the *hidden* and *exposed* node problems [33, 65]. On the other hand, using RTS/CTS control packets to advertise the transmission power level and the maximum tolerable interference (as in [29, 30]) imposes overhead and reduces the total channel throughput. Centralized scheduling and transmission power control for wireless ad hoc networks are proposed in [66, 67].

The optimal scheduling and transmission power control to maximize total throughput in a two-cell wireless network with only two links have been studied in [68]. In the network with two links, maximizing total throughput leads to binary power control. That is, each link should transmit at either the maximum power level or the minimum power level [68]. Motivated by optimality of binary power control in a two-cell network with only two links,

the binary power control is also proposed for multi-cell networks with more than two links in [69]. Distributed uplink power control in a cellular network to attain the target SINR levels of mobile stations is studied in [70, 71]. In current cellular networks, a *fractional power control* mechanism is used to determine transmission power level between a BS and a mobile node. In *fractional power control*, the transmission power of a link is adjusted to compensate for a fraction of the link's path loss power (in dB). Thus, the transmission power control policy can vary continuingly from fixed transmission power to fixed target SINR, as the compensation fraction of path loss power increases from 0 to 1. The total network throughput in a cellular network with different compensation factor values is studied in [72, 73] using simulation.

The effect of transmission power level on total energy consumption depends on the energy consumption pattern of the wireless adapter [21–24]. The energy consumption of a radio interface has two components: the energy consumed in the radio interface circuit, and the energy consumed in the amplifier. When the energy consumption in the amplifier dominates the energy consumed at the radio interface circuits, the energy consumption in a two-link network can be reduced by decreasing the transmission power level [21]. However, when the energy consumption in the radio interface circuit is much larger than the energy consumption in the amplifier, minimizing the energy consumption in a two-link network is equivalent to maximizing network throughput [21]. Generally, the transmission power level in which the energy consumption is minimized depends on the energy consumption pattern of the radio interface and the network condition. Thus, transmission at the minimum power level (as in [27, 28, 74, 75]) does not always reduce the energy consumption. Also, exchanging the RTS/CTS control packets (as in [27, 28, 74, 75]) imposes overhead and increases the total energy consumption. Energy consumption per transmitted data bit with consideration of both circuit power consumption and the transmission power level is

studied in [76]. They proposed a distributed power control scheme based on game theory to reduce energy consumption in network nodes.

2.5 Summary

There exist extensive research works on MAC and power saving for wireless ad hoc and local area networks. Despite the research efforts, the existing schemes still have low throughput and high energy consumption due to high collision and contention overhead, long radio interface idle-listening periods, power saving mechanism overhead, poor spatial spectrum utilization, and improper transmission power level. Also, the current cellular networks use fractional frequency reuse to prevent inter-cell interference, which cannot provide efficient spatial spatial spectrum utilization. The dense network of mobile nodes and APs in the next generation of wireless networks and diverse communications links (e.g., M2M communication links) necessitate developing novel MAC schemes to establish high throughput and energy efficient networks.

Chapter 3

MAC for a Fully Connected Network

As a first step, we propose a new MAC scheme for effective channel access coordination and radio interface sleep scheduling in a fully connected network. Using a temporary coordinator node, the proposed scheme reduces the energy consumption by scheduling the active and sleep times of node radio interfaces in a distributed way, and decreases MAC overhead and transmission collisions among nodes. A node contends only once to transmit a batch of packets, after that it will be assigned a contention-free time for transmission by the temporary coordinator node as long as it has packets ready for transmission. Nodes stay awake for a short time at the beginning of each beacon interval (to receive the transmission scheduling information) and during their packet transmission/reception times. The MAC scheme guarantees delay and packet loss rate requirements, and reduces energy consumption of nodes with realtime traffic such as voice or video calls that have stringent delay and packet loss requirements. Compared to existing power saving mechanisms, the proposed scheme has lower energy consumption, higher throughput, and shorter packet transmission delay.

The rest of this chapter is organized as follows: System model is presented in Section 3.1. In Section 3.2, we describe the proposed MAC protocol. Then, we present an analytical model to evaluate the performance of the proposed MAC scheme in Section 3.3. Numerical results are given in Section 3.4 to demonstrate performance of the proposed MAC scheme in comparison with existing MAC protocols. Section 3.5 summarizes this chapter.

3.1 System Model

Consider a single-channel wireless ad hoc network providing realtime and non-realtime services to mobile users. Let N denote the number of nodes with realtime traffic and K the number of nodes with non-realtime traffic. We assume that network is fully-connected. That is, all nodes are in the communication range of each other and at each instant only one node can transmit over the channel. If more than one node start transmission over the shared channel, collision happens and none of the packets will be received successfully at the receiver nodes. The destination node for each source node is randomly selected from the rest nodes. There is no central controller in the network and nodes coordinate their transmissions in a distributed way.

3.2 The MAC Protocol

Time is partitioned into beacon intervals of constant duration and all nodes are synchronized in time. The synchronization can be achieved by using a distributed beacon transmission mechanism, as in the IEEE 802.11 power saving mechanism [10].

Each beacon interval consists of three different periods: *announcement period*, *contention-free period*, and *contention period*. Figure 3.1 shows the structure of one beacon interval.

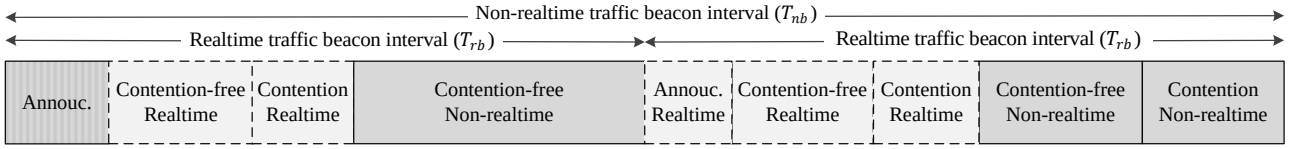

Figure 3.1: Structure of one beacon interval of the proposed scheme for $\beta = 2$.

The durations of the periods are adjusted dynamically by a temporary coordinator node called *head node*, based on the instantaneous network traffic load condition. The *head node* monitors the traffic demands of nodes in the previous beacon interval and records nodes' requests in a table called *demand table*. At the beginning of the current beacon interval, in the *announcement period*, the *head node* broadcasts the durations of the periods, and transmission schedule of the *contention-free period* based on the *demand table*. All nodes must be awake to receive the broadcast message in the *announcement period* from the current *head node*. The scheduled transmissions take place in the *contention-free period* with SIFS[1] intervals in between. Nodes, which have packets to transmit but have not informed the *head node* of their intent for transmission, contend in the *contention period* using a CSMA MAC mechanism to inform the *head node* of their intention for transmission by sending an RTS packet.

In the proposed MAC protocol, nodes need to wait for one beacon interval to transmit packets. Since realtime traffic (from voice and video calls) has a strict packet transmission delay requirement, the beacon interval for realtime traffic should be less than the maximum tolerable packet delay of realtime traffic. On the other hand, non-realtime traffic (such as in file transfer and web browsing) can tolerate a longer packet transmission delay, and a small beacon interval increases the energy consumption because nodes have less sleep times.

[1]The Short Inter-frame Space (SIFS) equals to time required for a node to sense the end of a packet transmission and start transmitting.

Therefore, we propose different beacon intervals for realtime traffic and non-realtime traffic respectively. We also assign unique transmission time to the realtime traffic for higher priority over non-realtime traffic flows.

The beacon interval duration of realtime traffic, T_{rb}, should not be longer than the maximum tolerable delay of realtime traffic, $D_{\max}$. i.e., $T_{rb} \leq D_{\max}$. We set the beacon interval duration for non-realtime traffic as, $T_{nb} = \beta T_{rb}$, where $\beta \geq 1$ is an integer. Figure 3.1 shows the structure of the realtime and non-realtime (traffic) beacon intervals for $\beta = 2$. That is, there are two realtime beacon intervals per non-realtime beacon interval. As β is increased, the throughput is increased and the energy consumption in nodes with non-realtime traffic is reduced due to less frequent *announcement period*s; however, the packet transmission queuing delay is increased because of larger non-realtime beacon intervals. The realtime traffic frame duration in a realtime beacon interval (T_{rf}), which is the summation of *contention-free period* and *contention period* of realtime traffic in one realtime beacon interval, is constant and should be adjusted to meet the packet loss rate requirement of realtime traffic in the network. The values of parameters T_{rb}, T_{rf}, and β, can be updated by the *head node* based on the network condition. In the following, we discuss detail operation of the proposed MAC protocol in a non-realtime beacon interval.

*Announcement period*s: There are β *announcement period*s per one non-realtime beacon interval. In each period, the *head node* regulates the transmission for the current beacon interval and announces the transmission schedule by broadcasting a *scheduling packet*, based on the requests in the *demand table* that it generated/updated in the previous beacon interval. When the number of requests is more than the packet transmissions that can be scheduled in the current beacon interval, the *head node* also broadcasts the pending requests. In the first *announcement period* at the beginning of each non-realtime beacon interval, all the nodes (with realtime and non-realtime traffic) stay awake and

the *head node* schedules the transmission for the current non-realtime beacon interval and the first realtime beacon interval. The *head node* also randomly selects one of the nodes that is involved in transmission/reception of current beacon interval as the new *head node* for the next beacon interval. The *scheduling packet* in the first *announcement period* contains the following information: the duration of realtime frames and the starting times of next $\beta - 1$ *announcement periods*, scheduling information for the first realtime beacon interval, the scheduling information for the non-realtime traffic in the current non-realtime beacon interval, and the node selected as the next *head node*. The scheduling information for the first realtime beacon interval determines the transmission in the first realtime *contention-free period*, the duration of realtime *contention period*, and the pending requests that cannot be scheduled in the first realtime beacon interval. The scheduling information for the non-realtime traffic determines the transmission schedule in the non-realtime *contention-free period*, the duration of non-realtime *contention period*, and the pending requests that cannot be scheduled in the current non-realtime beacon interval[2]. The node selected as the next *head node* should confirm with an ACK packet following the *scheduling packet*. If the selected node does not confirm, the *head node* will continue to serve as the *head node* for the next non-realtime beacon interval, and then will select a different *head node* at the first *announcement period* of the next non-realtime beacon interval. In the next $(\beta - 1)$ *announcement period*(s) of the current non-realtime beacon interval, only the nodes with realtime traffic are awake and the *head node* schedules the transmission in the realtime beacon intervals based on the transmission requests in the previous realtime beacon interval. The *scheduling packet*, transmitted by the *head node* in each *announcement period* at the beginning of next $\beta-1$ realtime beacon intervals, contains

[2]Note that the *contention-free period* and the *contention period* of non-realtime traffic may have more than one parts which are separated by realtime traffic frames.

the transmission schedule for that *realtime contention-free period*, and the pending requests that cannot be scheduled in that realtime beacon interval.

*Contention-free period*s: In these periods, the *head node* stays awake and the transmitter/receiver nodes that are scheduled for transmitting/receiving packets wake up at the assigned time to transmit/receive packets. The nodes with realtime traffic are scheduled to transmit/receive packets at the *realtime contention-free period*s and the nodes with non-realtime traffic are scheduled to transmit/receive the data packets in the *non-realtime contention-free period*s. Sender nodes with realtime traffic put their call status (*on* or *off*) in the header of the transmitted packets, and the sender nodes with non-realtime traffic put the number of the remaining packets ready for transmission in the header of their data packets. The *head node* uses the information to generate/update the *demand table*. Although transmission of packets is collision free in the *contention-free period*, the transmission may be corrupted by short-term channel fading. Therefore, receivers should acknowledge receiving non-realtime packets by transmitting an ACK packet[3]. In contrast, realtime packets will be useless if they are not transmitted before a deadline. Thus, no ACK packet is transmitted by the receiver for realtime packets.

*Contention period*s: In the *contention period*s, nodes (that have packets ready for transmission but were neither scheduled for transmission nor included in the pending traffic list transmitted by the *head node* in the previous *announcement period*) stay awake and contend for transmission using a CSMA MAC protocol to submit a transmission request. Nodes with realtime traffic submit transmission requests at the *realtime contention period*s and node with non-realtime traffic submit transmission requests at the *non-realtime contention period*s. Once a contending node's back-off counter reaches zero, it transmits an RTS packet

[3]Note that instead of transmitting an individual ACK for each packet, multiple packets can be acknowledged using a single Block ACK [10] to improve the MAC efficiency.

to the *head node*. The RTS packet of a node with realtime traffic includes information of the maximum tolerable delay, maximum tolerable packet loss rate, the sender node ID, and the destination node ID. The RTS packet of a node with non-realtime traffic contains the number of packets that are ready for transmission at the sender, the sender node ID, and the receiver node ID. The *head node* stays awake to monitor transmission requests and records them in the *demand table*. When a node successfully transmits a request without collision, the *head node* records the information in the *demand table* and uses this information to schedule transmission at the next beacon interval. Once a contending node has submitted a request to the *head node*, it powers off for the rest of the beacon interval. If a contending node does not have a chance to submit a request, it will contend again in the *contention period* of the next beacon interval. Figure 3.2 illustrates the operation of a node in the proposed MAC.

The proposed scheme dynamically adjusts the transmission schedule of the periods based on the current traffic load condition of all nodes. It has the following features:

1) The awake time of the nodes is short which reduces energy consumption.

Nodes with non-realtime traffic that are not involved in transmission/reception stay awake only at the first *announcement period* at each non-realtime beacon interval. Also, nodes with realtime traffic stay awake only at the *announcement period*s in each non-realtime beacon interval. The nodes that are scheduled to transmit or receive a packet wake up at the assigned time to transmit/receive without contention in the *contention-free period*s. In the *contention period*s, only the nodes that want to initiate a new transmission and the *head node* stay awake. The *head node* is the only node that stays awake for the whole beacon interval;

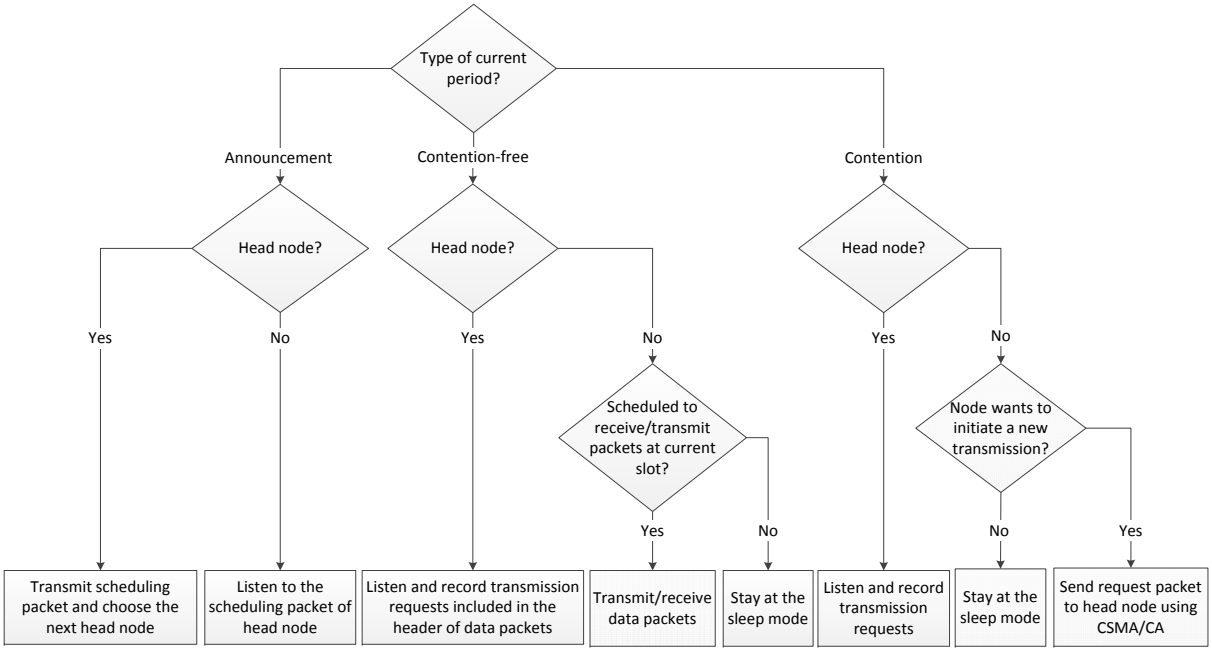

Figure 3.2: The flowchart operation of a node in the proposed MAC.

2) The contention and collision overhead is small, which reduces the energy consumption and enhances the network performance.

Nodes contend for the channel only when they want to initiate a new transmission. Once a node successfully submits a transmission request, it will be assigned a transmission time in the next beacon intervals as long as it has packets ready for transmission. Also, the number of contending nodes decreases because each node does not contend for transmission of each packet, but for transmission of a batch of packets available in its buffer;

3) It is distributed and adaptive to the network condition.

No dedicated cental controller is required to manage the network. Nodes cooperate and in each beacon interval a coordinator node (head node) schedules the transmissions based on the request from all nodes in the previous beacon interval. Since the *head node* has the information of all requests, it can efficiently schedule transmissions based on instantaneous network condition.

In the following section, we present an analytical model to evaluate the performance of the proposed MAC protocol. The analytical model enables us to determine the minimum required frame time for realtime traffic in each realtime beacon interval to meet the packet loss rate requirements of realtime traffic flows.

3.3 Performance Analysis for Realtime Traffic

Time is discretized and normalized to the duration of a mini-slot[4]. Consider constant rate, on-off realtime (voice or video) calls to make the analysis tractable. The duration of *on* and *off* modes are exponentially distributed with average t_{on} and t_{off} respectively. Packets are generated periodically with inter-arrival time t_a in the *on* mode, while no packet is generated in the *off* mode. Each packet has a payload of h bits. A sender node with realtime traffic aggregates the packets and transmits them as one packet at the assigned time in the *realtime contention-free period*s. The payload of an aggregated packet is $\rho = \frac{T_{rb}}{t_a}h$. If an aggregated realtime packet is not transmitted within a deadline $D_{\max}$, it will be removed at the sender. The maximum tolerable packet loss rate for each realtime

[4]A mini-slot is the summation of RxTx turn around time, channel sensing time, propagation delay, and MAC processing delay.

call is δ^*. Let δ_{ch} denote the packet error rate due to channel impairments and δ_{mac} denote the packet loss rate due to MAC contentions. The packet loss rate of each realtime call is given by

$$\delta = 1 - (1 - \delta_{mac})(1 - \delta_{ch}). \tag{3.1}$$

According to (3.1), the maximum allowable packet loss rate due to MAC contentions, δ^*_{mac}, is

$$\delta^*_{mac} = 1 - \frac{1 - \delta^*}{1 - \delta_{ch}}. \tag{3.2}$$

Let T_{rf} denote the realtime traffic frame duration which is the summation of *contention-free period* and *contention period* assigned to realtime traffic in each realtime beacon interval. Let τ_q denote the duration of one transmission request packet (including an SIFS) and τ_v denote the transmission time of one aggregated realtime packet (including an SIFS) over the channel. The maximum number of nodes with realtime traffic that can be scheduled for transmission in one realtime beacon interval is

$$M = \lfloor \frac{T_{rf}}{\tau_v} \rfloor \tag{3.3}$$

where $\lfloor . \rfloor$ denotes the floor function.

3.3.1 Markov modeling of the system

At any beacon interval, the sender node of a realtime call is in one of the following states:;

State 1 – The realtime call is in the *on* mode but the sender node is not included in the *demand table*. Thus, the sender node contends with other nodes in the *realtime contention period* to submit a transmission request;

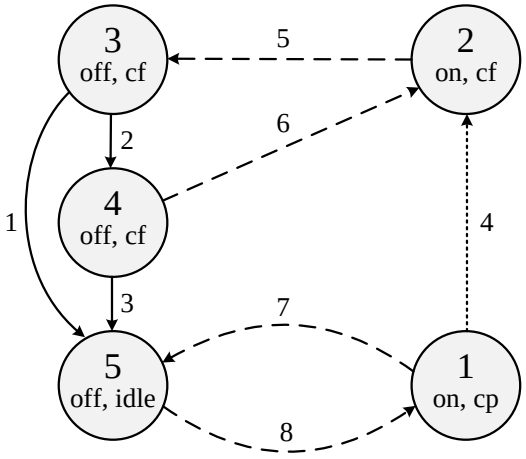

Figure 3.3: Sender node states of a realtime call.

State 2 – The realtime call is in the *on* mode and the sender node is included in the *demand table*;

State 3 – The realtime call has just switched to the *off* mode, the sender node is included in the *demand table* and has a pending packet for transmission whose transmission delay threshold has not passed yet. The sender node will inform its status change to the *head node* when transmitting in the *contention-free period*;

State 4 – The realtime call is in the *off* mode, and the sender node is included in the *demand table*. However, the sender node has no pending packet for transmission. The sender node will inform the *head node* of its *off* mode when transmitting in the *contention-free period*;

State 5 – The realtime call is in the *off* mode, and the node is not included in the *demand table*.

Figure 3.3 shows the sender node states of a realtime call. The state transitions illustrated by solid lines (transitions 1, 2 and 3) take place in the *contention-free period*. The transition represented by dotted line (transition 4) takes place in the *contention period*. The set of transitions indicated by dashed lines (transitions 5, 6, 7 and 8) are due to status changes of realtime call (from *on* to *off*, or from *off* to *on* mode) that we assume take place at the end of each realtime beacon interval. We assume that status of a realtime call does not change more than once during a realtime beacon interval, which is reasonable as average *on* and *off* periods of a realtime traffic call are in general much larger than the realtime beacon interval.

Let N_i denote the number of sender nodes with realtime traffic that are in state $i \in \{1, ..., 5\}$ at the beginning of each beacon interval. We have $N_5 = N - \sum_{i=1}^{4} N_i$. Denote the system state at each realtime beacon interval by $S = \big(N_1, N_2, N_3, N_4\big)$. Let $\mathcal{S}$ be the set of feasible system states in any beacon interval, $\mathcal{S} : \{s = (n_1, n_2, n_3, n_4) | n_i \geq 0, \sum_{i=1}^{4} n_i \leq N\}$. When the system is in state $s = \big(n_1, n_2, n_3, n_4\big)$, the number of nodes with realtime traffic that are scheduled for transmission at that beacon interval is

$$m(s) = \min(n_2 + n_3 + n_4, M) \tag{3.4}$$

and the corresponding durations of *contention-free period* $T_{cf}(s)$ and *contention period* $T_{cp}(s)$ are

$$T_{cf}(s) = m(s)\tau_v,\ T_{cp}(s) = T_{rf} - T_{cf}(s). \tag{3.5}$$

For a given number of realtime calls (no new call arrival and no call departures), since the duration of *on* and off periods are exponentially distributed, given the current system state, all state transitions during the current beacon interval are independent of the system states in the previous beacon intervals. As the system state in the next beacon interval only depends on the system state in the current beacon interval and the number of transitions

during the current beacon interval, the system state sequence satisfies the Markov property and is stationary. In the following subsection, we calculate the steady state probability of system states.

3.3.2 Steady state probability of system states

Let random vector $X = (X_1, ..., X_8)$ denote the number of transitions during a realtime beacon interval, where X_i, $i \in \{1, ..., 8\}$, is the number of nodes that have state transition i during the beacon interval. Let $\mathcal{X}(s, s')$ be the set of number of transitions $(x_1, ..., x_8)$ during a beacon interval that change the system state from $s = (n_1, n_2, n_3, n_4)$ to $s' = (n_1', n_2', n_3', n_4')$. We have

$$\mathcal{X}(s, s') = \left\{ (x_1, ..., x_8) \left| \begin{array}{l} x_8 - x_7 - x_4 = n_1' - n_1; \\ x_4 - x_5 + x_6 = n_2' - n_2; \\ x_5 = n_3'; \\ x_1 + x_2 = n_3; \\ x_2 - x_3 - x_6 = n_4' - n_4. \end{array} \right. \right\}. \tag{3.6}$$

The transition probability from system state s to system state s' after one beacon interval is

$$P_{s,s'} = \sum_{\mathcal{X}(s,s')} P_{X_1 ... X_8|S}(x_1, ..., x_8|s) \tag{3.7}$$

where $P_{X_1 ... X_8|S}(x_1, ..., x_8|s)$ is the conditional probability mass function (pmf) of the state transition numbers during a beacon interval, given the initial system state s. Using conditional probability,

$$P_{X_1 ... X_8|S}(x_1, ..., x_8|s) = P_{X_1 X_2 X_3|S}(x_1, x_2, x_3|s) P_{X_4|X_1 X_2 X_3 S}(x_4|x_1, x_2, x_3, s) \\ P_{X_5 ... X_8|X_1 ... X_4 S}(x_5, ..., x_8|x_1, ..., x_4, s). \tag{3.8}$$

In the right side of (3.8), the first term denotes the conditional pmf of state transition number (transitions 1, 2, 3) at the *contention-free period* given system state s. To calculate this term, we need to find the pmf of the node numbers in states 3 and 4 that are scheduled for transmission in the *contention-free period*. The second term in the right side of (3.8) is the conditional pmf of the state transition number (transition 4) at the *contention period* given system state s. This can be obtained by analysing the CSMA MAC protocol to find the pmf of the number of successful transmission requests in the *contention period*. The last term in the right side of (3.8) denotes the conditional pmf of the state transition numbers (transitions 5, 6, 7, and 8) due to status change of realtime calls given system state s, which can be found based on the distribution of *on* and off modes of realtime calls. We derive analytical expressions for these terms in Appendix A.

Finally, the steady state probability of the system states, $\pi(s), s \in \mathcal{S}$, can be found based on the transition probability between states given in (3.7) using the balance equations.

3.3.3 Minimum frame duration to guarantee the required QoS of realtime traffic

When the number of nodes in the *contention-free period* is more than M and/or when nodes do not get a chance to successfully submit a transmission request in the *contention period*, packet loss occurs. Although nodes in state 4 may be scheduled for transmission, they do not have a packet for transmission. Therefore, when the system is in state $s = (n_1, n_2, n_3, n_4)$, the average number of transmitted packets in one realtime beacon interval is

$$\bar{r}(s) = \min(n_2 + n_3 + n_4, M)\frac{n_2 + n_3}{n_2 + n_3 + n_4}\rho. \tag{3.9}$$

Nodes in states 1 and 2 are in the *on* mode. Thus, the number of packets generated in one realtime beacon interval in the system state $s = (n_1, n_2, n_3, n_4)$ is

$$\bar{g}(s) = (n_1 + n_2)\rho. \tag{3.10}$$

Using (3.9) and (3.10), the packet loss rate due to MAC contention can be calculated as

$$\delta_{mac} = 1 - \sum_{s \in \mathcal{S}} \pi(s) \frac{\bar{r}(s)}{\bar{g}(s)}. \tag{3.11}$$

To meet the required packet loss rate, the minimum frame time for realtime traffic T^*_{rf} can be calculated by solving the following optimization problem,

$$\begin{aligned} T^*_{rf} \quad &= \min T_{rf} \\ &\text{s.t. } \delta_{mac} \leq \delta^*_{mac}. \end{aligned} \tag{3.12}$$

Since the packet loss rate due to MAC contention (δ_{mac}) is a decreasing function of the dedicated time (T_{rf}) to realtime traffic in each realtime beacon interval, the optimization problem (3.12) can be solved using the binary search algorithm.

3.4 Numerical Results and Discussions

Similar to the IEEE standard [10], realtime and non-realtime packets are transmitted with the data channel rate and all control packets (including ATIM, ATIM-ACK, RTS, ACK, and the *scheduling packet*) are transmitted using the basic channel rate. The destination node for each source node is selected randomly from the rest nodes. We use 2.25W, 1.25W, 1.25W and .075W as values of power consumption by each radio interface in the transmit, receive, idle, and sleep states respectively, based on the data of *Cisco Aironet Wireless LAN Adapters 350 series* [9]. Simulations are performed using MATLAB for 100 seconds of the channel time, with error-free transmissions.

3.4.1 Non-realtime traffic

In this subsection, we consider only non-realtime traffic in the network and compare the throughput, energy consumption, and delay performance of our proposed scheme with the IEEE 802.11 DCF scheme without power saving (hereafter referred to as DCF-W) and in power saving mode (PSM).

The beacon interval T_{nb} for both proposed scheme and PSM is set to $100ms$, which is the value specified for the PSM [10]. Since the PSM performance significantly depends on the ATIM window size, we vary the ATIM window size from $2ms$ to $10ms$, which includes 4ms as specified in the standard [10]. In the proposed scheme, the *contention period* duration varies, depending on the *contention-free period*. However, a minimum of $2ms$ is dedicated to the *contention period* in each beacon interval to ensure that contending nodes can submit a request for the *demand table* even when the network is overloaded. Other simulation parameters are given in Table 3.1.

We compare the proposed scheme, DCF-W, and PSM as the network traffic load changes. Packets are generated at each node according to a Poisson process. The network load is defined as the aggregate packet generation rate in all the nodes. Three metrics are used as performance measures to compare the MAC schemes:

1. *Aggregate throughput,* which is defined as the total number of transmitted packets per second in the network;

2. *Energy consumption,* which is the average energy consumption per packet, and is calculated as the ratio of total energy consumption to the total number of transmitted packets in the network;

Table 3.1: Simulation Parameters

Parameter	Value
Slot time	20 μs
SIFS	10 μs
DIFS	50 μs
W	32
$CW_{\min}$	15
$CW_{\max}$	1023
PHY preamble	192 μs
RTS size	160 bits
CTS size	112 bits
ACK size	112 bits
ATIM size	224 bits]
ATIM-ACK size	112 bits
Scheduling size for one transmission	160 bits
Non-Realtime Beacon interval	100 ms
Realtime Beacon interval	50 ms
Data rate	11 Mbps
Basic rate	2 Mbps
t_{on}	1.8 seconds
t_{off}	1.2 seconds
Voice codec	G.711 (64Kbps)
Voice packet inter arrival time	20 ms
Voice packet payload	160 bytes
User datagram protocol (UDP) overhead	8 bytes
Realtime transport protocol (RTP) overhead	12 bytes
IP overhead	20 bytes
MAC overhead	20 bytes
Maximum voice packet delay	50 ms
Voice packet loss rate threshold	1%
Data packet size	1024 bytes

3. *Average packet delay,* which is the packet delay averaged over all the data packets transmitted in the network with packet delay being the duration from the instant that a packet is ready for transmission to the instant that the packet is successfully received at the receiver.

Similar metrics are also used as performance measures in [13, 48, 50, 60, 77]. Figures 3.4-3.6 show the aggregate throughput, energy consumption, and average packet delay of the proposed scheme, DCF-W and PSM versus the network load when there are $K = 10$, 20, 50 nodes in the network. It is observed that the PSM performance depends on the ATIM window size. The PSM throughput is less sensitive to the ATIM window size when the network is light-loaded. However, as the traffic load increases, the ATIM window size significantly affects the PSM throughput. Generally, the ATIM window size should be adjusted based on the number of the contending nodes in the network. We consider a PSM scheme whose ATIM window size is dynamically adjusted to achieve the highest throughput (here after referred to as best-PSM), without imposing any overhead on the network. According to Figure 3.4, the ATIM size of best-PSM depends on the node number and is $2ms$, $4ms$ and $8ms$ for $K = 10$, $K = 20$ and $K = 50$ nodes in the network respectively. In each scheme, the maximum achievable throughout decreases as the number of nodes increases, due to higher contention among nodes that causes more collision overhead. The results indicate that, for different network sizes ($K = 10, K = 20$, and $K = 50$ nodes), the proposed scheme provides 18%-23% higher throughput than the best-PSM and 27%-43% higher than the DCF-W.

Energy consumption per transmitted packet using different schemes is shown in Figure 3.5. As the number of nodes increases, the energy consumption per transmitted packet increases in each scheme due to more contention and collision among nodes. Although the total energy consumption in each scheme increases as the network load increases,

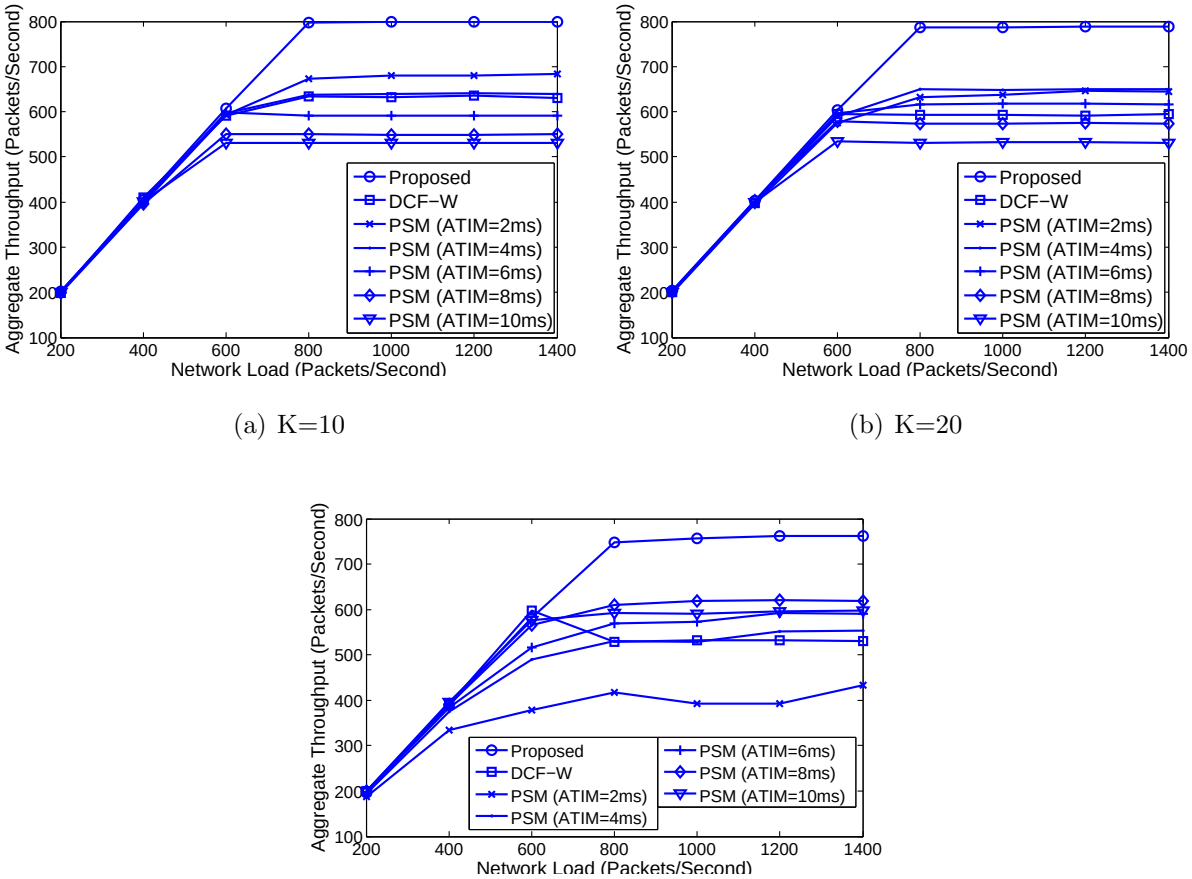

(a) K=10

(b) K=20

(c) K=50

Figure 3.4: Aggregate throughput of the proposed scheme, PSM, and DCF-W

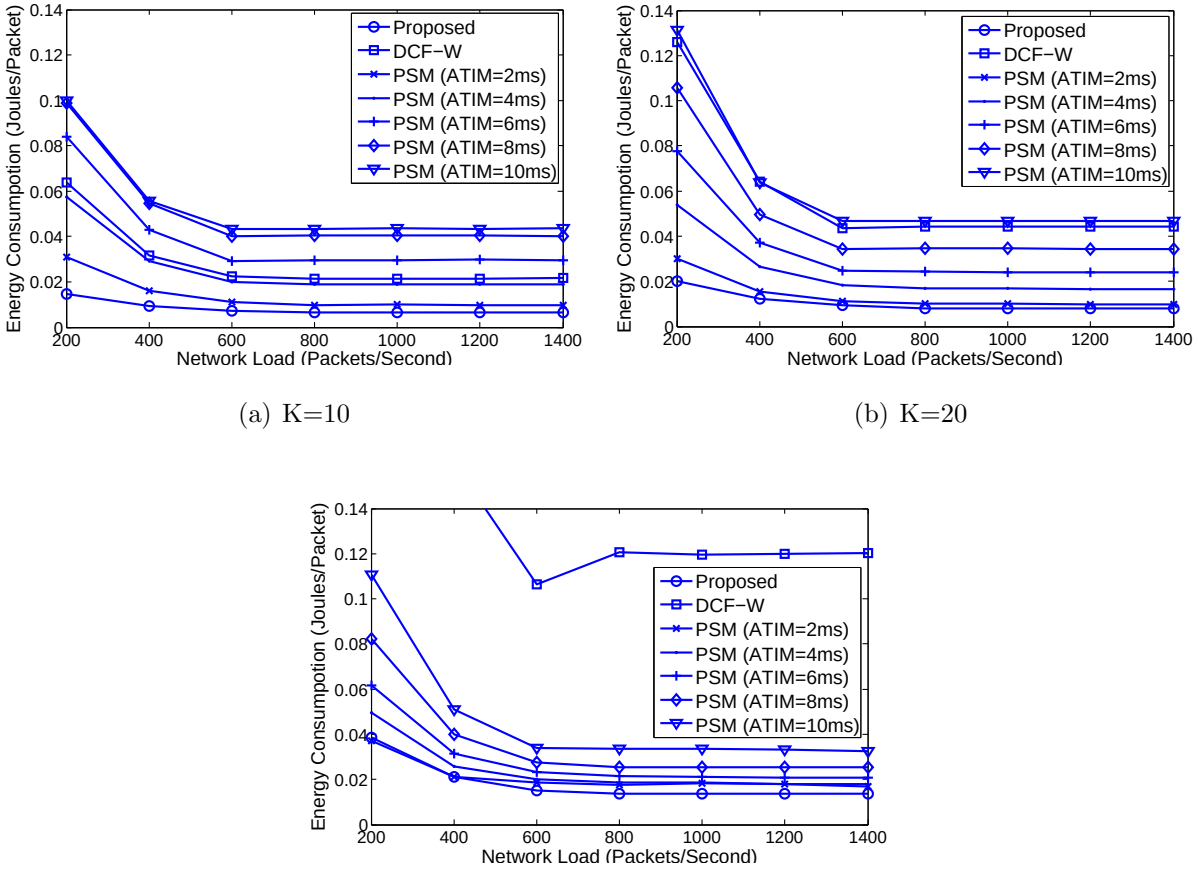

(a) K=10

(b) K=20

(c) K=50

Figure 3.5: Energy consumption per packet of the proposed scheme, PSM, and DCF-W

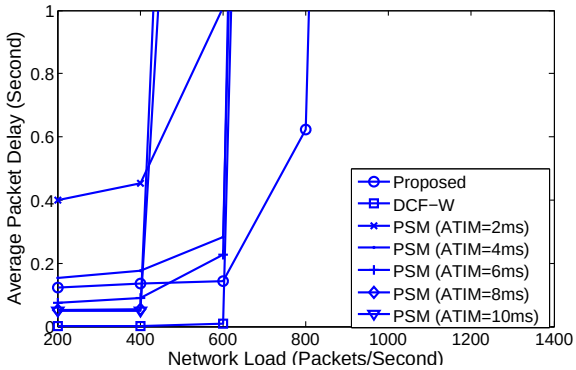

(a) K=10

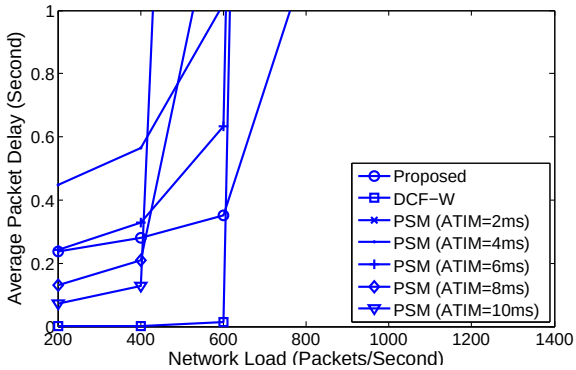

(b) K=20

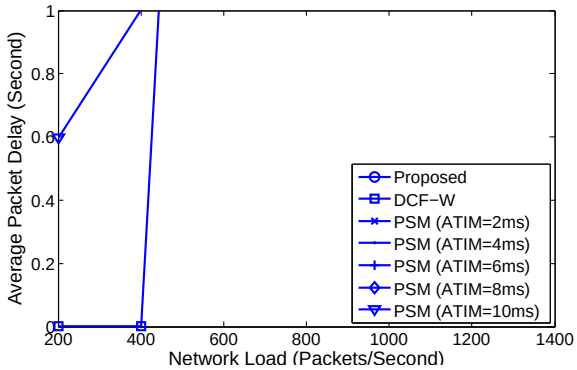

(c) K=50

Figure 3.6: Average packet transmission delay of the proposed scheme, PSM, and DCF-W

Table 3.2: EDCA-W Parameters

Access category	CWmin	CWmax	AIFSN	MAX TXOP
Realtime (Voice)	3	7	2	1.504 ms
Non-realtime (Best Effort)	15	1023	3	0

all the schemes have the highest energy consumption per packet when the network load is the lowest. It is observed that the proposed scheme has a significantly lower energy consumption per transmitted packet, which is 48%-55% of the best-PSM.

Figure 3.6 demonstrates that the proposed scheme and PSM have longer average packet delays than the DCF-W, as expected. When the number of nodes increases and/or the network load increases, the average packet delay increases in each scheme. However, the proposed scheme provides a significantly lower average packet transmission delay as compared to the best-PSM.

3.4.2 Realtime traffic

In this subsection, we calculate the minimum required frame duration that should be assigned to the realtime traffic to guarantee the required QoS, based on the analytical model presented in Section IV, and compare it with the simulation results. Consider the realtime traffic generated by voice codec G.711 (64 Kbps) at the nodes. Table 4.1 lists the voice traffic parameters. Since a maximum end-to-end delay of $150ms$ is recommended in [78] for VoIP and video conferencing, we restrict the maximum tolerable delay of each voice packet to $50ms$ in the wireless network. We set the beacon interval duration $T_{rb} = 50ms$, and the maximum tolerable packet error rate of each voice call $\delta^*_{mac} = 0.01$. Other parameters are

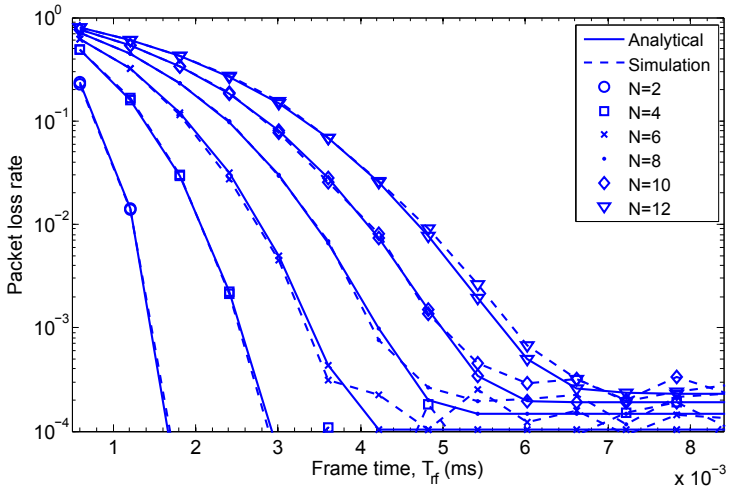

Figure 3.7: Packet loss rate of realtime traffic

given in Table 3.1.

Figure 3.7 shows the packet loss rate versus the frame duration assigned to realtime traffic for different numbers of realtime nodes based on the analytical model and simulation. It is evident that there is a good match between the analytical and simulation results. The packet loss rate decreases almost exponentially as the frame duration increases. Figure 3.8 shows the minimum required frame time (T^*_{rf}) to guarantee the required packet loss rate, as the number of nodes with realtime traffic changes. The required channel time per realtime node (for constant average traffic load per node) decreases as the number of realtime nodes increases, due to a higher multiplexing gain.

3.4.3 Mixed realtime and non-realtime traffic

Consider both realtime (voice) and non-realtime traffic in the network. We compare the performance of our proposed protocol with the Enhanced Distributed Channel Access

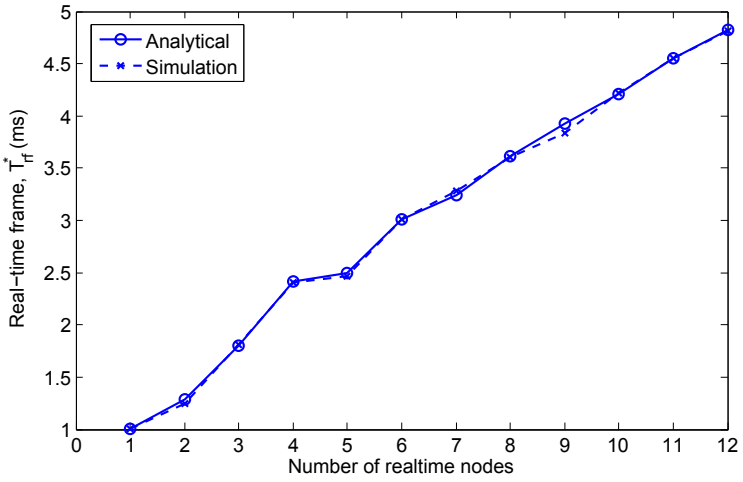

Figure 3.8: Minimum required realtime frame duration to guarantee packet loss rate no larger than 1%

without power saving mode (here after EDCA-W) which is defined in the IEEE 802.11e standard to provide the QoS guarantee for realtime traffic. We use default EDCA-W parameters as specified in the standard, given in Table 4.1. The network traffic load is evenly distributed between nodes with non-realtime traffic. Figure 3.9(a) shows the aggregate throughput of non-realtime traffic versus the network traffic load as the number of node with realtime traffic changes, with $K = 20$. It is observed that the aggregate throughput of nodes with non-realtime traffic decreases as the number of nodes with realtime traffic increases in both proposed scheme and EDCA-W scheme. The packet loss rate of realtime traffic is illustrated in Figure 3.9(b). Figure 3.9(c) shows the total power consumption of both realtime and non-realtime traffic. The results show that both proposed scheme and EDCA-W guarantee the required packet loss rate of realtime traffic; However, the proposed scheme has much lower power consumption and provides significantly higher throughput for non-realtime traffic.

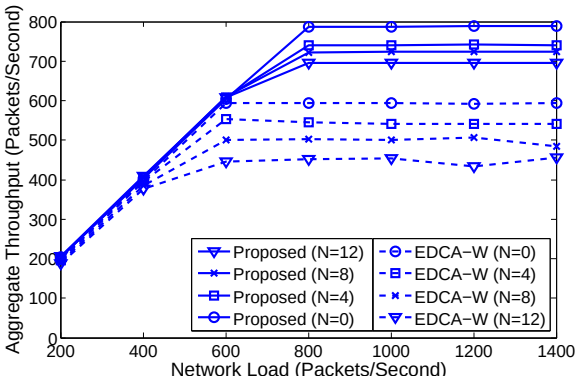

(a) Aggregate throughput of none-realtime nodes

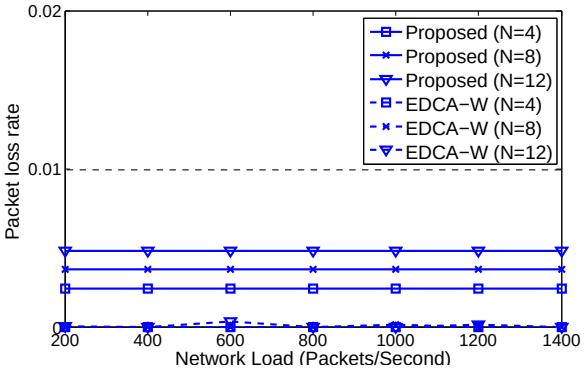

(b) Packet loss rate at each real time node

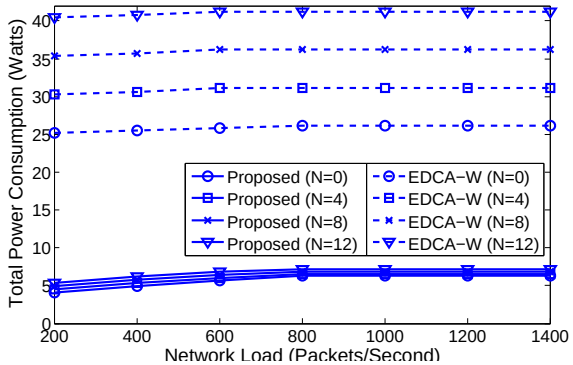

(c) Total power consumption

Figure 3.9: Performance of the proposed scheme, and EDCA-W for mixed realtime and non-realtime traffic (K=20 nodes)

3.5 Summary

In this chapter, we present a novel distributed MAC protocol for fully-connected wireless networks. A temporary coordinator node (*head node*) regulates transmissions dynamically based on the network traffic load condition. In the proposed protocol, nodes contend once to transmit a batch of packets, after that they will be assigned contention-free times for data transmission. Contention-free data transmission reduces contention overhead and allows nodes to put their radio interfaces into sleep mode when they are not scheduled to transmit or receive a packet. We present an analytical model to evaluate the performance of proposed scheme that enables us to determine the minimum required channel time to realtime traffic. We compare the proposed scheme with the DCF scheme of IEEE 802.11 without power saving (DCF-W), the EDCA scheme of IEEE 802.11e without power saving (EDCA-W), and a dynamic version of IEEE 802.11 power saving mechanism, where the ATIM window size is adjusted dynamically based on the network traffic load conditions to provide highest throughput (best-PSM). The performance measures include aggregate throughput and average packet delay of non-realtime traffic, packet loss rate of realtime traffic, and the total energy consumption in the network. Numerical results show that the proposed scheme guarantees the QoS requirement of realtime traffic, significantly reduces the energy consumption, and considerably enhances the network performance in terms of throughput and packet transmission delay in comparison with the existing protocols. In comparison with the best-PSM, the newly proposed scheme provides around 20% higher throughput, 50% less energy consumption, and reduces the packet transmission delay by 50%.

Chapter 4

MAC for Exploiting Spatial Spectrum Reuse

In this chapter, we propose a novel medium access mechanism for a wireless ad hoc network with the consideration of spatial spectrum reuse. The proposed scheme combines the opportunistic spectrum access feature of WiFi networks and the deterministic transmission feature of cellular network to efficiently utilize shared spectrum and minimize energy consumption. A set of coordinators distributed in the network area are chosen to dynamically coordinate contention-free time slots for all data transmissions/receptions based on transmission requests from source nodes. Each coordinator periodically broadcasts a scheduling packet to schedule all transmissions/receptions in its proximity. For each scheduled transmission, sufficient space area around the receiver node is reserved to avoid transmission collision and enhance spatial spectrum reuse. A coordinator collects nodes' transmission requests and overhears the scheduling packets of its neighboring coordinators. Accordingly, each coordinator schedules a transmission only if the transmission of the source node does

not interfere with other scheduled receptions and the other scheduled transmissions do not interfere with the reception at the destination. Dynamic assignment of the shared radio spectrum and effective spatial reuse increase spectrum efficiency. Moreover, a deterministic transmission/reception time warrants nodes to put their radio interface into the sleep mode when they are neither transmitting nor receiving a packet, which reduces energy consumption. Comparing with existing schemes, the proposed MAC provides significantly higher throughput and greatly reduces node energy consumption.

The rest of this chapter is organized as follows: The system model is presented in Section 4.1. We describe the proposed MAC mechanism in Section 4.2. Simulation results are presented in Section 4.3 to evaluate the performance of proposed MAC scheme in comparison with existing schemes. Section 4.4 summarizes this chapter.

4.1 System Model

Consider a single-channel wireless ad hoc network with coverage area A. We focus on single-hop transmissions as, at the MAC layer, each node communicates with one or more of its one-hop neighboring nodes. Nodes are randomly distributed over the network coverage area and the destination of each node is randomly selected from the rest nodes within distance $d_{\max}$. Let $l \in \{1, 2, ..., L\}$ denote a single-hop link in the network, where L is the number of links in the network. The source and destination nodes of link l are represented by S_l and D_l, respectively. We denote the distance between the source node of link l and the destination node of link k by d_{lk}. The channel gain between source node of link l and the destination node of link k is $h_{lk} = cd_{lk}^{-\alpha}$, where c is a constant and α is the path loss

exponent[1]. Let $\bar{\boldsymbol{\gamma}} = (\gamma_1, \gamma_2, ..., \gamma_L)$ denote the transmission power vector, where γ_l denotes the transmission power level of source node of link l. Let $\bar{\boldsymbol{u}} = (u_1, u_2, ..., u_L)$ denote the transmission vector, where $u_l = 1$ denotes that link l is scheduled for transmission and $u_l = 0$ otherwise. Thus, SINR at the destination of link l is given by

$$\eta_l = \frac{u_l \gamma_l h_{ll}}{N_0 + \sum_{k \neq l} u_k \gamma_k h_{kl}} \tag{4.1}$$

where N_0 is background noise power and $\sum_{k \neq l} u_k \gamma_k h_{kl} \triangleq I_l$ is the amount of interference at the destination of link l. All control/scheduling packets are transmitted at power level γ_s at rate R_s bps and all data packets are transmitted at power level γ_d at rate R_d bps. The corresponding minimum required SINR at a receiver node to successfully receive control/scheduling and data packets are denoted by η_s and η_d respectively.

4.2 Medium Access Control

In order to efficiently utilize the radio channel and minimize energy consumption in a wireless ad hoc network, we use the following main strategies:

1. Dynamic coordination of access to the shared medium based on instantaneous traffic load by a set of coordinators distributed in the network area;

2. Preventing transmission collisions and minimizing idle listening power consumption by periodic assignment of deterministic time slots for data transmissions/receptions;

[1]We assume that Physical-Layer coding deals with channel fading. Considering channel fading information in the MAC-Layer can be beneficial for effective scheduling of transmissions, however, acquiring channel fading state information requires additional signaling overhead.

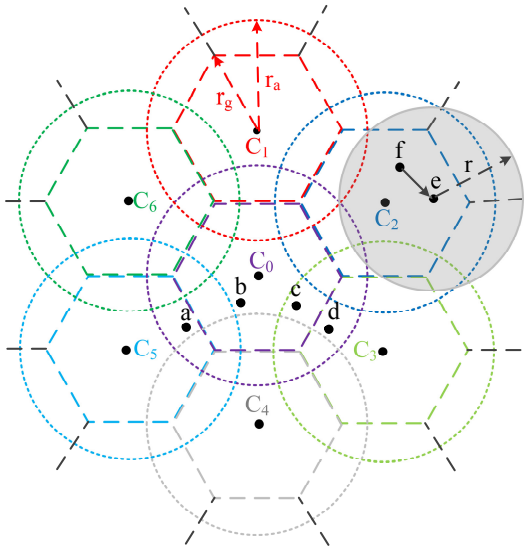

Figure 4.1: Partitioning the network area into hexagonal cells, where C_i, $i \in \{1, 2, ..., m\}$, denotes the coordinator of cell i, the dotted circle centred at C_i shows the area that C_i broadcasts all scheduled transmissions/receptions, and the shaded area shows the space reserved for transmission from node f to node e.

3. Effective spatial channel reuse by space-reservation for scheduled transmissions/receptions and by exchanging scheduling information among adjacent coordinators.

The network coverage area is partitioned into hexagonal cells, as shown in Figure 4.1. The distance between the center and a vertex of a cell is denoted by r_g, which is set such that $r_g \geq d_{\max}$. Therefore, the source and destination nodes of each single-hop link are either in one cell or adjacent cells. A node at the center of each cell coordinates all the transmissions/receptions for nodes inside the cell. We assume that coordinators have higher energy capacity and do not move frequently (e.g., APs). Thus, the network planning does not need to be updated frequently.

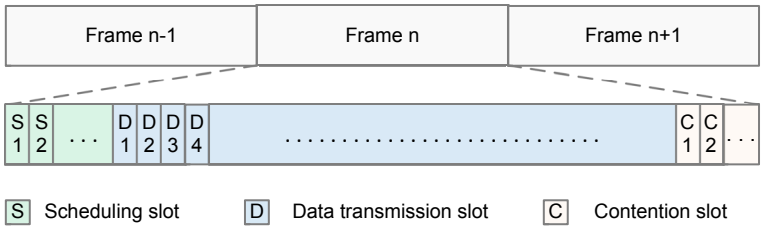

Figure 4.2: Structure of one frame of the proposed scheme.

All nodes are synchronized in time, and time is partitioned into frames. Each frame consists of three types of time slots, i.e., *scheduling slots*, *contention-free slots*, and *contention slots*. In scheduling time slots, located at the beginning of each frame, coordinators transmit scheduling packets to coordinate transmissions of the current frame. The scheduling packet of a coordinator should be received by all nodes in the cell and adjacent coordinators. Data packet transmissions take place in contention-free time slots, as scheduled by coordinators. A source node scheduled for transmission in contention-free slots can notify the cell coordinator of its transmission request for the next frame by including information in the header of one data packet. During contention slots, source nodes that want to initiate a new transmission contend with each other to send a transmission request to the cell coordinator. Figure 4.2 shows the structure of a frame[2]. In the following, we describe transmission policy in each time slot, and then the detail operation of the MAC protocol.

[2]Although we consider a single-channel wireless network, the proposed MAC scheme can be extended to a multi-channel wireless network. For instance, the scheduling and contention slots can be on a main channel and the rest channels can be utilized as contention-free transmissions that are scheduled on the main channel.

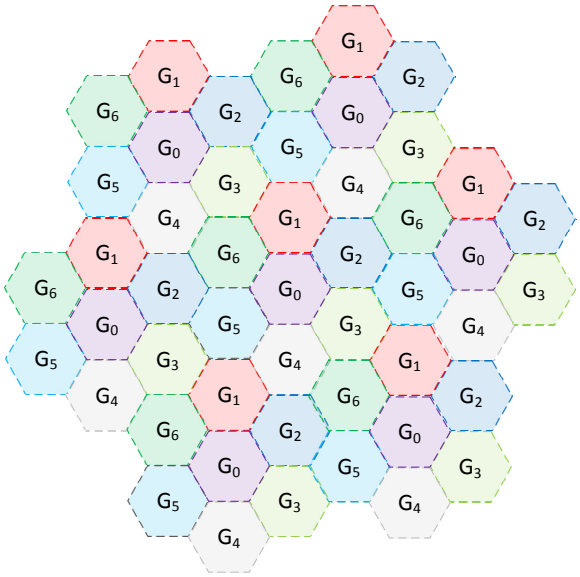

(a)

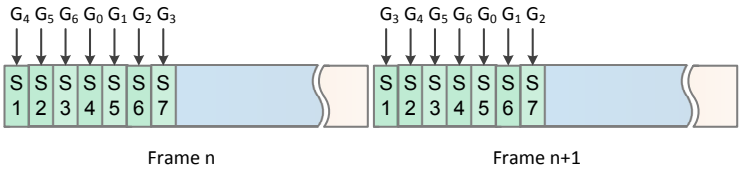

(b)

Figure 4.3: Assignment of scheduling time slots to coordinators, in which a scheduling time slot is assigned to all the coordinators of cells of a same group/color.

4.2.1 Transmission policies in the different time slots

Scheduling slots: Scheduling time slots are assigned to coordinators such that a scheduling time slot, assigned to a coordinator, is not assigned to any other two-hop neighboring coordinator. Let J denote the number of scheduling slots in a frame and $j \in \{1, 2, .., J\}$, denote slot index. Let $G_i, i \in \{0, 1, 2, ..., J-1\}$ denote the set of coordinators that can be assigned same scheduling time slot. Similar to frequency reuse in cellular networks, with J $(= 7)$ scheduling time slots, as illustrated in Figure 4.3, every coordinator can acquire a scheduling time slot that is not assigned to any other two-hop neighboring coordinator node. To ensure fair channel access for nodes in different cells, we change transmission order of coordinators in each frame as illustrated in Figure 4.3(b). In frame n, coordinators G_i are assigned the j^*th scheduling time slot where $j^* = (n \mod i+1)+1$. Moreover, the size (r_g) of cells, transmission power level (γ_s) for scheduling packets, and data transmission rate (R_s) of scheduling packets are selected such that a scheduling packet is received by all nodes inside the cell and all adjacent coordinators (with SINR $\geq \eta_s$).

Contention-free slots: Data packet transmissions are scheduled in contention-free time slots. For each scheduled transmission, no other node should be scheduled for transmission in a reserved area around the receiver to guarantee required SINR at the destination. The shaded area in Figure 4.1 shows the reserved space for transmission from node f to node e, where no other node is scheduled for transmission in the area to guarantee the required SINR at node e. The reserved area for a scheduled link can be parts of several adjacent cells (as in Figure 4.1), which is determined by exchanging real-time scheduling information among adjacent coordinators. The proposed space-reservation mechanism is to provide effective spatial spectrum reuse to improve spectrum efficiency while avoiding transmission collisions. In addition, for each scheduled source node in the current frame, the space

around the cell coordinator is reserved during one contention-free slot to enure that the cell coordinator receives the transmission request of source node (for the next frame) that is included in the header of a data packet. When a link is scheduled for transmission, all other nodes in the reserved area around the receiver (and around coordinators) are denoted as interfering nodes and should not be scheduled for transmission. Let $r(d)$ denote the radius of the circular reserved area centered at the receiver node when the distance between the transmitter and receiver is d. The amount of interference imposed on the receiver due to transmissions outside the reserved area has an upper bound given by

$$I(d) \leq \hat{I}(d) \triangleq c' \frac{c\gamma_d}{r(d)^\alpha}, \tag{4.2}$$

where c' is a constant and depends on the node density and network traffic load. Therefore, the received SINR at the destination can be represented by

$$\eta \geq \frac{\frac{c\gamma_d}{d^\alpha}}{N_0 + \hat{I}(d)}. \tag{4.3}$$

Using (4.2) and (4.3), the minimum radius of the reserved circular area centred at the receiver to guarantee $\eta \geq \eta_d$ can be calculated as

$$r(d) = \Big(\frac{c' c\gamma_d}{\frac{c\gamma_d}{d^\alpha \eta_d} - N_0} \Big)^{1/\alpha}. \tag{4.4}$$

Under the assumption $\hat{I}(d) \gg N_0$,

$$r(d) \approx (c'\eta_d)^{1/\alpha} d. \tag{4.5}$$

According to (4.4) and (4.5), as c' increases, the reserved circular area increases, which decreases the probability of packet collisions. However, spectrum reuse is decreased as a result of the larger reserved area per transmission.

Contention slots: Each coordinator marks a few time slots as contention slots, in which nodes inside the cell (that are not currently scheduled for transmission) can send a request

to initiate a new transmission. In the contention slots, nodes contend with each other using a CSMA MAC scheme to send a transmission request to their cell coordinators. Adjacent coordinators mark the same idle time slot(s) as contention slots. Coordinators dynamically adjust the number of contention slots and contention window size based on the traffic load condition. In Appendix, we present a mathematical model to calculate the number of successful transmission requests in the contention slots and the average delay to initiate a new transmission. Using the analytical model, we propose a mechanism to dynamically adjust the contention window size and the number of contention slots based to the network load and the required delay to initiate a new transmission.

4.2.2 Operation of the MAC protocol

A coordinator node stays awake during the following time slots in a frame:

1. Scheduling slots – to transmit a scheduling packet and to receive the scheduling packets transmitted by adjacent coordinators;

2. One of the contention-free slot(s) scheduled for the transmission of each source inside the cell – to receive the information of transmission request for the next frame, included in the header of a packet transmitted by the source node scheduled for transmission;

3. Contention slots – to receive transmission requests from nodes inside the cell that want to initiate a new transmission.

Each coordinator has the location information of all nodes inside the cell and the nodes whose transmission/reception is advertised by adjacent coordinators[3]. A coordinator maintains two tables:

1. *Demand table*, which contains the transmission requests of source nodes (i.e., source ID, destination ID, and the number of packets ready for transmission), and is updated/generated based on the nodes' transmission requests in previous frames and scheduling packets of adjacent coordinators;

2. *Scheduling table*, which contains the information of scheduled transmissions (and correspondingly the reserved space for each scheduled transmission) for the current frame, and is updated based on scheduling packets of coordinator and scheduling packets broadcasted by adjacent coordinators.

Based on the demand table and scheduling table, each coordinator transmits a scheduling packet at its assigned scheduling time slot in each frame. The scheduling packet contains the following information:

1. the schedule of transmissions (scheduled by the coordinator and/or adjacent coordinators) within distance r_a of the coordinator, where $r_a \in [r_g, 2r_g]$;

2. cancelation of scheduled transmissions by adjacent coordinators within distance r_a of the coordinator that interfere with transmissions scheduled by other adjacent coordinators;

[3]We assume that node location information is updated at coordinators as they move in the network. A higher node mobility imposes higher signaling overhead due to more frequent signaling required to update location information at the coordinators.

3. announcement of the contention slots and contention window size for the current frame.

Figure 4.4 shows the area centred at a coordinator in which the coordinator obtains the information of scheduled transmissions by overhearing scheduling packets of adjacent coordinators. A coordinator will schedule a transmission from a source to a destination in a contention-free time slot only when neither an interfering node to the source is scheduled for reception nor an interfering node to the destination is scheduled for transmission. Also, each coordinator will cancel scheduled transmissions by adjacent coordinators within range r_a that interfere with other existing scheduled transmissions. This mechanism ensures that a scheduled link for transmission by a coordinator does not interfere with transmissions of nodes within range r_a of the coordinator or adjacent coordinators. In Figure 4.1, a scheduled link for transmission by coordinator C_0 does not interfere with any other scheduled transmission in area $A_0 \cup A_1 \cup ....A_6$, where $A_i, i \in \{0, 1, ...6\}$ denote the area within range r_a from coordinator C_i. To illustrate, consider frame n where scheduling time slots are assigned as in Figure 4.3(b) and $C_i \in G_i$, $i \in \{0, 1, 2, ..., 6\}$. A transmission scheduled by coordinator C_0 will not interfere with any scheduled transmission in area A_4, A_5, A_6, and A_0, because coordinator C_0 receives the scheduling packets of C_4, C_5, and C_6 before transmitting its scheduling packet and it does not schedule an interfering transmission. Also, coordinators C_1, C_2, and C_3, which overhear the scheduled transmission from coordinator C_0 before transmitting their own scheduling packets, will not schedule an interfering transmission and will cancel any interring transmission scheduled by their adjacent coordinators in area A_1, A_2, and A_3 respectively.

When both source and destination nodes are in one cell, the cell coordinator finds time slot(s) to schedule contention-free transmission and broadcast the scheduled transmission in its scheduling time slot of current frame. However, when the source and destination

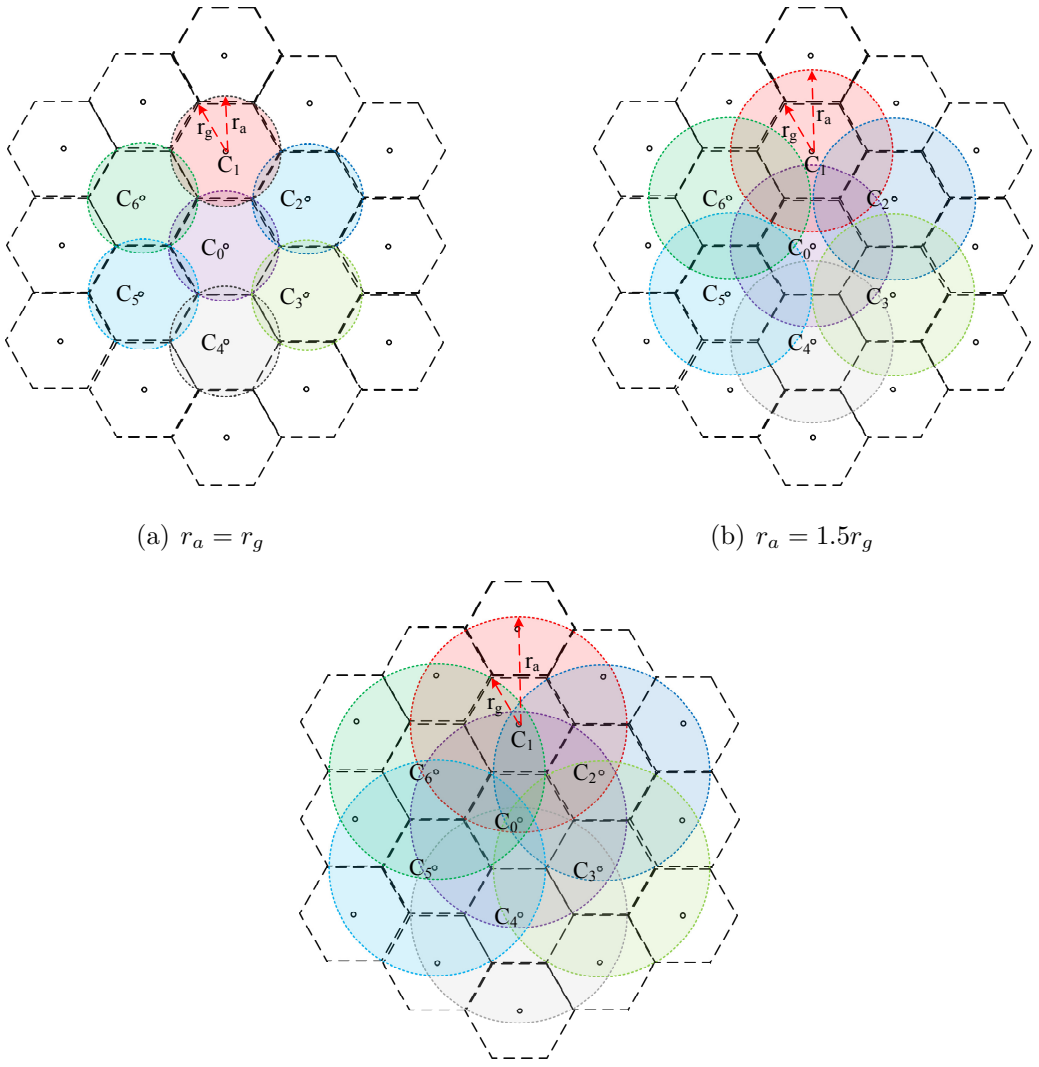

(a) $r_a = r_g$

(b) $r_a = 1.5r_g$

(c) $r_a = 2r_g$

Figure 4.4: The area centred at coordinator C_0 in which the coordinator obtains the information of scheduled transmissions by overhearing scheduling packets of adjacent coordinators, where a circular area centred at each coordinator denotes the area that the coordinator broadcasts the information of scheduled transmissions.

nodes are located in adjacent cells, the coordinator of source schedules the transmission in the current frame only if its scheduling time slot is before the scheduling time slot of the coordinator of destination node. Thus, the coordinator of destination node can inform the destination node of the scheduled transmission in its scheduling time slot of the current frame. Otherwise, the coordinator of source node finds time slots to schedule contention-free transmission in the next frame and includes the scheduled transmission in its scheduling packet for the current frame. In the next frame, both the coordinators of source and destination again broadcast the scheduled transmission in their scheduling time slots. Consider the network as illustrated in Figure 4.1, where scheduling time slots are assigned to coordinators as in Figure 4.3(b) and $C_i \in G_i$, $i \in \{0, 1, 2, ..., 6\}$. Coordinator C_0 can schedule transmission between nodes b and c (that are inside the cell) in each frame and inform both source and destination in its scheduling time slot. Also, it can schedule transmission from source node c to destination node d in frame n, in which coordinator C_3 can inform destination node d of the scheduled transmission in the same frame. However, coordinator C_0 will not schedule a transmission from source nodes b to destination node a in frame n, in which the scheduling time slot of coordinator C_5 comes before C_0. In frame n, coordinator C_0 finds time slots to schedule the transmission (from source node b to destination node a) for frame $n + 1$, broadcasts the scheduled transmission at frame $n + 1$, and includes the information in its scheduling time slot of frame n. In frame $n + 1$, both coordinators C_0 and C_5 broadcast the scheduled transmissions in their scheduling time slots.

Figures 4.6 and 4.5 illustrate the operations of a coordinator node and a non-coordinator node in each time slot. Every non-coordinator node in the network stays awake during the scheduling time slot of its cell coordinator to receive the information of scheduled transmissions (in the contention-free slots) and contention slots in the current frame. A

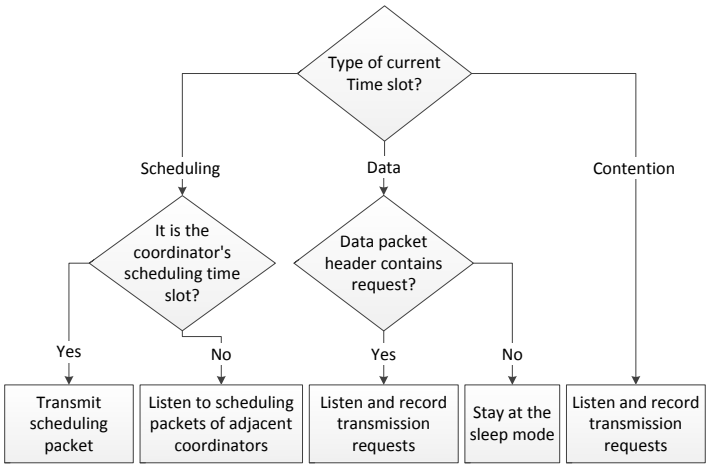

Figure 4.5: The flowchart operation of a non-coordinator node in each time slot.

node scheduled for transmission will also stay awake during the scheduling time slots of the adjacent coordinators within distance r_a from the node to receive cancelation information of transmission (from adjacent coordinators). In Figure 4.3(b), nodes a and b stay awake during scheduling time slot of coordinator C_0 in every time slot. Also, node b stays awake during scheduling time slot of C_5 only if it is scheduled for transmission in the current frame. The source and destination nodes wake up at the assigned contention-free slots to perform transmissions as scheduled by cell coordinators. Source nodes will also include their transmission request for next frame in the header of one packet (as determined by cell coordinator). The cell coordinators will use this information to update its demand table for next frame. The source nodes that want to initiate a new transmission wake up at the assigned contention slots and contend with each other using a CSMA MAC scheme to send transmission request to cell coordinators. The coordinator will also record this information to update/generate its demand table for the next frame.

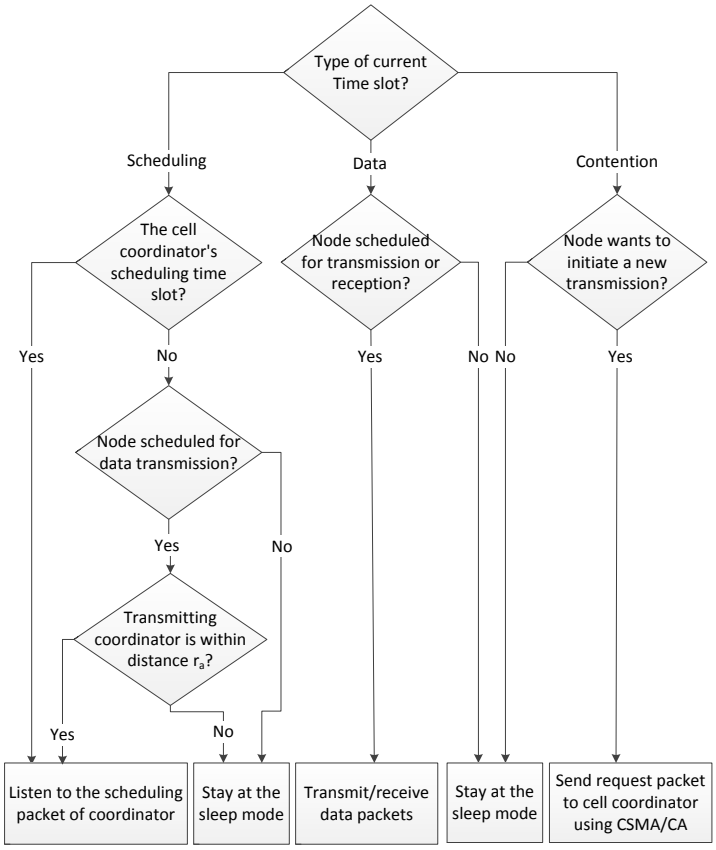

Figure 4.6: The flowchart operation of a coordinator node in each time slot.

4.3 Numerical Results

Consider single-hop transmissions in a wireless ad hoc network with dimensions $6d_{\max} \times 6d_{\max}$. N nodes are randomly distributed over the network coverage area and the destination of each source node is randomly selected from the rest nodes in its proximity at a distance less than $d_{\max}$.

We compare performance of the proposed scheme with the IEEE 802.11 DCF scheme without power saving (hereafter referred to as DCF) and in power saving mode (here-

Table 4.1: Simulation Parameters

Parameter	Value
Mini-slot	20 μs
SIFS	10 μs
PHY preamble	192 μs
RTS size	160 bits
CTS size	112 bits
ACK size	112 bits
ATIM size	224 bits
ATIM-ACK size	112 bits
$CW_{\min}$	15
$CW_{\max}$	1023
Scheduling size for one transmission	200 bits
Scheduling time slot	1ms
Contention-free time slot	1ms
Contention time slot	1ms
Data packet+SIFS+ACK+DIFS duration	1ms
γ_d	100 mW
γ_s	$100 - 180$ mW
c	0.0001
c'	3
α	3.4
Carrier sensing threshold	-80 dBm
$d_{\max}$	20
R_d	18 Mbps, 24 Mbps
R_s	6 Mbps
η_d	9 dB, 17 dB
η_s	6 dB
Beacon interval	100 ms
Frame duration	100 ms
Power consumption in sleep mode	0.075 W
Power consumption in receive mode	1.15 W
Power consumption in transmit mode	$2.25 - 3.15$ W

after referred to as PSM). Packets are generated according to a Poisson process at each source node. All control/scheduling packets (including RTS, ACK, ATIM, ATIM-Back, and scheduling packets) are transmitted at the control/scheduling channel rate (R_s) and all data packets are transmitted at the data channel rate (R_d). The required SINR at the destination for control/sceduling and data packets are $\eta_s = 6$ dB and $\eta_d = 9$ dB, 17 dB respectively [4]. The network load is defined as the aggregate packet generation rate in all the nodes. The following metrics are used as performance measures to compare the MAC schemes:

1. *Throughput*, which is defined as the summation of the numbers of packets transmitted per second from all nodes in network, weighted by the packet transmission distance;

2. *Energy consumption*, which is the average energy consumption per data packet, and is calculated as the ratio of total energy consumption in all nodes (including coordinators in our proposed scheme) to the total number of transmitted data packets in the network;

3. *Collision rate*, which is the ratio of collided data packets to the total number of transmitted data packets in the network.

Similar metrics are used as performance measures in [13, 31–33, 48, 50, 77], and [60]. Each performance metric is calculated as the average performance over 10 different random node distributions in the network area. In our proposed MAC scheme, the network coverage area is partitioned into hexagon cells and a coordinator node is placed at the center of each cell as in Figure 4.1. We set $r_g = hd_{\max}$ and $r_a = qr_g$, where $h \in \{1, 1.5, 2\}$ and

[4]The corresponding control/scheduling and data rates, according to data in [79] for IEEE 802.11g, are $R_s = 6$ Mbps and $R_d = 18, 24$ Mbps respectively.

$q \in \{1, 1.2, ..., 2\}$. The frame duration is 100 ms and the duration of each scheduling, contention-free, and contention slot is 1 ms. Since the performance of DCF in a wireless ad hoc network significantly depends on the carrier sensing range of the nodes, we vary carrier sensing range from $1.8d_{\max}$ to $3.0d_{\max}$. The beacon interval size of PSM is set to 100 ms [10]. The ATIM size varies from 2 ms to 10 ms, which include the 4ms as specified in [10]. Simulations are performed using MATLAB for 20 seconds of the channel time. Other simulation parameters are given in Table 4.1.

Figure 4.7 shows the throughput of IEEE 802.11 DCF MAC scheme versus traffic load as the carrier sensing range changes from $1.8d_{\max}$ to $3.0d_{\max}$. It is observed that the throughput of DCF can be maximized by choosing $r_c = 2.0d_{\max}$ and $r_c = 2.8d_{\max}$ when $\eta_d = 9$ dB and $\eta_d = 17$ dB respectively. Figure 4.8 shows the performance of PSM as the ATIM size changes from 2 ms to 10 ms using carrier sensing range corresponding to the highest throughput of DCF in Figure 4.7. According to Figure 4.8, the optimal choice of ATIM size to maximize the throughput depends on the network traffic load and required SINR at the receiver, η_d. We consider a DCF scheme and a PSM scheme whose carrier sensing range and ATIM size are adjusted for highest throughput, referred to as best-DCF and best-PSM hereafter.

Figures 4.9-4.11 show the throughput, energy consumption and collision rate of the proposed MAC (PMAC), best-DCF, and best-PSM versus traffic load when $\eta_s = 6$ dB and $\eta_d = 9$ dB. From Figure 4.9, the proposed MAC provides 20% higher throughput than best-DCF and best-PSM. The proposed MAC mechanism can achieve high throughput by opportunistically utilizing the spectrum in space and time domains and reducing signaling overhead. Reserving the required space for each transmission and sharing the information of scheduled transmissions among adjacent coordinators facilitate efficient spatial channel reuse, while avoiding transmission collisions, which significantly improve the network

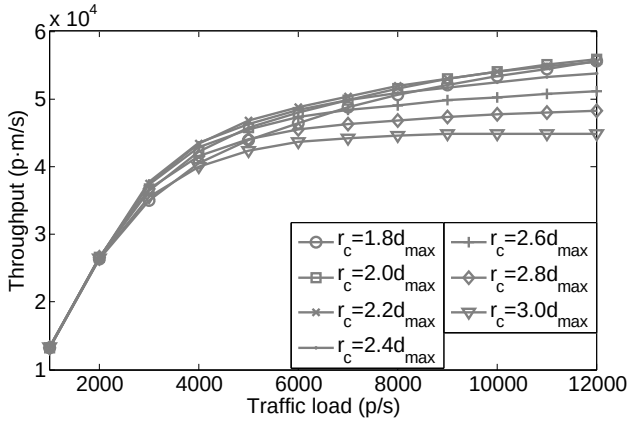

(a) $\eta_d = 9$ dB

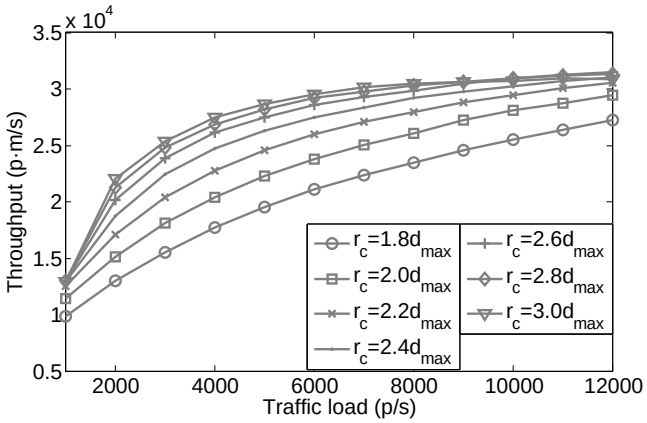

(b) $\eta_d = 17$ dB

Figure 4.7: Throughput of the IEEE 802.11 DCF MAC vs traffic load for different carrier sensing ranges (N=100, $\eta_s = 6$ dB).

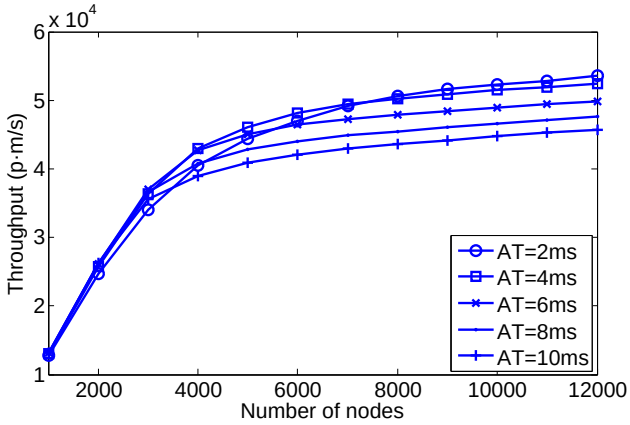

(a) $\eta_d = 9$ dB

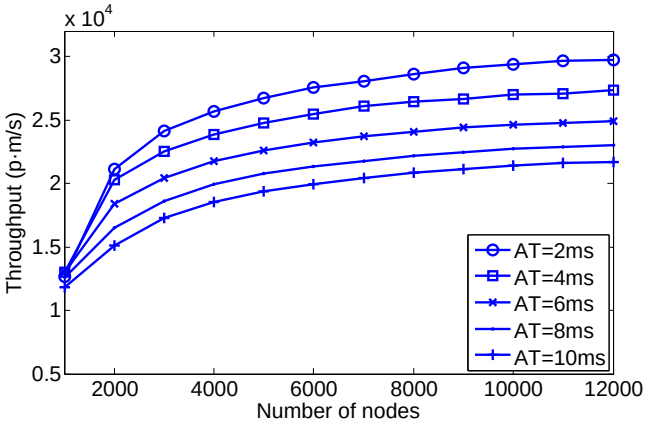

(b) $\eta_d = 17$ dB

Figure 4.8: Throughput of the IEEE 802.11 DCF MAC in power saving mode (PSM) vs traffic load for different ATIM sizes when the carrier sensing range is set for highest throughput (N=100, $\eta_s = 6$ dB).

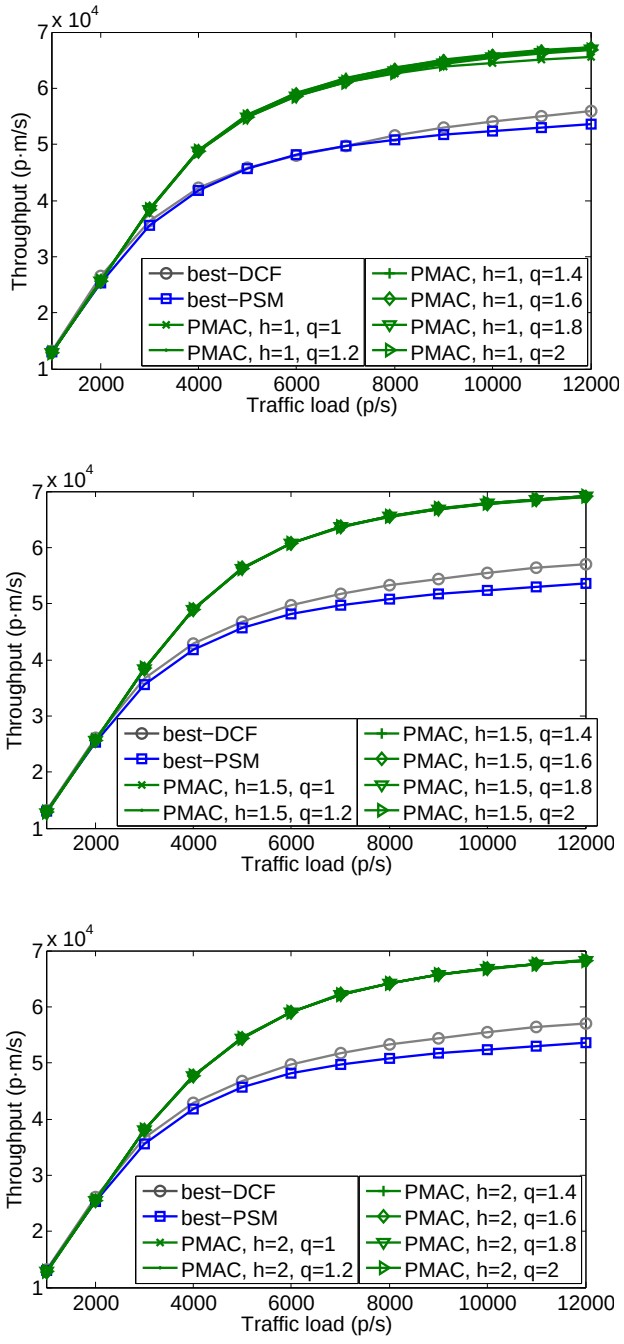

Figure 4.9: Throughput of the proposed MAC (PMAC), best-DCF, and best-PSM (N=100, $\eta_s = 6$ dB and $\eta_d = 9$ dB).

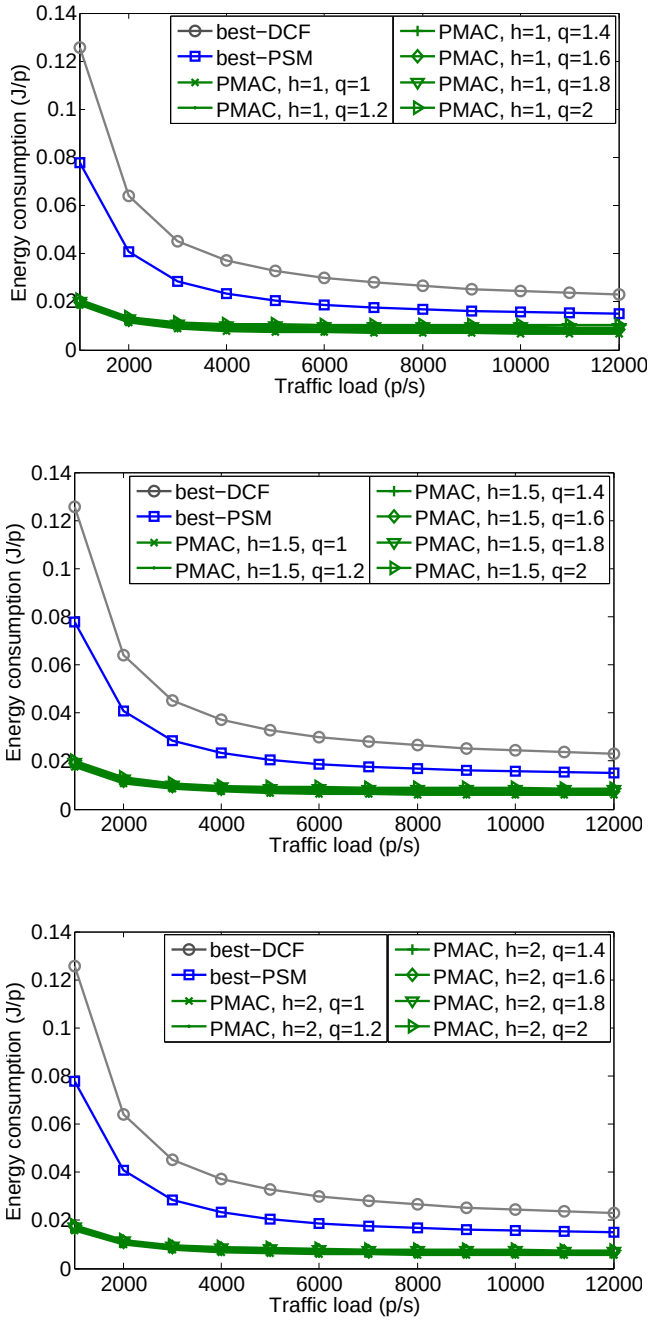

Figure 4.10: Energy consumption of the proposed MAC (PMAC), best-DCF, and best-PSM (N=100, $\eta_s = 6$ dB and $\eta_d = 9$ dB).

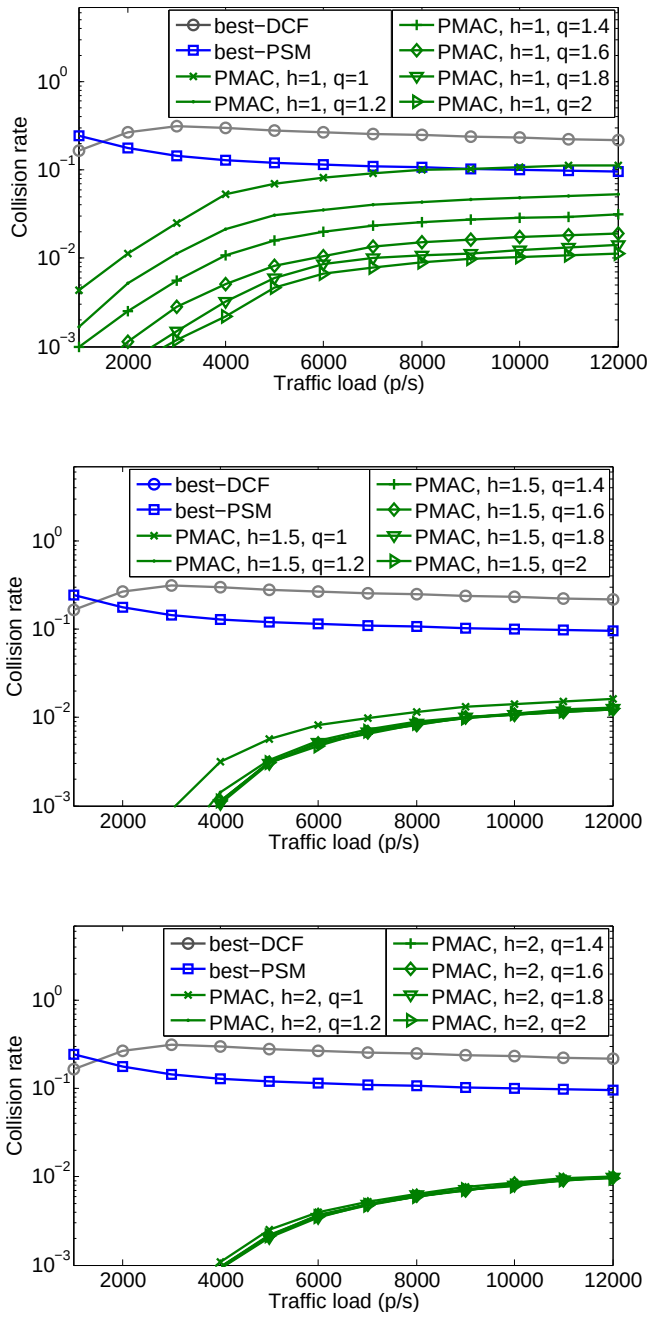

Figure 4.11: Collision rate of the proposed MAC (PMAC), best-DCF, and best-PSM (N=100, $\eta_s = 6$ dB and $\eta_d = 9$ dB).

throughput. In addition, a cell coordinator schedules all data transmissions for nodes inside the cell by transmitting only a scheduling packet in each frame. The reduced scheduling overhead provides more time data transmission to increase throughput.

Energy consumption per transmitted data packet is shown in Figure 4.10. Although the total energy consumption in each scheme increases as the network load increases, the highest energy consumption per packet occurs at the lowest network traffic load. The results indicate that the proposed MAC has significantly lower energy consumption per transmitted data packet, which is 25%-50% of the best-PSM energy consumption. The high energy efficiency of the proposed MAC scheme is the result of minimizing energy wastage because of node idle listening and transmission collisions, which is achieved by periodic assignment of deterministic time slots for transmissions. In the proposed scheme, a node stays awake only during the scheduling time slot of cell coordinator, in its data time slot(s) either for transmission or reception, and when initiating a new transmission in the contention slots. Also, energy wastage caused by transmission collisions is minimized by reserving space exclusively for each scheduled data transmission and sharing the scheduling information among adjacent cell coordinators.

The packet collision rate for the different protocols is demonstrated in Figure 4.11. The high transmission collision rate in the DCF and PSM MAC schemes is due to the hidden node problem of CSMA MAC in a wireless ad hoc network. In the proposed MAC, the packet collision rate is reduced as r_a and/or r_g increases, which increases the area range around a coordinator that it is aware of scheduled transmissions/receptions. As the results indicate, the proposed MAC has a much lower packet collision rate in compassion with the best-DCF and best-PSM. The proposed MAC scheme can effectively minimize transmission collisions by assigning contention-free time slots for data transmissions and reserving space around a scheduled link to prevent collisions.

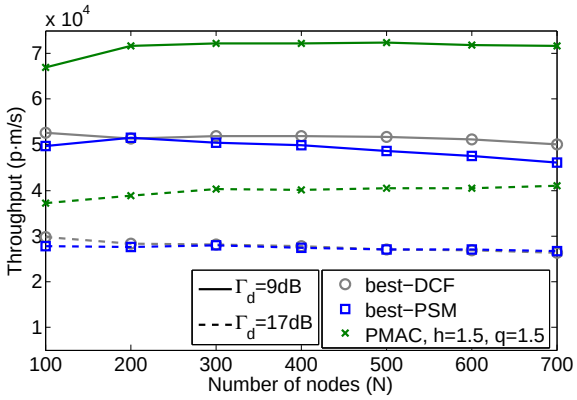

(a) Throughput

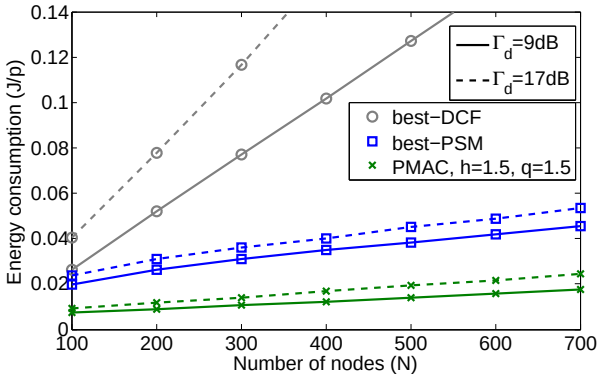

(b) Energy consumption

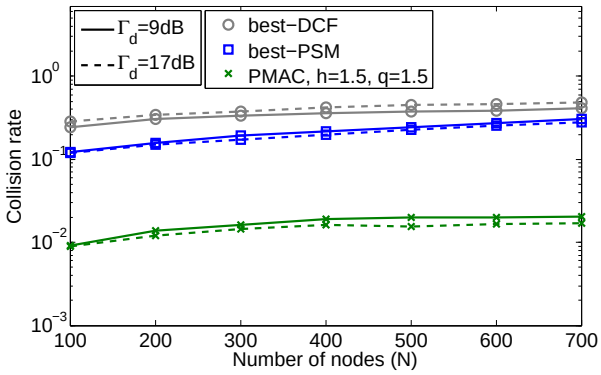

(c) Collision rate

Figure 4.12: Performance of the proposed MAC (PMAC), best-DCF, and best-PSM versus node density (Traffic load=8000 p/s, $\eta_s = 6$ dB and $\eta_d = 9$, 17 dB).

Figure 4.12 shows the performance of the proposed MAC (PMAC), best-DCF, and best-PSM in high traffic load (8000 packets/s) as the node density changes and for $\eta_d = 9$ dB and 17 dB respectively. The number of transmitted packets per second decreases in each scheme as η_d increases, because a larger channel space required for each transmission in each MAC scheme to meet the higher SINR requirement at the receiver node. According to Figure 4.12(a), the proposed MAC scheme provides 25%-50% higher throughput than best-DCF and best-PSM. As illustrated in Figure 4.12(b), the energy consumption per packet increases in each scheme as the node density and/or η_d increases. It is observed that the energy consumption of the proposed MAC mechanism is about 35%-45% of the best-PSM. Figure 4.12(c) shows that the transmission collision rate in the proposed MAC scheme is always lower than 0.02, which is about 10 times smaller than the transmission collision rate in the best-DCF and best-PSM.

4.4 Summary

In this chapter, we present a novel coordination-based MAC protocol for a wireless ad hoc network. In the proposed MAC scheme, the network area is partitioned into cells and a coordinator node periodically schedules all transmissions/receptions for nodes inside its cell. For each scheduled transmission/reception, the channel in both time and space domains are reserved to avoid transmission collisions. Adjacent coordinators actively exchange scheduling information to maximize spatial spectrum reuse while avoiding transmission collisions. A source node contends only once to transmit a batch of packets. After that it can request for transmission by including the information in the header of one data packet. Moreover, periodic scheduling of transmission time slots for data packets allows a node to put its radio interface into the sleep mode when not transmitting/receiving a packet in order to reduce

energy consumption. We compare the performance of the proposed scheme with the IEEE 802.11 DCF scheme without power saving and in power saving mode, whose carrier sensing range and ATIM window size are dynamically adjusted to provide highest throughput. The performance measures include aggregate throughput, average energy consumption per packet and packet collision rate. Simulation results show that the proposed scheme achievers substantially higher throughput, significantly reduces energy consumption, and has a much smaller packet collision rate in comparison with the existing protocols.

Chapter 5

Joint Scheduling and Transmission Power Control

In this chapter, we study efficient joint scheduling and transmission power control in a wireless ad hoc network. We discuss that the optimal scheduling and transmission power control are solutions of an NP-hard problem with network wide information. However, we show that the asymptotic optimal solution can be determined when node density in the network goes to infinity and the network area is unbounded. By analyzing the asymptotic joint optimal scheduling and transmission power control, we determine the fundamental limits of maximum spectrum and energy efficiencies in a wireless network. To approach the maximum spectrum and energy efficiencies in a practical wireless ad hoc network, we assign a transmission power level and a target interference power level to each link that are determined based on the asymptotic optimal values. The concurrent transmissions at each time slot are scheduled such that the actual power of interference at the scheduled links are close to the target interference levels for efficient spectrum and energy utilization. We

present a distributed implementation of the proposed scheduling and transmission power control scheme based on our proposed MAC framework in Chapter 4. The simulation results show that the proposed scheme achieves 70% of the asymptotic network capacity, which is about 78% of the asymptotic network capacity without consideration of the MAC overhead. The achieved throughput is about 35% higher than the throughput obtained using existing schemes. Also, the energy consumption in the proposed scheme is less than 20% of the consumed energy using existing schemes.

The rest of this chapter is organized as follows: The system model is presented in Section 5.1. In Section 5.2, we analyze asymptotic joint optimal scheduling and transmission power control and determine the maximum spectrum and energy efficiencies in a wireless network. We propose a scheduling and transmission power control mechanism to approximate the optimal solution in a practical wireless network in Section 5.3. In Section 5.4, we present distributed implementation of our proposed scheduling and transmission power control scheme using local network information. We present simulation results in Section 5.5 to evaluate the performance of the proposed scheme. Finally, Section 5.6 summarizes this chapter.

5.1 System Model

Consider a wireless ad hoc network with coverage area A where all network nodes use a shared radio spectrum for transmissions. We focus on single-hop transmissions as, at the MAC layer, each node communicates with one or more of its one-hop neighboring nodes. Nodes are randomly distributed in the network area and the destination of each source node is randomly selected from the rest nodes within maximum data transmission distance $d_{\max}$. Let L denote the number of links and $l \in \{1, 2, ..., L\}$ denote a single-hop link in the

network; The source and destination nodes of link l are denoted by S_l and D_l, respectively. We denote the distance from the source node of link l to the destination node of link k by d_{lk}. The channel gain between the source node of link l and the destination node of link k is $h_{lk} = c{d_{lk}}^{-\alpha}$, where c is a constant and α is the path loss exponent[1].

Time is partitioned into slots of constant durations. Consider a scheduling interval of T slots, and let $t \in \{1, 2, ..., T\}$ denote time slot index[2]. We assume that d_{lk}, with $l, k \in \{1, 2, ..., L\}$, is constant over T time slots (i.e., node mobility during T time slots is negligible). Let $\bar{\boldsymbol{\gamma}} = [\gamma_{lt}]_{L\times T}$ denote the transmission power matrix, where γ_{lt} denotes the transmission power level of source node of link l at time slot t. Let $\bar{\boldsymbol{u}} = [u_{lt}]_{L\times T}$ denote the scheduling matrix, where $u_{lt} = 1$ if link l is scheduled for transmission at time slot t and $u_{lt} = 0$ otherwise. A scheduled link transmits a data packet during a time slot that is scheduled. The signal to noise plus interference ratio (SINR) at the destination of link l at slot t is given by

$$\eta_{lt} = \frac{u_{lt}\gamma_{lt}h_{ll}}{N_0 + \sum_{k\neq l} u_{kt}\gamma_{kt}h_{kl}} \tag{5.1}$$

where N_0 is background noise power and $\sum_{k\neq l} u_{kt}\gamma_{kt}h_{kl} \triangleq I_{lt}$ is the power of interference at the destination of link l at slot t. The achievable channel rate in bit/s/Hz over link l at slot t, using *Shannon formula*[3], is

$$R_{lt} = \log_2(1 + \eta_{lt}) \tag{5.2}$$

[1]We assume that Physical-Layer coding deals with channel fading. Considering channel fading information is advantageous for effective packet scheduling and transmission power control, however, acquiring channel fading state information requires additional signaling overhead.

[2]The scheduling interval should be determined based on data traffic and network dynamics. A very large scheduling interval causes slow adaptation to data traffic and network changes. Also, a small scheduling interval leads to higher scheduling overhead due to more frequent scheduling/signaling slots.

[3]Shannon's equation provides an upper bound of link data rate. In practice, link data rate is usually a discrete step function of SINR [10].

and the average data rate (in bit/s/Hz) at link l can be written as

$$R_l = \frac{1}{T}\sum_{t=1}^{T} R_{lt} = \frac{1}{T}\sum_{t=1}^{T} \log_2\big(1 + \frac{u_{lt}\gamma_{lt}h_{ll}}{N_0 + \sum_{k\neq l} u_{kt}\gamma_{kt}h_{kl}}\big). \tag{5.3}$$

A radio interface can be in transmit, receive, idle and sleep modes. The power consumption of a radio interface in the transmit mode to transmit at power level γ is $\Gamma_c + g_a\gamma$, where Γ_c is the circuit power consumption and $g_a > 1$ is the inverse of the power efficiency of radio interface amplifier. The power consumption in the receive and idle modes is Γ_c and in the sleep mode is Γ_0. We assume that each node puts its radio interface into sleep mode when it is not transmitting/receiving data to save energy (i.e., nodes do not consume energy because of idle-listening). Thus, the sum of power consumption at the source and destination nodes of link l at slot t is

$$P_{lt} = u_{lt} \times (2\Gamma_c + g_a\gamma_{lt}) + (1 - u_{lt}) \times (2\Gamma_0) \tag{5.4}$$

and the average power consumption (in Joule/s) at link l can be written as

$$P_l = \frac{1}{T}\sum_{t=1}^{T} P_{lt} = \frac{1}{T}\sum_{t=1}^{T}\big[u_{lt} \times (2\Gamma_c + g_a\gamma_{lt}) + (1 - u_{lt}) \times (2\Gamma_0)\big]. \tag{5.5}$$

The average energy consume per transmitted bit (in Joule/(bit/Hz)) at link l can be written as

$$E_l = \frac{P_l}{R_l} \tag{5.6}$$

where P_l and R_l are defined in (5.5) and (5.3) respectively.

Joint optimal scheduling and transmission power control are to find a scheduling matrix

and a transmission power matrix that maximize the network objective function. i.e.,

$$\begin{aligned} \max_{\bar{\boldsymbol{u}},\bar{\gamma}} & \sum_{l=1}^{L} w_l R_l \\ \text{s. t. : } & R_l \leq \hat{R}_l,\ l \in \{1,2,...,L\} \\ & E_l \leq \hat{E}_l,\ l \in \{1,2,...,L\} \end{aligned} \tag{5.7}$$

where $w_l \in [0,\infty)$ is the weighting factor of data rate of link l, $\hat{R}_l$ denotes the maximum required data rate at link l, and $\hat{E}_l$ denotes the maximum energy consumption per bit constraint at link l. To find an optimal solution in (5.7), we need to solve a non-convex mixed integer non-linear problem, which is known to be NP-hard. In Section 5.2, we show that the optimal scheduling and transmission power control can be calculated for the asymptotic node density in an unbounded network area. We use asymptotic analysis to study the maximum spectrum and energy efficiencies in a wireless network and to develop scheduling and transmission power control methods to approximate the optimal solution.

5.2 Asymptotic Joint Optimal Scheduling and Transmission Power Control

In this section, we study scheduling and transmission power control in a wireless network as the density of nodes goes to infinity and when the network area is unbounded. Consider a symmetric link scheduling in an unbounded network area as illustrated in Figure 5.1. The network area is partitioned into equal size hexagonal cells and a link is scheduled inside each cell. The source and destination distance is the same for all links and the position of the source and destination nodes of every scheduled link with respect to all other scheduled source nodes is identical. Due to the symmetry of scheduled links, the optimal transmission

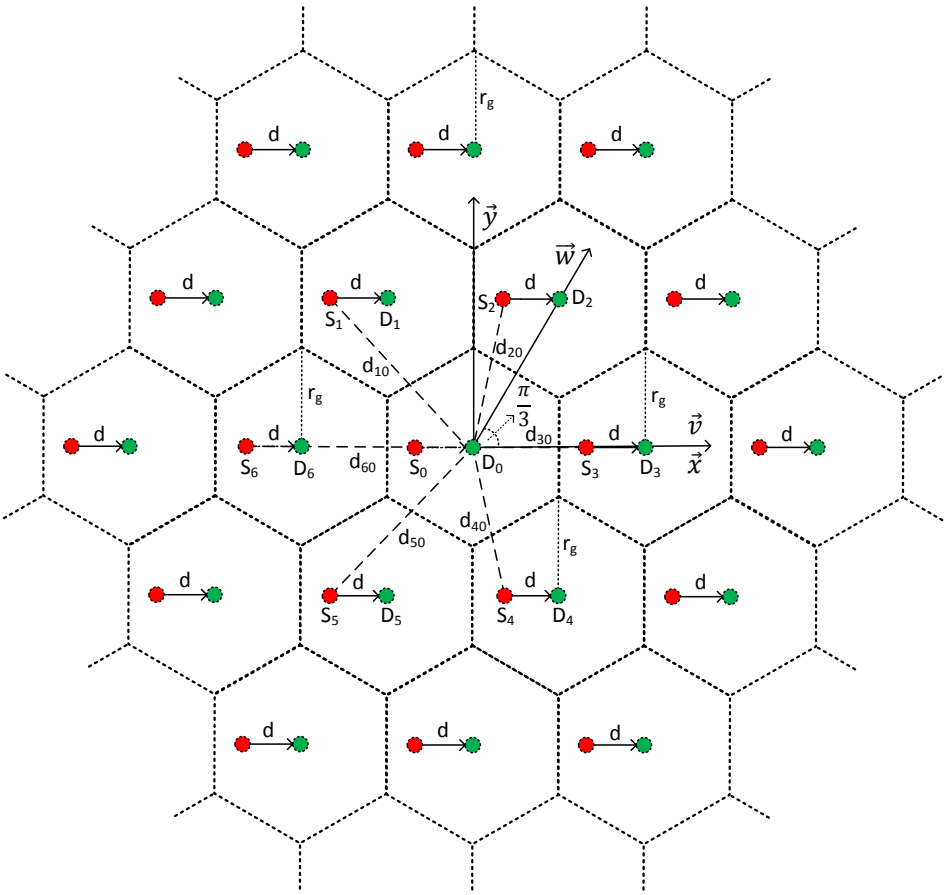

Figure 5.1: Symmetric scheduling paradigm

power should be the same for every scheduled link. Thus, the asymptotic optimal joint scheduling and transmission power control is to find a cell size and a transmission power level that maximize the network objective function. In the following, we analyze the spectrum and energy efficiencies in the network as the cell size and transmission power level vary, in order to determine optimal scheduling and transmission power control based on the network objective function.

Let d denote the distance between the source and destination of a link, r_g the distance between the center and a vertex of a cell in Figure 5.1, and γ the transmission power of every scheduled source node. The signal power at a destination node depends on the transmission power level of the source node and the distance between source and destination node. The signal power at a destination node can be written as

$$\gamma^{(r)} = c\gamma d^{-\alpha}. \tag{5.8}$$

The interference power at a destination node depends on the transmission power γ, the distance d, and the distances between scheduled links. It can be calculated as

$$I = \sum_{i=1}^{\infty} c\gamma {d_{i0}}^{-\alpha} \tag{5.9}$$

where $d_{i0}, i \in \{1, 2, ...\}$, denotes the distance from the source node of an interfering link to the destination node. As illustrated in Figure 5.1, using unity vectors $\bar{v}$ and $\bar{w}$, we have

$$d_{i0} = \big|\big|m\sqrt{3}r_g\bar{v} + n\sqrt{3}r_g\bar{w} - d_l\bar{v}\big|\big| = \big|\big|(m\sqrt{3}r_g - d_l)\bar{v} + n\sqrt{3}r_g\bar{w}\big|\big| \tag{5.10}$$

for some $(m, n) \in \{..., -2, -1, 0, 1, 2, ...\}^2, (m, n) \neq (0, 0)$, where $||\cdot||$ denotes the euclidian distance. By changing coordinates in (5.10), we have

$$\begin{aligned} d_{i0} &= \big|\big|(m\sqrt{3}r_g - d)\bar{x} + n\sqrt{3}r_g\cos(\pi/3)\bar{x} + n\sqrt{3}r_g\sin(\pi/3)\bar{y}\big|\big| \\ &= \big|\big|(m\sqrt{3}r_g + \frac{n\sqrt{3}r_g}{2} - d)\bar{x} + \frac{3nr_g}{2}\bar{y}\big|\big| = \sqrt{\Big(m\sqrt{3}r_g + \frac{n\sqrt{3}r_g}{2} - d\Big)^2 + \Big(\frac{3nr_g}{2}\Big)^2}. \end{aligned} \tag{5.11}$$

Using (5.8)-(5.11), with the assumption that $I \gg N_0$, the SINR at a destination node can be calculated as

$$\eta = \frac{\gamma^{(r)}}{N_0 + I} \approx \frac{c\gamma d^{-\alpha}}{\sum_{i=1}^{\infty} c\gamma {d_{i0}}^{-\alpha}} = \frac{1}{\sum_{(m,n)\neq(0,0)} \left[\Big(\frac{m\sqrt{3}r_g}{d} + \frac{n\sqrt{3}r_g}{2d} - 1\Big)^2 + \Big(\frac{3nr_g}{2d}\Big)^2\right]^{-\alpha/2}} \triangleq F(\tfrac{r_g}{d}). \tag{5.12}$$

Also, with frequency reuse, the network space occupied by each scheduled link can be written as

$$S = \frac{3\sqrt{3}}{2} \times r_g^2. \tag{5.13}$$

Using (5.12) and (5.13), the total transmitted data rate (bit/s/Hz) per unit network area can be written as

$$\tilde{R} = \frac{\log_2(1+\eta)}{S} = \frac{\log_2\left(1+F(\frac{r_g}{d})\right)}{\frac{3\sqrt{3}}{2} \times {r_g}^2} = \frac{1}{d_l^2} \times \frac{\log_2\left(1+F(\frac{r_g}{d})\right)}{\frac{3\sqrt{3}}{2} \times \left(\frac{r_g}{d_l}\right)^2}. \tag{5.14}$$

According to (5.14), the total data rate depends on the ratio, $r_g/d \triangleq r'_g$, and can be maximized by choosing r'_g to maximize $\frac{\log_2\left(1+F(r'_g)\right)}{\frac{3\sqrt{3}}{2} \times {r'_g}^2} \triangleq G(r'_g)$. Function $G(\cdot)$ is plotted in Figure 5.2 for different path loss exponent values. The maximum achievable data rate is inversely proportional to the square of the link distance. i.e.,

$$\max_{r'_g} \tilde{R} = \frac{1}{d^2} \times \max_{r'_g} G(r'_g). \tag{5.15}$$

On the other hand, energy consumption per transmitted data bit (Joule/(bit/Hz)) in the network can be written as

$$E = \frac{\frac{1}{S} \times (2\Gamma_c + g_a\gamma)}{\tilde{R}} = \frac{2\Gamma_c + g_a\gamma}{\log_2\left(1+F(\frac{r_g}{d})\right)} \tag{5.16}$$

where $2\Gamma_c + g_a\gamma$ denotes the sum of power consumption in the source and destination nodes of a link, assuming that energy consumption in non-scheduled links (which are in the sleep mode) is negligible. According to (5.16), the energy consumption per transmitted data bit decreases as the distance between scheduled links increases (i.e., as r_g increases).

We set the objective of joint scheduling and transmission power control to maximize the total data rate per unit of network area (i.e., maximize spectrum efficiency) while keeping the amount of consumed energy per transmitted data bit below a threshold as an energy

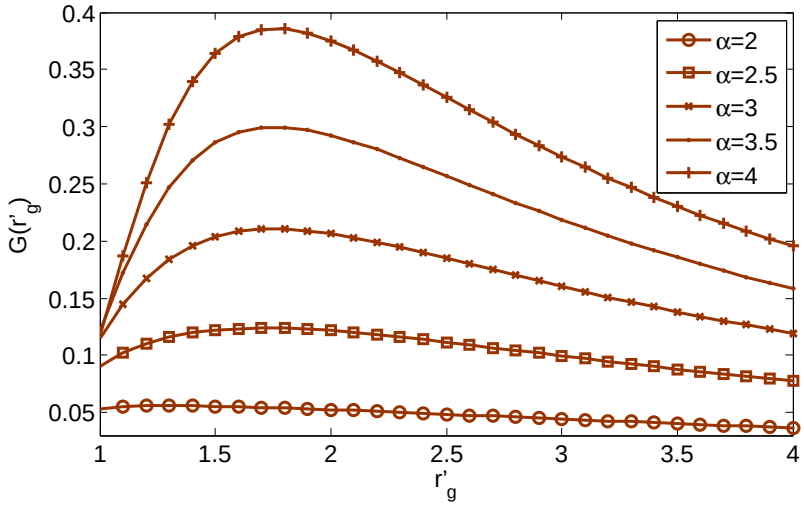

Figure 5.2: Plot of function $G(\cdot)$ for different path loss exponent values

efficiency constraint. i.e.

$$\begin{aligned} &\max_{\gamma, r_g} \tilde{R} \\ &\text{s. t. : } E \leq \hat{E} \end{aligned} \tag{5.17}$$

where $\tilde{R}$ denotes the total transmitted data rate per unit network area, E denotes energy consumption per transmitted data bit and $\hat{E}$ denotes the maximum energy consumption per bit threshold. The objective function in (5.17) is consistent with (5.7) in which weighting factors of links' data rates are set such that $w_l = w_k$ if $d_{ll} = d_{kk}$, the maximum required data rate of links $\hat{R}_l = \infty$, and energy efficiency constraints are set such that $\hat{E}_{ll} = \hat{E}_{kk} = \hat{E}$ if $d_{ll} = d_{kk}$, for every link l and k in the network. Therefore, the asymptotic optimal

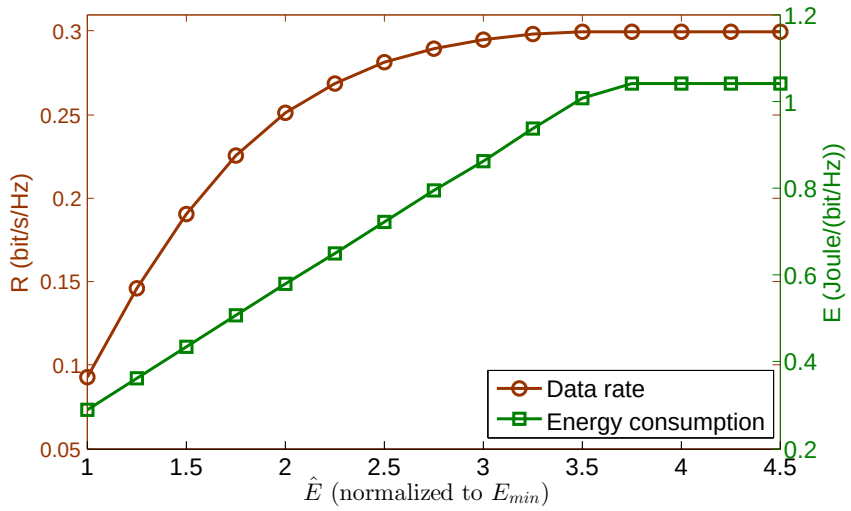

Figure 5.3: Data rate per unit of network area versus energy consumption per transmitted bit as $\hat{E}$ in the network objective function varies ($\Gamma_c = 1.25$ mW, $\gamma \in [1, 100]$ mW, $g_a = 10$, $\alpha = 3.5$, $d = 1$, $r_g \in [d, 4d]$.)

scheduling and transmission power control problem can be written as

$$\begin{aligned} &\max_{\gamma, r_g} \frac{1}{d^2} \times \frac{\log_2\left(1 + F(\frac{r_g}{d})\right)}{\frac{3\sqrt{3}}{2} \times \left(\frac{r_g}{d}\right)^2} \\ &\text{s. t. :} \quad \frac{2\Gamma_c + g_a\gamma}{\log_2\left(1 + F(\frac{r_g}{d})\right)} \leq \hat{E}. \end{aligned} \tag{5.18}$$

Figure 5.3 shows spectrum efficiency and energy consumption per bit with optimized transmission power and cell size, as the the energy consumption constraint $\hat{E}$ varies.

In the symmetric scheduling, the transmission power level of source nodes and the cell size determine the power of interference at destination nodes. Using (5.12), we have

$$r_g = d \times F^{-1}\left(\frac{c\gamma d^{-\alpha}}{I}\right) \tag{5.19}$$

where $F^{-1}(\cdot)$ denote the inverse of function F defined in (5.12). By substituting (5.19) in (5.14) and (5.16), the asymptotic data rate per unit of network area and the energy consumption per bit can be obtained based on the transmission power level of a source node and the power of interference at a receiver node as

$$\tilde{R} = \frac{1}{d^2} \times \frac{\log_2\left(1 + \frac{c\gamma d^{-\alpha}}{I}\right)}{\frac{3\sqrt{3}}{2} \times \left(F^{-1}\left(\frac{c\gamma d^{-\alpha}}{I}\right)\right)^2} \tag{5.20}$$

and

$$E = \frac{2\Gamma_c + g_a\gamma}{\log_2\left(1 + \frac{c\gamma d^{-\alpha}}{I}\right)} \tag{5.21}$$

respectively. Thus, the optimal transmission power of a source and the optimal power of interference at a destination can be calculated as

$$\begin{aligned} [\gamma^*, I^*] = \arg\max_{\gamma, I} \ & \frac{1}{d^2} \times \frac{\log_2\left(1 + \frac{c\gamma d^{-\alpha}}{I}\right)}{\frac{3\sqrt{3}}{2} \times \left(F^{-1}\left(\frac{c\gamma d^{-\alpha}}{I}\right)\right)^2} \\ \text{s. t. : } & \frac{2\Gamma_c + g_a\gamma}{\log_2\left(1 + \frac{c\gamma d^{-\alpha}}{I}\right)} \leq \hat{E} \end{aligned} \tag{5.22}$$

where γ^* and I^* denote the asymptotic optimal transmission power of a source and the optimal power of interference at a destination node respectively.

5.3 Scheduling and Transmission Power Control

In Section 5.2, we determine the asymptotic optimal scheduling and transmission power level to maximize spectrum efficiency in the wireless network (i.e., data rate per unit of network area) given the required energy consumption per bit constraint in the symmetric link scheduling. In a practical wireless network, however, links likely are not placed in a

symmetric manner, because the density of the nodes is finite and the distances between source and destination of the links are not identical. Also, scheduling and transmission power control should be adaptive, as node's location and link's required data rate (i.e., traffic load) vary over time in a wireless network. In this section, we develop a scheduling and transmission power control mechanism to approximate the optimal solution in a practical wireless network.

The data rate and energy consumption of a link depend on the transmission power of the source and the power of interference at the destination node. Thus, as an approximation of optimal scheduling and transmission power control, we schedule links for transmissions in a practical network such that the transmission power of source nodes and the power of interference at destination nodes follow the asymptotic optimal values. For this purpose, we assign a transmission power level to the source and a target interference power level to the destination of each link, which maximize asymptotic spectrum efficiency while satisfying the energy consumption per bit constraint of the link. Then, we schedule concurrent links for transmissions such that the actual power of interference at the destination of each scheduled link is as close as possible to the determined target interference power of the link. If the actual interference at a destination node is more than the target interference power, the data will not be successfully decoded at receiver (because the actual SINR at the destination node will be lower than the expected SINR value used to adjust transmission data rate at the source node). However, it is desired to schedule links such that the actual interference at destinations are close to the target interference of the schedule links to pack scheduled links together and allow more concurrent transmissions. In Subsection 5.3.1, we determine efficient transmission power and target interference power of different links for efficient radio spectrum and energy utilization. In Subsection 5.3.2, we investigate how to schedule concurrent links (based on their transmission power and target interference

power) such that the actual interference power levels at the scheduled links are close to their target interference power levels for efficient spatial spectrum reuse.

5.3.1 Transmission power and target interference power

We determine the transmission power and target interference power for a link to maximize the asymptotic spectrum efficiency (data rate per unit of area) while maintaining the energy consumption per bit of the link below a threshold as an energy efficiency constraint. According to analysis in Section 5.2, for transmission between a pair of source and destination nodes with distance d_{ll}, setting the transmission power to γ_l and the target interference power to $\tilde{I}_l$ provides the asymptotic spectrum efficiency

$$\tilde{R}_l = \frac{1}{{d_{ll}}^2} \times \frac{\log_2\left(1 + \frac{c\gamma_l {d_{ll}}^{-\alpha}}{\tilde{I}_l}\right)}{\frac{3\sqrt{3}}{2} \times \left(F^{-1}\left(\frac{c\gamma_l {d_{ll}}^{-\alpha}}{\tilde{I}_l}\right)\right)^2} \tag{5.23}$$

and energy consumption per transmitted bit

$$E_l = \frac{2\Gamma_c + g_a\gamma}{\log_2\left(1 + \frac{c\gamma_l {d_{ll}}^{-\alpha}}{\tilde{I}_l}\right)}. \tag{5.24}$$

According to (5.23), the asymptotic spectrum efficiency is proportional to the inverse of second power of link distance ${d_{ll}}^2$ and depends on the ratio of transmission power γ_l and target interference power $\tilde{I}_l$. Also, the optimal ratio of γ_l and $\tilde{I}_l$ to maximize the asymptotic spectrum efficiency in a link depends on the link distance d_{ll}.

In a practical wireless network, the distances between the source and destination nodes of different links are different in general and links cannot be scheduled based on the symmetric link distribution studied in the asymptotic analysis. Also, the asymptotic optimal ratios of transmission power and interference power for links with different distances are

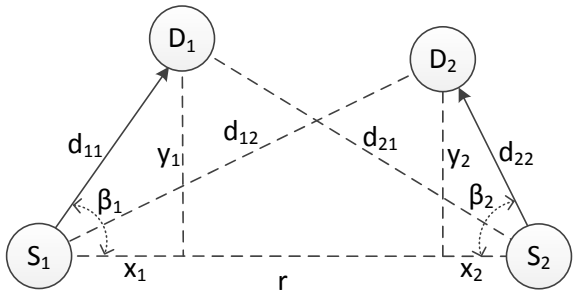

Figure 5.4: A two-link network

different. Given the asymptotic optimal ratios of transmission power and interference power for the links, the transmission power and target interference power values should be prudently chosen such that non-symmetric links can be scheduled with actual interference power close to the target interface power at every scheduled link for efficient spatial spectrum reuse. To study how to effectively choose the transmission power and target interference value of different links for non-symmetric link scheduling, we consider a two-link network as illustrated in Figure 5.4. We assume that β_1 and β_2 are independent and uniformly distributed in $[0, 2\pi]$. Also, the distance between source and destination of the links, d_{11} and d_{22}, are independent and have an identical distribution. Let $E(d_{11}) = E(d_{22}) = m_1$ and $E({d_{11}}^2) = E({d_{22}}^2) = m_2$. We consider the distance between the two source nodes (r in Figure 5.4) as a measure of the space occupied by the two scheduled links in the network. Thus, it is desired to minimize the expected distance r (over random realization of β_1, d_{11}, β_2 and d_{22}) to minimize the average occupied space for the scheduled links and, as a result, maximize spatial spectrum reuse. Let $\gamma_1, \tilde{I}_1$ and $\gamma_2, \tilde{I}_2$ denote the transmission power level and target interference power levels of the links respectively. Both links can be scheduled concurrently only if the actual interference power at each link is not greater than their

target interference power level. i.e., we must have

$$I_1 = c\gamma_2 {d_{21}}^{-\alpha} \leq \tilde{I}_1 \Rightarrow d_{21} \geq \left(\frac{c\gamma_2}{\tilde{I}_1}\right)^{1/\alpha} \tag{5.25}$$

and

$$I_2 = c\gamma_1 {d_{12}}^{-\alpha} \leq \tilde{I}_2 \Rightarrow d_{12} \geq \left(\frac{c\gamma_1}{\tilde{I}_2}\right)^{1/\alpha}. \tag{5.26}$$

According to Figure 5.4, we have

$$d_{12} = \sqrt{(r - x_2)^2 + {y_2}^2} = \sqrt{(r - d_{22}\cos(\beta_2))^2 + (d_{22}\sin(\beta_2))^2} \tag{5.27}$$

and

$$d_{21} = \sqrt{(r - x_1)^2 + {y_1}^2} = \sqrt{(r - d_{11}\cos(\beta_1))^2 + (d_{11}\sin(\beta_1))^2}. \tag{5.28}$$

By substituting (5.27) and (5.28) in (5.25) and (5.26), the required conditions to schedule both links concurrently can be written as

$$r^2 - 2rd_{22}\cos(\beta_2) + {d_{22}}^2 \geq \left(\frac{c\gamma_2}{\tilde{I}_1}\right)^{2/\alpha} \tag{5.29}$$

and

$$r^2 - 2rd_{11}\cos(\beta_1) + {d_{11}}^2 \geq \left(\frac{c\gamma_1}{\tilde{I}_2}\right)^{2/\alpha}. \tag{5.30}$$

Taking expectation (with respect to β_1, d_{11}, β_2 and d_{22}) from both sides of (5.29) and (5.30), we obtain

$$E(r^2) \geq \max\left(\left(\frac{c\gamma_2}{\tilde{I}_1}\right)^{2/\alpha} - m_2, \left(\frac{c\gamma_1}{\tilde{I}_2}\right)^{2/\alpha} - m_2\right). \tag{5.31}$$

According to (5.31), the expected square of distance, $E(r^2)$, increases as transmission power levels increase and target interference power levels decrease. Also, the $E(r^2)$ value can be decreased by setting

$$\left(\frac{c\gamma_2}{\tilde{I}_1}\right)^{2/\alpha} - m_2 = \left(\frac{c\gamma_1}{\tilde{I}_2}\right)^{2/\alpha} - m_2 \Rightarrow \frac{\gamma_2}{\tilde{I}_1} = \frac{\gamma_1}{\tilde{I}_2} \Rightarrow \gamma_1 \times \tilde{I}_1 = \gamma_2 \times \tilde{I}_2 = \lambda \tag{5.32}$$

where λ is a constant. Thus, the average occupied space for scheduling non-symmetric links is decreased (i.e., actual interference power levels are close to the target interference power levels in both links) when the product of transmission power and target interference power is identical for every link. Motivated by the analysis for the two-link network, we maintain the product of transmission power and target interference power a fixed value for all links in a practical network for efficient spatial spectrum utilization when scheduling non-symmetric links.

Therefore, we determine the transmission power and target interference power of the links as follows:

1. The product of transmission power and target interference power is a fixed value for every link;
2. The energy consumption per bit in each link is less than a threshold [4];
3. The transmission power and target interference of each link are chosen to maximize its asymptotic spectrum efficiency based on the link distance.

Based on (5.23) and (5.24), the transmission power level and target interference power for link l are chosen as

[4]The energy consumption per bit threshold of the links can be adjusted periodically based on network condition. For instance, when the network throughput is less than traffic load, the energy consumption per bit thresholds can be incremented to increase spectrum efficiency (i.e., improve network throughput). However, when the network throughput is greater than traffic load the energy consumption per bit thresholds can be decremented to reduce energy consumption.

$$
\begin{aligned}
[\gamma_l^*, \tilde{I}_l^*] = \arg\max_{\gamma_l, \tilde{I}_l} \ & \frac{1}{{d_{ll}}^2} \times \frac{\log_2\left(1 + \frac{c\gamma_l {d_{ll}}^{-\alpha}}{\tilde{I}_l}\right)}{\frac{3\sqrt{3}}{2} \times \left(F^{-1}\left(\frac{c\gamma_l d_{ll}^{-\alpha}}{\tilde{I}_l}\right)\right)^2} \\
\text{s. t. :} \ & \frac{2\Gamma_c + g_a\gamma_l}{\log_2\left(1 + \frac{c\gamma_l d_{ll}^{-\alpha}}{\tilde{I}_l}\right)} \leq \hat{E}_l \\
& \gamma_l \times \tilde{I}_l = \lambda
\end{aligned}
\tag{5.33}
$$

where $\hat{E}_l$ is the maximum energy consumption per bit threshold at link l, and constant λ should be chosen based on the feasible range of transmission power and interference bound of the links in the network.

5.3.2 Link scheduling

In Subsection 5.3.1, we discuss how to choose the transmission power and target interference power levels for each link to approach the optimal values. Given the determined transmission power and target interference of different links in a network, the set of concurrent links for transmissions at each time slot should be carefully determined such that the actual power of interference at the receiver of scheduled links are close to their target interference power levels for efficient spatial spectrum utilization. For instance, consider the scheduling scenario illustrated in Figure 5.5. The first column in the figure shows six links that are to be scheduled in two time slots. For simplicity of illustration, we use the circular areas around the links to show the conflicting links based on their transmission power and target interference power levels. Any two links can be scheduled simultaneously in a time slot only if their circular space areas do not overlap. The scheduled links are indicated by solid line and shaded circular areas in the second and third columns of the figure. The second column shows a weak scheduling plan in which only four links are scheduled

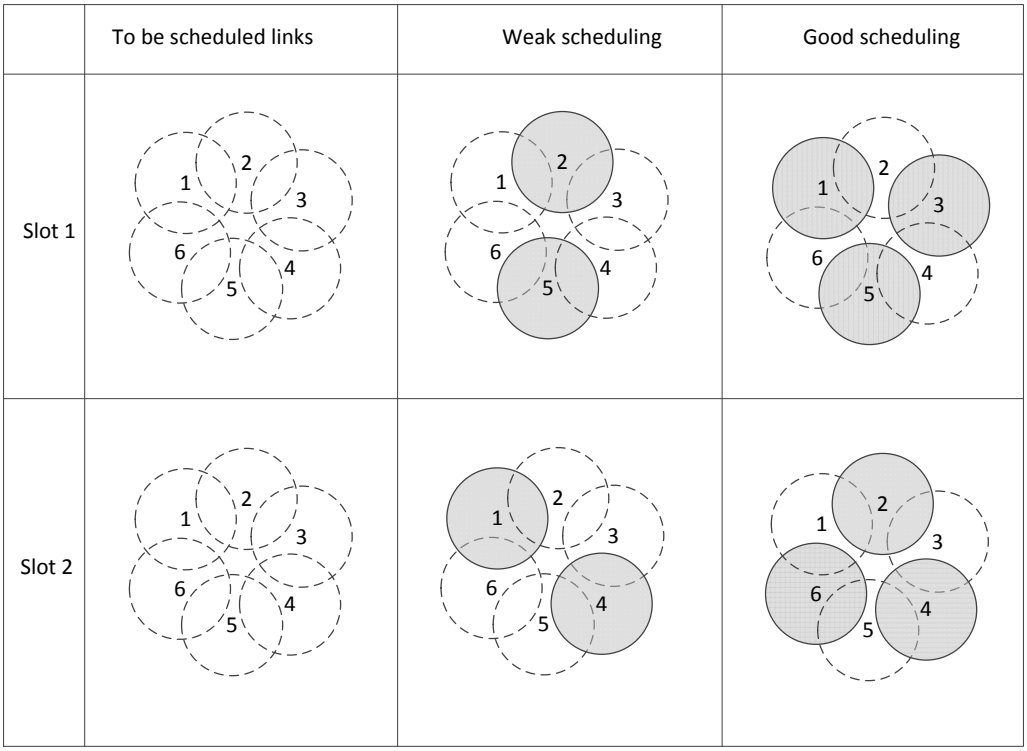

Figure 5.5: Weak link scheduling plan versus good link scheduling plan

in both time slots and no new link can be scheduled any more. A better scheduling plan is represented in the third column of the figure in which all six links are scheduled by carefully selecting the set of concurrent scheduled links in each time slot. The better scheduling plan that schedules more concurrent links (by efficient spatial spectrum utilization) corresponds to the situation where the actual interference power levels are closer to the target interference power levels in the scheduled links in comparison to the weak scheduling plan. In the following, we investigate how to effectively select the set of concurrent links in each time slot based on the determined transmission power and target interference power levels of the links such that actual interference power levels at the scheduled links are close to their target interference power levels for efficient spatial spectrum utilization.

The actual power of interference at the destination of link l at time slot t is $I_{lt} = \sum_{k \neq l} u_{kt} \gamma_k^* h_{kl}$. If link l is scheduled at time slot t (i.e., $u_{lt} = 1$), we must have $I_{lt} \leq \tilde{I}_l^*$ to guarantee successful data reception at the destination of link l. Also, it is desired to schedule links such that I_{lt} is close to $\tilde{I}_l^*$ for efficient spatial spectrum utilization.

We consider a sequential link scheduling algorithm to avoid high complexity. At each step, a link is scheduled for transmission at a time slot. Let $\bar{\boldsymbol{u}}^i = [u_{lt}^i]_{L \times T}$ denote the scheduling matrix after step i, with $\bar{\boldsymbol{u}}^0 = [0]_{L \times T}$. The data rate of link l up to sequential scheduling step i is

$$R_l^i = \frac{1}{T} \sum_{t=1}^{T} \log_2 \Big(1 + \frac{u_{lt}^i \gamma_l^* h_{ll}}{\tilde{I}_l^*} \Big). \tag{5.34}$$

Let $\hat{\gamma}_{lt}^i$ denote the maximum transmission power at the source node of link l at slot t that does not increase the interference power at any already scheduled link before step i to more than its target interference power level, i.e.,

$$\begin{aligned} &\hat{\gamma}_{lt}^i = \max \gamma \\ &\text{s. t.: } \gamma h_{lk} + \sum_{j \neq k} u_{jt}^{i-1} \gamma_j^* h_{jk} \leq I_k^*,\ k \neq l,\ u_{kt}^{i-1} = 1. \end{aligned} \tag{5.35}$$

We have

$$\hat{\gamma}_{lt}^{i} = \min_{\substack{k \neq l \\ u_{kt}^{i-1}=1}} \Big(\frac{\tilde{I}_{k}^{*} - \sum_{j \neq k} u_{jt}^{i-1} \gamma_{j}^{*} h_{jk}}{h_{lk}} \Big). \tag{5.36}$$

Also, let $\hat{I}_{lt}^{i}$ denote the minimum possible target interference power for link l at slot t in the presence of already scheduled links before step i, i.e.,

$$\begin{aligned} \hat{I}_{lt}^{i} &= \min I \\ \text{s. t.:} \ & \sum_{k \neq l} u_{kt}^{i-1} \gamma_{k}^{*} h_{kl} \leq I. \end{aligned} \tag{5.37}$$

We have

$$\hat{I}_{lt}^{i} = \sum_{k \neq l} u_{kt}^{i-1} \gamma_{k}^{*} h_{kl}. \tag{5.38}$$

Thus, at step i, link l can be scheduled at time slot t if

$$\hat{\gamma}_{lt}^{i} \geq \gamma_{l}^{*} \text{ and } \hat{I}_{lt}^{i} \leq \tilde{I}_{l}^{*}. \tag{5.39}$$

On the other hand, the ratio $\hat{I}_{lt}^{i}/\tilde{I}_{l}^{*}$ indicates how close the target interference power and the actual interference power are at link l, after scheduling link l at slot t at i^{th} step. Also, the ratio $\gamma_{l}^{*}/\hat{\gamma}_{lt}^{i}$ indicates how close the target interference power and the actual interference power are at the closest scheduled link to link l, after scheduling link l at slot t at i^{th} step. Thus, at step i, we schedule a link at a time slot with the highest ratios $\hat{I}_{lt}^{i}/\tilde{I}_{l}^{*}$ and $\gamma_{l}^{*}/\hat{\gamma}_{lt}^{i}$. i.e., the link to be scheduled and the time slot of its transmission at step i are

$$\begin{aligned} [l^{i}, t^{i}] = \arg\max_{l,t} & \left(\frac{\gamma_{l}^{*}}{\hat{\gamma}_{lt}^{i}} \times \frac{\hat{I}_{lt}^{i}}{\tilde{I}_{l}^{*}} \right) \\ \text{s. t.:} \ & \hat{\gamma}_{lt}^{i} \geq \gamma_{l}^{*} \text{ and } \hat{I}_{lt}^{i} \leq \tilde{I}_{l}^{*} \\ & R_{l}^{i} < \hat{R}_{l} \\ & l \in \{1, 2, ..., L\}, \, t \in \{1, 2, ..., T\} \end{aligned} \tag{5.40}$$

where l^{i} and t^{i} denote the link and its transmission slot scheduled at step i respectively. To maintain fair link scheduling, scheduling is performed in several rounds and in each round

a link is scheduled at most in one time slot. The sequential scheduling steps in each round continue until every node is either scheduled once or cannot be scheduled. The scheduling rounds continue until no new link can be scheduled.

5.4 Distributed Scheduling and Transmission Power Control

In Section 5.3, we present a scheduling and transmission power control scheme for the wireless network. In this section, we discuss distributed implementation of the proposed scheduling and transmission power control scheme based on local network information. We also present a distributed MAC framework to adaptively schedule links for transmissions based on required data rates of network links.

In the proposed scheduling and transmission power control in Section 5.3, the transmission power and target interference power are determined for each link as described in Subsection 5.3.1. According to (5.33), the transmission power and target interference power of a link are determined based on the link distance and the maximum energy consumption per bit constraint of the link ($\hat{E}_l$). Therefore, the transmission power and target interference power can be determined independently at each link using (5.33).

In the proposed scheduling and transmission power control in Section 5.3, links are scheduled for transmission as described in Subsection 5.3.2. The link scheduling algorithm schedules links over a period of T time slots iteratively based on the information of already scheduled links in the network using (5.40). However, the information of local scheduled links is the most relevant information to schedule links for transmission/reception, because the power of interference decreases exponentially with distance in a wireless network. The

power of interference at the destination node of link l at time slot t can be written as

$$I_{lt} = \sum_{k \neq l} u_{kt} \gamma_{kt}^{*} h_{kl} = \sum_{\substack{k \neq l \\ d_{kl} < d_0}} u_{kt} \gamma_{kt}^{*} h_{kl} + \sum_{\substack{k \neq l \\ d_{kl} \geq d_0}} u_{kt} \gamma_{kt}^{*} h_{kl}. \tag{5.41}$$

At the right side of (5.41), the first term denotes the total interference caused by source nodes of the scheduled links within distance d_0 from the destination of link l, and the second term denotes the total interference caused by source nodes of the scheduled links at distance d_0 or farther. We have

$$\sum_{\substack{k \neq l \\ d_{kl} \geq d_0}} v_{kt} \gamma_{kt} h_{kl} \leq c_0 \gamma_{\max} {d_0}^{-\alpha} \triangleq I_0 \tag{5.42}$$

where c_0 is a constant and $\gamma_{\max}$ denotes the maximum transmission power level. i.e., the interference caused by links that are farther than d_0 (> 0) is bounded by I_0. Thus, using only the information of scheduled local links within distance d_0 and I_0, we can estimate the power of interference at a link to calculate (5.36) and (5.38) that are required for the link scheduling algorithm in (5.40). To coordinate distributed link scheduling, we employ a set of coordinator nodes distributed over the network area to collect and exchange local network information and to periodically schedule links in a distributed manner. Each coordinator node schedules its associated links for transmissions according to (5.40) with consideration of already scheduled local links that are announced by its adjacent coordinators. In the following, we describe the proposed MAC framework (which is based on our proposed medium access framework in Chapter 4) to coordinate all transmissions in the network based on source node transmission requests.

The network coverage area is partitioned into hexagonal cells as shown in Figure 5.6. The distance r_g between the center and a vertex of a cell is chosen such that $r_g \geq d_{\max}$. Therefor, the destination node of each source node is either in the same cell or an adjacent

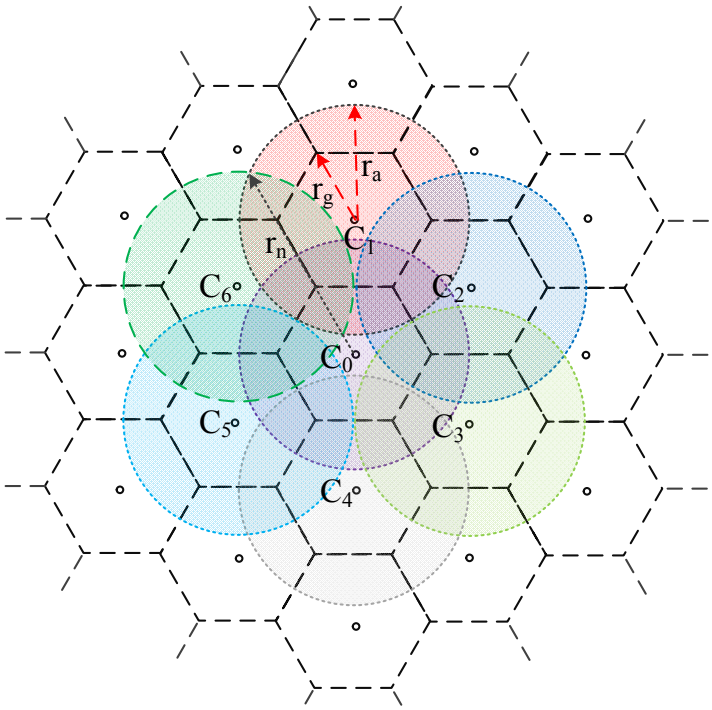

Figure 5.6: Partitioning the network area into hexagonal cells, where C_i, $i \in \{0, 1, 2, ...\}$, denotes the coordinator of cell i. A circular area centred at each coordinator denotes the location area of the nodes that their scheduling information is broadcasted by the coordinator ($r_a = 1.5r_g$).

cell. We assume that a coordinator node is placed at the center of each cell to coordinate all transmissions for nodes inside the cell. Figure 5.7 shows the frame structure. Each frame consists of three types of time slots:

1. *Contention slots:* During contention slots, the source nodes that want to initiate a transmission contend with each other using a truncated CSMA MAC scheme to send a request packet to the cell coordinators;

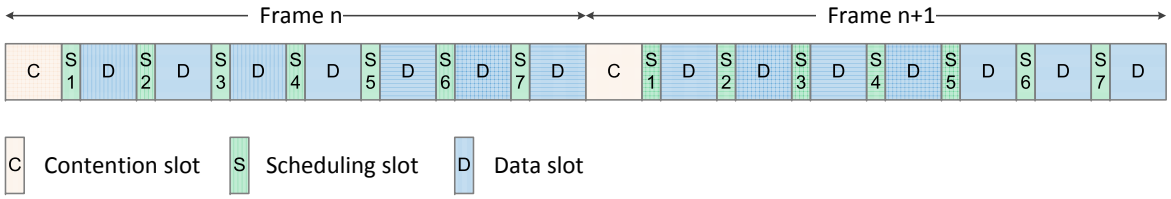

Figure 5.7: Structure of one frame of the proposed MAC framework.

2. *Scheduling slots:* Each coordinator node has a scheduling time slot in every frame, in which it broadcasts a scheduling packet to coordinate all transmissions in its vicinity;

3. *Data slots:* Data packet transmissions are performed during contention-free data slots as scheduled by the coordinators[5].

A coordinator node maintains the following information about each link in its vicinity (i.e., all links within its cell and all links that their scheduling information is advertised by adjacent coordinators):

1. The source and destination nodes IDs and their location information[6];

2. The transmission power level of the link;

3. The target interference power of the link;

4. The set of future data slots that link is scheduled for transmission;

[5]A link may transmit/receive one or more data packets during a data slot that is scheduled for transmssion/reception.

[6]We assume that node location information is updated at coordinators as they move in the network. A higher node mobility imposes higher signaling overhead due to more frequent signaling required to update location information at the coordinators.

5. The amount of data that link has for transmission (which indicates the maximum required link data rate $\hat{R}_l$).

A coordinator receives transmission requests from source nodes during contention slots. Also, a coordinator receives the information of scheduled links for the future data slots by overhearing scheduling packets of adjacent coordinators during scheduling slots. The scheduling packets of a coordinator contains the information of all future scheduled data transmissions for every node within distance $r_a \geq r_g$ from the coordinator. Figure 5.6 shows the area centred at a coordinator where the coordinator obtains the information of scheduled transmissions by overhearing scheduling packets of adjacent coordinators. According to Figure 5.6, a coordinator node acquires the information of scheduled transmissions within distance $r_n = 1.5r_g + \sqrt{{r_a}^2 - 0.75{r_g}^2}$ and for each link, depending on destination node's location in the cell, we have $d_0 \in [r_n - r_g, r_n]$. Based on the source node requests for transmission and the information of already scheduled links, each coordinator periodically schedules data transmissions for every link with the destination inside its cell. A coordinator node schedules links for transmission according to the proposed link scheduling algorithm in Subsection 5.3.2 (with the consideration of already scheduled links by adjacent coordinators) and broadcasts a scheduling packet in its scheduling slot to announce the scheduling information to nodes inside its cell and its adjacent coordinators. The scheduled links perform data transmissions during data time slots as scheduled by cell coordinators and announced during scheduling slots. Every node puts its radio interface into sleep mode when it is not transmiting/receiving a scheduling, data or request packet to save energy.

5.5 Numerical Results

Consider area of 19 hexagonal cells as illustrated in Figure 5.6. There are N nodes randomly distributed over the area. The destination node of each link is randomly selected from the nodes within distance $d_{\max}$ from the source node. The ranges of feasible transmission power level, target interference power level and SINR value for a link are provided in Table 5.1 based on IEEE 802.11 standard [10]. We set the energy consumption per bit constraint, $\hat{E}_l = \theta \times \min E_l$ for every link l, where $\theta \geq 1$. Thus, $\theta = 1$ corresponds to setting transmission power and target interference power for lowest energy consumption per bit in each link, while as θ increases, the energy consumption constraint is relaxed and the transmission power and target interference of a link are determined based on the values that provide highest asymptotic spectrum efficiency. Figures 5.8, 5.9 and 5.10 show respectively the optimal transmission power, target interference power and SINR of a link versus θ as the link distance varies. The corresponding asymptotic spectrum efficiency and the energy consumption per bit are depicted in Figures 5.11 and 5.12 respectively. According to Figure 5.10, the SINR is set to the highest value for a link when the objective is to minimize energy consumption per bit (i.e., $\theta = 1$). However, the optimal SINR value to maximize the asymptotic spectrum efficiency when the energy consumption constraint is weakened is always about 8 dB, independent of the link distance.

We evaluate the performance of our proposed scheduling and transmission power control via simulation. The following metrics are used as performance measure to compare different schemes:

1. *Throughput:* Throughput is defined as the summation of all transmitted data bits per second, weighted by the transmitted distance [80];

2. *Energy consumption:* Energy consumption is defined as the ratio of total energy

Table 5.1: Simulation Parameters

Parameter	Value
c	0.0001
α	3.4
$d_{\max}$	20 m
Bandwidth	2 MHz
$\gamma_{\max}$	100 mW
$\gamma_{\min}$	1 mW
$I_{\max}$	-45 dB
$I_{\min}$	-80 dB
$\eta_{\max}$	30 dB
$\eta_{\min}$	6 dB
R_s	6 Mbps
Frame length	100 ms
Data time slot	1 ms
Scheduling time slot	1 ms
Contention time slot	1 ms
Number of data slots	90
Number of scheduling slots	7
Number of contention slots	3
Data packet length	1 ms
Scheduling packet length	1 ms
Scheduling size for one transmission	200 bits
Request packet size	160 bits
Contention window size	32
Beacon interval	100 ms
Data packet length	1 ms
ATIM size	224 bits
ATIM-ACK size	112 bits
Mini-slot	20 μs
SIFS	10 μs
PHY preamble	72 μs
$CW_{\min}$	15
$CW_{\max}$	1023
Γ_c	1.25 W
g_a	10
Γ_0	0 W

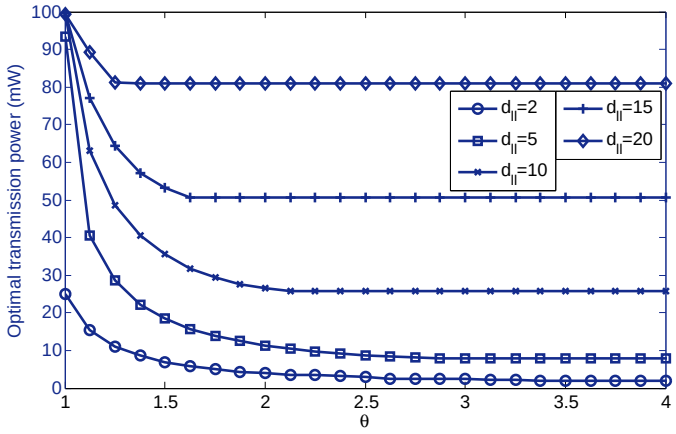

Figure 5.8: The optimal transmission power as energy consumption constraints vary ($\hat{E}_l = \theta \times \min E_l$).

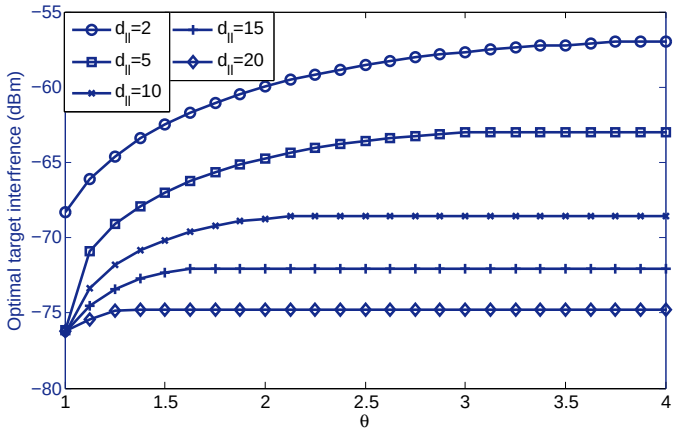

Figure 5.9: The optimal target interference power as energy consumption constraints vary ($\hat{E}_l = \theta \times \min E_l$).

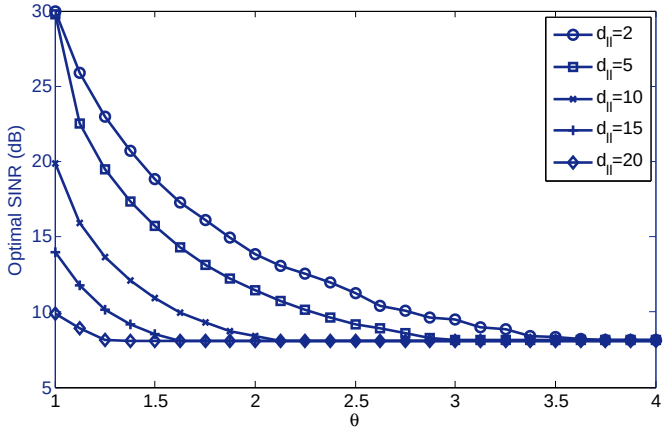

Figure 5.10: The optimal SINR as energy consumption constraints vary ($\hat{E}_l = \theta \times \min E_l$).

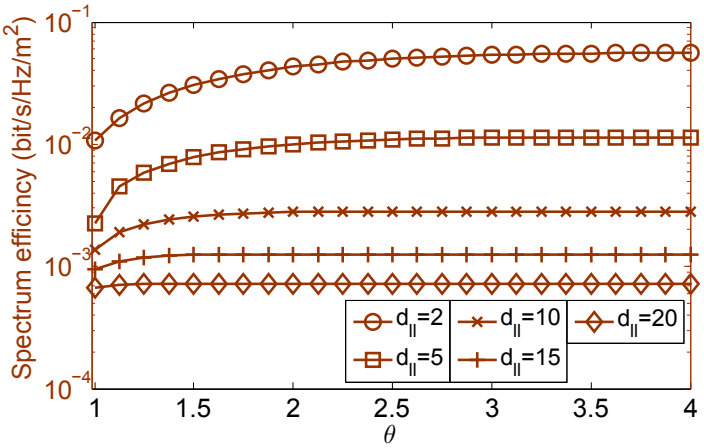

Figure 5.11: The asymptotic spectrum efficiency as energy consumption constraints vary ($\hat{E}_l = \theta \times \min E_l$).

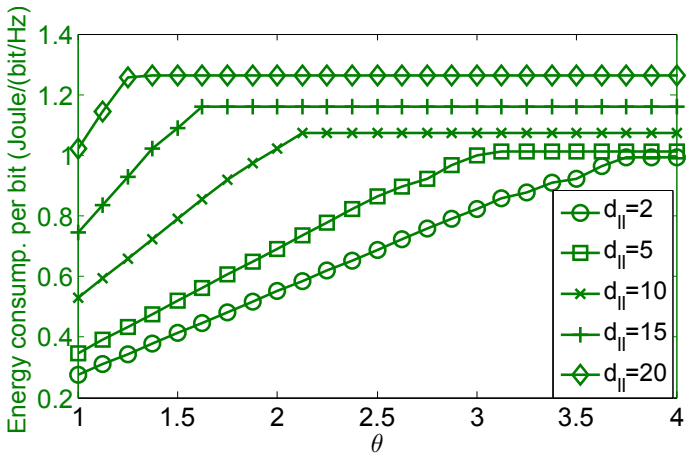

Figure 5.12: The energy consumption per bit as energy consumption constraints vary ($\hat{E}_l = \theta \times \min E_l$).

consumed in the nodes to the total number of transmitted data bits. Similar metrics are also used in [13, 33, 48];

3. *Scheduling efficiency:* According to (5.14), the spectrum efficiency for transmission distance d is bounded by $\tilde{R} = 1/d^2 \times \max G(\cdot)$. Thus, the summation of all transmitted data bits per second, weighted by the second power of the transmitted distance, $\sum_l R_l d_{ll}^2 \leq \max G(\cdot) \times A$, where A denotes the area size and the equality holds under asymptotic optimal scheduling and transmission power control. Therefore, we define scheduling efficiency as the ratio $\sum_l R_l d_{ll}^2 / (\max G(\cdot) \times A)$.

The performance metrics are evaluated based on the transmitted data and energy consumption of the nodes in an inner region of the network area to eliminate edge effects. Links with source nodes located inside the 7 central hexagonal cells (of the 19 hexagonal cells) in Figure 5.6 and all coordinator nodes inside this area are considered in evaluating the performance metrics. We compare the performance of our proposed scheme with IEEE

802.11 DCF MAC with and without power saving and with optimized transmission power levels and carrier sensing threshold based on the analysis provided in [25, 26]. Also, we examine the effectiveness of each strategy that we use for determining transmission power and target interference power levels and for link scheduling by evaluating the throughput without the strategy. The compared schemes are as follows:

1. The proposed scheme, denoted by "Proposed";

2. "P - $g_{\max}$", "P - $I_{\min}$" and "P - arb. g, I", representing proposed scheme when the product of transmission power and target interference power is not maintained at a fixed value, but respectively the transmission power is set to the maximum value, the target interference level is set to the minimum value and the transmission power and target interference level are chosen arbitrary;

3. "P - ran. sch.", representing the proposed scheme when the link scheduling by coordinators at each scheduling step is not according to the link scheduling algorithm described by (5.40), instead a link and a data slot are randomly selected from the set of links and slots that can be scheduled;

4. "best-DCF" and "best-PSM", representing the DCF MAC of IEEE 802.11 respectively without and with power saving mode, with optimized transmission power levels and carrier sensing threshold based on the analysis provided in [25] and with optimized ATIM window size.

In each scheme, all control and signaling packets are transmitted using signaling rate R_s, which requires minimum SINR $\eta_{\min}$ during entire packet transmission time for successful reception at the destination. Data packets are transmitted using variable bit rate which is

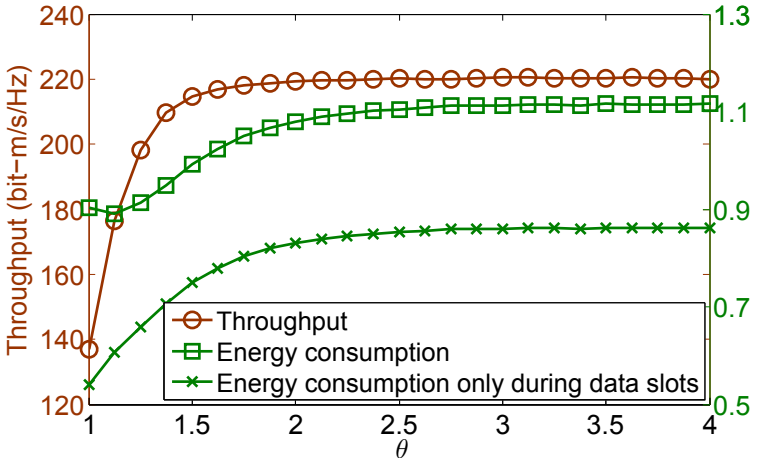

Figure 5.13: Throughput and energy consumption of proposed scheme as θ varies with saturated data traffic at all nodes ($N = 400$).

optimized for each link based on the statistics of SINR at destination during past transmitted packets to obtain highest average link data rate. A data packet is successfully received if the SINR at the destination node during the entire packet transmission time is not less than the required SINR for the used data transmission rate. The data packet duration is 1 ms in each scheme and the data packet header and ACK packet overheads are neglected in every scheme. Data packets are generated according to a Poisson process in each source node. The network load is defined as the aggregate bit generation rate in all nodes in the entire network area and is equally distributed among all nodes. Other simulation parameters are given in Table 5.1. The simulations are performed using MATLAB for five seconds of the channel time and the performance metrics are averaged over five different random realization of the network.

Figure 5.13 shows throughput versus energy consumption of the proposed scheme as the energy consumption per bit constraint varies. The energy consumption including only

consumed energy during data slots (without considering energy consumed during scheduling slots and contention slots) is also plotted in the figure. According to Figure 5.13, as the energy consumption constraints vary from no constrains to the minimum energy consumption per bit constraints in every link, the network throughput is decreased by 38% and energy consumption is reduced by 18%, while the energy consumption for data transmissions/receptions only is reduced by 37%.

Figures 5.14(a) and 5.14(b) show the throughput and energy consumption using different schemes, as network traffic load changes. The throughput and energy consumption versus number of nodes in the network are shown in Figures 5.15(a) and 5.15(b) respectively. The proposed scheme provides about 40% higher throughput than best-DCF and best-PSM. Figure 5.14(a) shows the effectiveness of the strategies used for choosing transmission power and target interference power of the links and for link scheduling in our proposed scheme. Also, according to Figures 5.14(b) and 5.15(b), the energy consumption of the proposed scheme is less than 10% of best-DCF and about 20% of best-PSM. Figure 5.16 compares the energy consumption of the proposed scheme and best-PSM when θ is adjusted such that the proposed scheme provides the same throughput as best-PSM. The energy consumption of the proposed scheme to achieve the same network throughput as best-PSM is less than 15% of the consumed energy by best-PSM .

Figure 5.17 compares the data transmission rate of the nodes using different schemes. In each scheme, nodes are sorted based on data transmission rate and the horizonal line shows node index. It is observed that the proposed scheme provides better fairness compared to best-DCF and best-PSM, as the link scheduling algorithm in the proposed scheme is to maintain fairness while efficiently choosing concurrent transmissions in each data slot.

Figure 5.18 compares the scheduling efficiency using different schemes. The scheduling efficiency of the proposed scheme is about 35% higher than best-DCF and best-PSM.

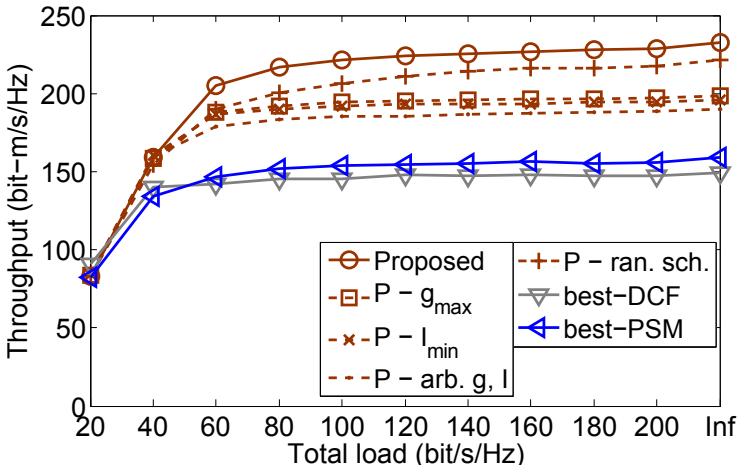

(a) Throughput

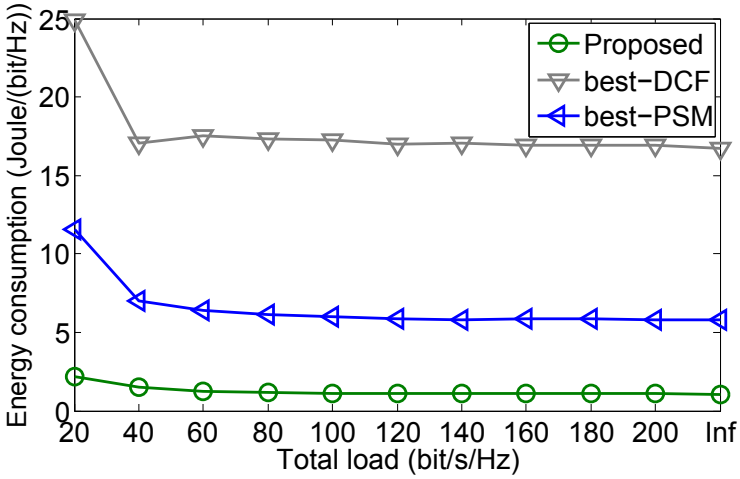

(b) Energy consumption

Figure 5.14: Throughput and energy consumption of different schemes as network traffic load varies ($N = 400$, $\theta = \infty$).

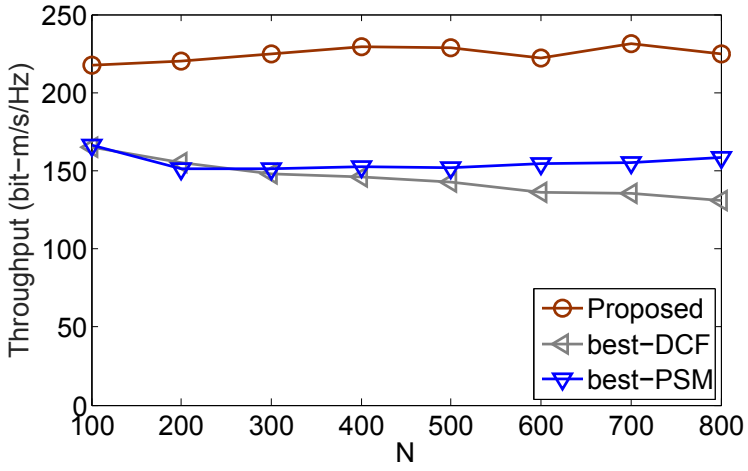

(a) Throughput

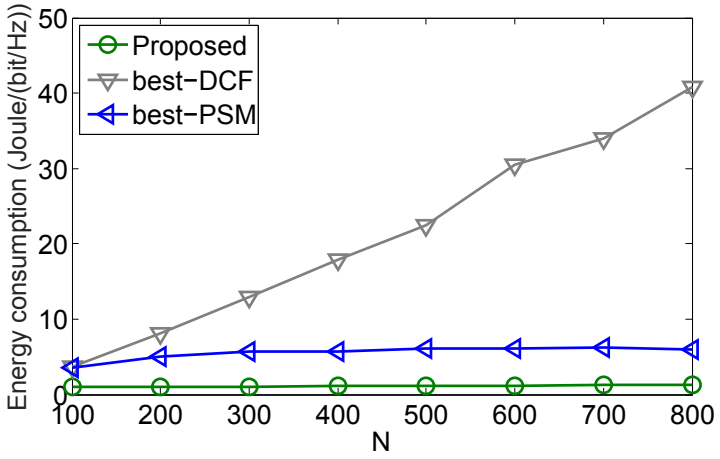

(b) Energy consumption

Figure 5.15: Throughput and energy consumption of different schemes as number of nodes varies with saturated data traffic at all nodes ($\theta = \infty$).

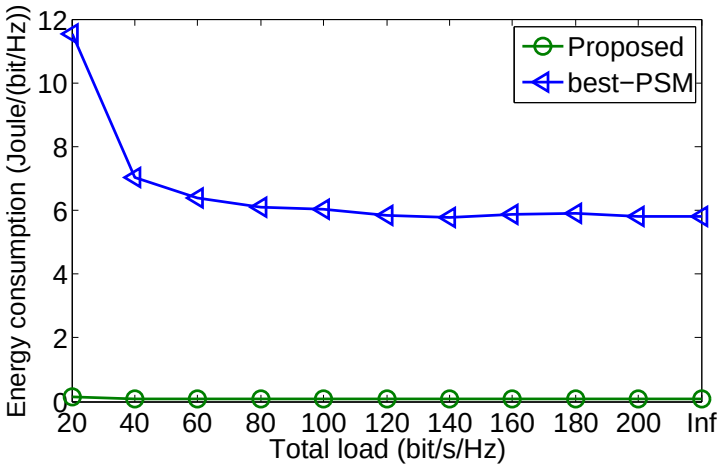

Figure 5.16: Energy consumption of proposed scheme and best-PSM as network traffic load varies ($N = 400$, θ is adjusted such that the proposed scheme provides the same throughput as best-PSM).

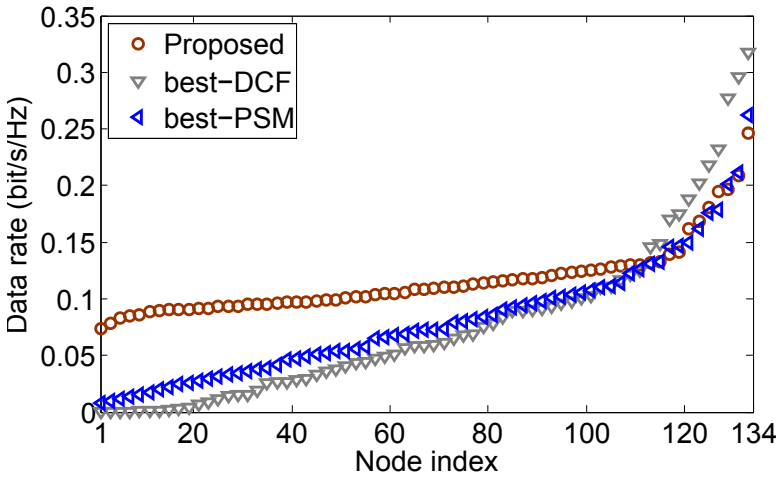

Figure 5.17: Data transmission rate of the nodes using different schemes with saturated data traffic at all nodes ($N = 400$, $\theta = \infty$).

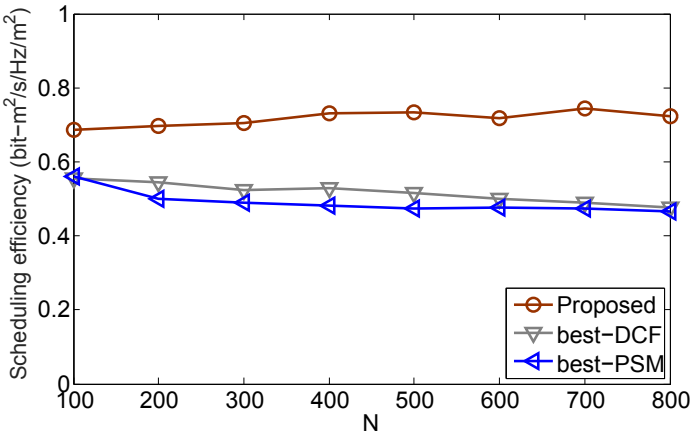

Figure 5.18: Scheduling efficiency of different schemes as number of nodes varies with saturated data traffic at all nodes ($\theta = \infty$).

Indeed, the scheduling efficiency of our proposed scheme is about 70% of the asymptotic optimal scheduling and transmission power control. The achieved scheduling efficiency is about 78% in data slots, as 90% of slots are data slots and the rest are scheduling and contention slots in the proposed scheme.

5.6 Summary

In this chapter, we study joint scheduling and transmission power control for spectrum and energy efficient communication in a wireless ad hoc network. We analyze the asymptotic optimal joint scheduling and transmission power control and determine the maximum spectrum efficiency in a wireless network subject to an energy efficiency constraint. Based on the asymptotic analysis, we propose a scheduling and transmission power control scheme

to approach maximum spectrum and energy efficiencies in a practical wireless ad hoc network. A transmission power level and a target interference power level are determined for each link to maximize the asymptotic spectrum efficiency subject to the link's energy consumption constraint. Concurrent links are scheduled for transmission such that the actual level of interference at each destination node is close to its target interference level for efficient spatial spectrum utilization. We discuss that local network network information is sufficient to implement the proposed scheduling and transmission power control scheme, and present a distributed MAC framework to implement the proposed scheme. Simulation results show that the proposed scheme can achieve 70% of the asymptotic optimal throughput, which is more than 35% higher than existing schemes. Also, the energy consumption of the proposed scheme is less than 20% of existing schemes.

Chapter 6

Conclusions and Future Work

6.1 Conclusions

The objective of this research is to develop a medium access control mechanism with high throughput and low energy consumption for wireless ad hoc networks. To achieve the objective, we focus on four fundamental approaches:

- The access to the shared channel should be dynamically coordinated with low MAC overhead;
- The active and sleep times of the radio interface should be effectively planned to minimize energy consumption without adverse effects on the throughput and packet transmission delay;
- The concurrent transmissions should be properly scheduled to improve spatial spectrum utilization;

- The transmission power level of each link should be adjusted based on the network condition to maximize spectrum and energy efficiencies.

At the first step, we present a new energy efficient MAC protocol for a fully connected wireless network. A temporary coordinator node regulates transmissions dynamically based on the instantaneous network traffic load condition. In the proposed protocol, nodes contend once to transmit a batch of packets, after that they will be assigned a contention-free time for transmission as long as they have packets for transmission. Contention-free data transmission time reduces collision and MAC contention overheads and minimizes idle-listening radio interface energy consumption. Also, a unique transmission time is assigned to realtime traffic in order to provide higher priority for realtime traffic over non-realtime traffic. We present an analytical model to efficiently allocate channel time to realtime and non-realtime traffic. Using the proposed protocol, the awake time of the nodes is short, signaling for power saving and MAC contention overhead is relatively small, and transmission schedule is adaptive to the network traffic load condition, which results in low energy consumption and high performance. Numerical results show that the proposed scheme guarantees the QoS requirement of realtime traffic, significantly reduces the energy consumption, and considerably enhances the network performance in terms of throughput and packet transmission delay in comparison with the existing protocols.

We present a novel MAC scheme based on dynamic space-reservation for a wireless ad hoc network. All data transmissions are dynamically scheduled by a set of coordinator nodes that are distributed over the network coverage area. A coordinator node receives transmission requests from source nodes inside its cell during the contention slots and exchanges scheduling information with adjacent coordinators in the scheduling time slots. Each coordinator node periodically schedules data transmissions for nodes inside its cell

by transmitting a scheduling packet in its scheduling slot. Data transmissions are performed during the data time slots, as determined by coordinators. For each scheduled transmission, adequate space area around the receiver node is reserved to guarantee the required SINR. The reserved space area can be parts of several adjacent cells which is coordinated through active exchange of scheduling information among adjacent coordinators to enhance spatial spectrum reuse. Moreover, the deterministic data transmission time allows nodes to stay awake only when they are transmitting/receiving a packet to minimize idle-listening energy consumption. Simulation results show that the proposed MAC scheme provides substantially higher throughput and has significantly lower energy consumption in comparison with existing MAC schemes.

We study efficient joint scheduling and transmission power control in a wireless ad hoc network. The optimal scheduling and transmission power control in general are solutions of an NP-hard problem with network wide information. The optimal solution can be determined for the asymptotic node density in an unbounded network area. By analyzing the asymptotic optimal joint scheduling and transmission power control, we determine the fundamental limit of the wireless network throughput, subject to an energy consumption per bit constraint. Based on the asymptotic analysis, we present a novel scheduling and transmission power control mechanism to approach the optimal solution in a practical wireless ad hoc network. In the proposed scheme, the concurrent transmissions are scheduled such that the transmission power level of scheduled source nodes and the interference power level at scheduled destination nodes follow the asymptotic optimal values. We present distributed implementation of our proposed scheduling and transmission power control based on local network information. Simulation results show that the proposed scheme provides about 40% higher throughput than existing schemes. The energy consumption of the proposed scheme is less than 20% of existing schemes. Also, the scheduling efficiency

of proposed scheme is 70% of the asymptotic optimal solution, which is about 35% higher than existing schemes.

6.2 Future Research Directions

In this research, we treat the interference from the concurrent transmissions as noise at the receiver node of a link. However, using multiple antennas and more sophisticated signal processing algorithms (or using directional antennas at transmitters/receivers) allow canceling (or reducing) interference at receivers. An interesting future research direction is to investigate efficient joint scheduling and transmission power control with the consideration of multiuser MIMO (and/or discretional antennas) at transmitter and receiver nodes in a wireless ad hoc network.

The dense deployment of Internet APs in the future wireless networks allows the required data of a mobile node to be downloaded/uploaded through several APs in its vicinity. Also, multi-hop data transmission can be carried through different set of intermediate relays. Efficient data transmission path selection jointly considered with scheduling and transmission power control is another important research direction to enhance spectrum and energy efficiencies in next generation wireless networks.

In the proposed MAC framework (in Chapter 4), we assume that a coordinator node is placed at the center of each cell. In a wireless ad hoc network with low node density, a node may not exist at the center of every cell to serve as cell coordinator. A further research direction is to study how to efficiently determine the set of coordinator nodes when presence of a coordinator node at the center of every cell is not practical due to network environment limitations.

Appendix A

Derivation of Conditional Probabilities

Derivation of $P_{X_1X_2X_3|S}(x_1, x_2, x_3|s)$

Since all nodes in states 2, 3 and 4 are equally likely to be scheduled for transmission, $P_{X_1X_2X_3|S}(x_1, x_2, x_3|s)$ can be obtained as in (A.1).

$$P_{X_1X_2X_3|S}(x_1, x_2, x_3|s) =$$
$$\begin{cases} 1, & n_2 + n_3 + n_4 \leq M, x_1 = n_3, x_2 = 0, x_3 = n_4; \\ \dfrac{\binom{n_3}{x_1}\binom{n_4}{x_3}\binom{n_2}{M - x_1 - x_3}}{\binom{n_2 + n_3 + n_4}{M}}, & n_2 + n_3 + n_4 > M, x_1 + x_2 = n_3, x_1 + x_2 + x_3 = M, \\ 0, & \text{Otherwise.} \end{cases} \tag{A.1}$$

Derivation of $P_{X_4|X_1X_2X_3S}(x_4|x_1, x_2, x_3, s)$

In a *contention period*, each contending node chooses a random backoff window size w, uniformly distributed between $[0, W-1]$, waits for w mini-slots of idle channel time, and then transmits a transmission request. Let random vector $\bar{w}(s) = (w_1, ..., w_{n_1})$ denote the back-off times chosen by the contending nodes, where w_i is the backoff window size chosen by contending node $i \in \{1, 2, .., n_1\}$ at system state s and $w_i \in [0, W-1]$. Denote the set of all possible outcomes of random vector $\bar{w}(s)$ by $\mathcal{W}(s)$. Since nodes choose their random back-off times independently and uniformly between $[0, W-1]$, different outcomes have equal probability and the size of $\mathcal{W}(s)$ is

$$|\mathcal{W}(s)| = W^{n_1}. \tag{A.2}$$

Consider random vector $U = (X_4, X_4', W_l)$, where X_4 and X_4' are the numbers of successful and collided transmissions respectively during the *contention period*, and W_l is the backoff window chosen by node(s) which sends the last transmission request in the *contention period*. Let $I_{cp}(u, s)$ denote the number of mini-slots that channel is idle during the *contention period* in system state s when event $U = u \triangleq (x_4, x_4', w_l)$ occurs. We have

$$I_{cp}(u, s) = T_{cp}(s) - (x_4 + x_4')t_q. \tag{A.3}$$

Contending nodes do not initiate transmissions (even if their back-offs reach zero) if there is not enough time remained in the *contention period* to complete at least one request. Thus, in the system state s and event u, a contending node that has chosen backoff time $w > T_{cp}(s) - t_q - (x_4 + x_4')t_q = I_{cp}(u, s) - t_q$ does not start transmission. Also event u is feasible in system state s if

$$(x_4 + x_4') - 1 \leq w_l \leq w_x(u, s) = \min(I_{cp}(u, s) - t_q, W - 1). \tag{A.4}$$

Let $\mathcal{Y}(u,s)$ denote a subset of $\mathcal{W}(s)$ that leads to event u in system state s. In the event, there are x_4 successful requests and x_4' collisions, and the backoff window of node(s) that had the last transmission is w_l; thus, $x_4+x_4'-1$ transmissions have backoff $w \in [0, w_l)$, one transmission has backoff time $w = w_l$, none of the other nodes has backoff $w \in (w_l, w_x(u,s)]$ and all other contending nodes have backoff $w \in (w_x(u,s), W-1]$. In addition, one node transmits at each successful transmission and at least two nodes in a collision. Therefore, the size of $\mathcal{Y}(u,s)$ is

$$|\mathcal{Y}(u,s)| = \binom{w_l}{x_4+x_4'-1}\binom{x_4+x_4'}{x_4} \frac{n_1!}{(n_1-x_4-2x_4')!2^{x_4'}}\Big(W-1-w_x(u,s)+x_4'\Big)^{n_1-x_4-2x_4'}. \quad \text{(A.5)}$$

Using (A.2) and (A.5), the probability of event u at system state s can be calculated by

$$P_{U|S}(u|s) = \frac{|\mathcal{Y}(u,s)|}{|\mathcal{W}(s)|} \quad \text{(A.6)}$$

and $P_{X_4|S}(x_4|s)$ can be calculated using (A.6) as

$$P_{X_4|S}(x_4|s) = \sum_{x_4',w_l} P_{U|S}(u|s). \quad \text{(A.7)}$$

Since the right side of (A.7) is independent of x_1, x_2, and x_3, we have

$$P_{X_4|X_1X_2X_3S}(x_4|x_1,x_2,x_3,s) = P_{X_4|S}(x_4|s). \quad \text{(A.8)}$$

Derivation of $P_{X_5...X_8|X_1...X_4S}(x_5,...,x_8|x_1,...,x_4,s)$

Let p denote the probability that a realtime call switches from the *off* mode to the *on* mode in one realtime beacon interval, and q the probability that a realtime call switches

from the *on* mode to the *off* mode in one realtime beacon interval. With the exponentially distributed *on* and *off* periods, we have

$$p = 1 - e^{-\frac{T_{rb}}{t_{off}}},\ q = 1 - e^{-\frac{T_{rb}}{t_{on}}}. \tag{A.9}$$

Since the realtime calls are independent *on* and *off* periods, the pmf of transition number due to call status changes can be calculated as

$$\begin{aligned} &P_{X_5...X_8|X_1...X_4S}(x_5,...,x_8|x_1,...,x_4,s) = \\ &\qquad P_{X_5|X_1...X_4S}(x_5|x_1,...,x_4,s)P_{X_6|X_1...X_4S}(x_6|x_1,...,x_4,s) \\ &\qquad\qquad P_{X_7|X_1...X_4S}(x_7|x_1,...,x_4,s)P_{X_8|X_1...X_4S}(x_8|x_1,...,x_4,s) \end{aligned} \tag{A.10}$$

where all terms at the right side of (A.10) have binomial distribution, as given by

$$P_{X_5|X_1...X_4S}(x_5|x_1,...,x_4,s) = \binom{n_2+x_4}{x_5} q^{x_5}(1-q)^{n_2+x_4-x_5}, \tag{A.11}$$

$$P_{X_6|X_1...X_4S}(x_6|x_1,...,x_4,s) = \binom{n_4+x_2-x_3}{x_6} p^{x_6}(1-p)^{n_4+x_2-x_3-x_6}, \tag{A.12}$$

$$P_{X_7|X_1...X_4S}(x_7|x_1,...,x_4,s) = \binom{n_1-x_4}{x_7} q^{x_7}(1-q)^{n_1-x_4-x_7}, \tag{A.13}$$

$$P_{X_8|X_1...X_4S}(x_8|x_1,...,x_4,s) = \binom{n_5+x_1+x_3}{x_8} p^{x_8}(1-p)^{n_5+x_1+x_3-x_8}. \tag{A.14}$$

Appendix B

Determining the Number of Contention Slots and Contention Window Size

In this section, we present a mathematical model to analyze the number of successful transmission requests in the contention slots and the average delay to initiate a new transmission. Based on the analytical model, we propose a mechanism to dynamically adjust the contention window size and the number of contention slots according to the traffic load and required delay to initiate a new transmission.

In the contention slots, the nodes that want to initiate a new transmission contend with each other using CSMA/CA MAC to send a transmission request packet to their cell coordinators. Each contending node chooses a random back-off time uniformly distributed in the range $[0, W-1]$, where W is the contention window size that is dynamically set by coordinators. After each idle mini-slot, a contending node decreases its back-off window

by one and transmits its request packet when its back-off window reaches zero. Nodes freeze their back-off window while the channel is busy and restart reducing the back-off window when the channel is idle again. We set the carrier sensing range, r_c, large enough (comparing to the maximum transmission range of requests, r_g,) such that the hidden node problem is avoided, in order to reduce the probability of transmission request collisions. We also assume that contending nodes are uniformly distributed in the network area. Let N' denote the number of contending nodes within a circular area with radius r_c. Thus, when a node starts to transmit a request packet, $N' - 1$ other nodes (which are in the transmitting node's carrier sensing range) have to stay silent until the nodes finishes the transmission of its request packet. Let T_{cp} denote the total duration of contention slots in a frame, t_s denote the duration of a mini-slot, and T_r denote the duration of a transmission request packet.

Since contending nodes choose their back-off time uniformly distributed in the range $[0, W-1]$, when the channel is not busy a contending node starts to initiate transmission request packet in a mini-slot with probability $1/W$. Therefore, the probability that $X \in [0, N']$ nodes within a circular area with radius r_c start transmission in a mini-slot (when the channel is not busy) can be written as

$$P(X = i) = \binom{N'}{i} (\frac{1}{W})^i (1 - \frac{1}{W})^{N'-i}. \tag{B.1}$$

Using (B.1), the probability that a mini-slot is idle is

$$\delta_i = P(X = 0) = (1 - \frac{1}{W})^{N'}, \tag{B.2}$$

the probability of starting a successful transmission request in a mini-slot is

$$\delta_s = P(X = 1) = \frac{N'}{W}(1 - \frac{1}{W})^{N'-1}, \tag{B.3}$$

and the probability of a transmission collision in a mini-slot is

$$\delta_c = P(X \geq 2) = 1 - \delta_i - \delta_s. \tag{B.4}$$

Consider a cycle as the time between two consecutive idle detection of mini-slots. The probability of initiating a transmission (successful or collision) after M idle mini-slots is

$$P(M = m) = \delta_i^{m-1}(1 - \delta_i). \tag{B.5}$$

Thus, the average number of idle mini-slots in a cycle is

$$\bar{m} = \sum_{m \geq 1} mP(m) = \frac{1}{1 - \delta_i} = \frac{1}{1 - (1 - \frac{1}{W})^{N'}} \tag{B.6}$$

and the average duration of a cycle is

$$\bar{T}_{cy} = \bar{m}t_s + T_r = \frac{t_s}{1 - (1 - \frac{1}{W})^{N}} + T_r. \tag{B.7}$$

Since the contention window size is W and on average $\bar{m}$ idle mini-slots exits in a cycle, the expected number of cycles in the contention slots of a frame is

$$\bar{u} = \min\left(\frac{W}{\bar{m}}, \frac{T_{cp}}{\bar{T}_{cy}}\right) = \min\left(\frac{W}{\frac{1}{1-(1-\frac{1}{W})^{N'}}}, \frac{T_{cp}}{\frac{t_s}{1-(1-\frac{1}{W})^{N'}} + T_r}\right). \tag{B.8}$$

Therefore, in a circular area with radius r_c, the expected number of successful transmission requests in the contention slots of one frame can be written as

$$\bar{Q} = \bar{u} \times \frac{\delta_s}{\delta_s + \delta_c} = \min\left(\frac{W}{\frac{1}{1-(1-\frac{1}{W})^{N'}}}, \frac{T_{cp}}{\frac{t_s}{1-(1-\frac{1}{W})^{N'}} + T_r}\right) \times \frac{\frac{N'}{W}(1 - \frac{1}{W})^{N'-1}}{1 - (1 - \frac{1}{W})^{N'}}. \tag{B.9}$$

Figure B.1 shows the the expected number of successful transmission requests (during 1 ms contention time) using different contention window sizes as the number of contending nodes varies. Figure B.2 shows the expected number of successful transmission requests in one frame as the total duration of contention slots increases for a different number of contending

nodes (in each case, the contention window is adjusted for the best performance). Using (B.9), the probability that a contending node successfully sends a transmission request to the coordinator in a frame is

$$P_s = \frac{\bar{Q}}{N'}. \tag{B.10}$$

Therefore, the probability that a node successfully sends its request to the coordinator after contending in Y frames is

$$P(Y = y) = P_s(1 - P_s)^{y-1} \tag{B.11}$$

and the expected delay to initiate a new transmission is

$$\bar{D} = \sum_y yP(Y = y)T_f = \frac{T_f}{P_s} = \frac{T_f N'}{\bar{Q}}, \tag{B.12}$$

where T_f is the duration of a frame. Figure B.3 shows the average delay to initiate a new transmission as the total contention slot duration increases for a different number of contending nodes in the carrier sensing range (the contention window is adjusted for the best performance).

The coordinators measure δ_i, δ_s and δ_c by monitoring contention slots of the most recent frame. Based on (B.2), (B.3) and (B.4) and the value of contention window size in the previous frame, they estimate the number of contending nodes within the carrier sensing range. The optimal value of contention window size can be calculated using (B.9) for the estimated number of contending nodes. Also, the number of contention slots can be adjusted for the required transmission request delay using (B.12). Accordingly, the number of contention slots and the contention window size are dynamically updated and announced by the coordinators.

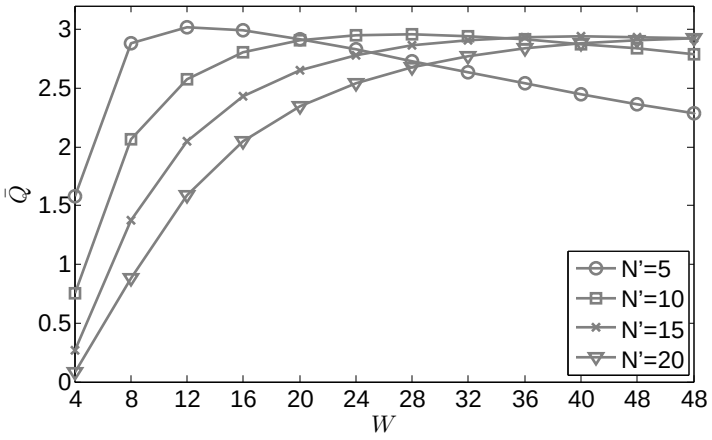

Figure B.1: The number of successful transmission requests in 1 ms.

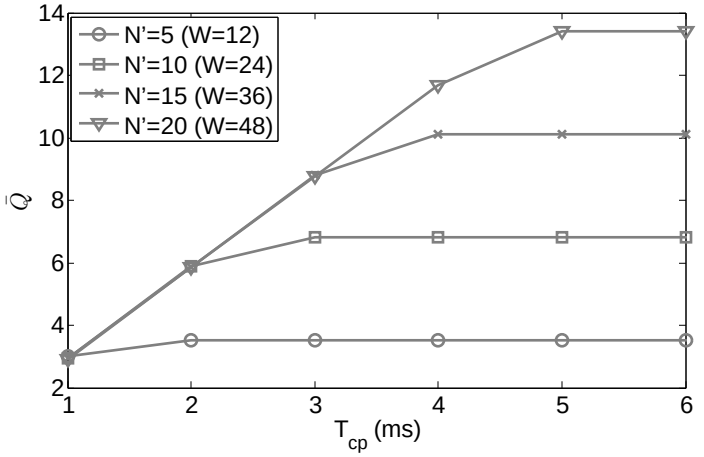

Figure B.2: The expected number of successful transmission requests in one frame (with the optimal contention window size).

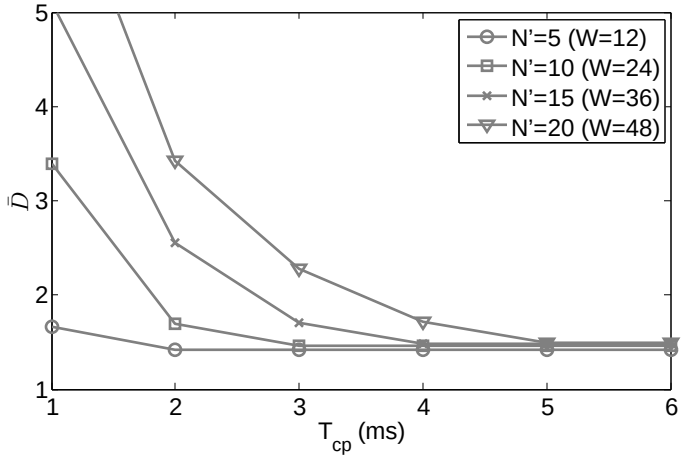

Figure B.3: The average delay to initiate a new transmission normalized to frame duration (with the optimal contention window size).

Bibliography

[1] Cisco visual networking index: Global mobile data traffic forecast update, 2013-2018. White Paper, Feb. 2014.

[2] I. Hwang, B. Song, and S. S. Soliman. A holistic view on hyper-dense heterogeneous and small cell networks. *IEEE Communications Magazine*, 51(6):20–27, June 2013.

[3] A. Asadi, Q. Wang, and V. Mancuso. A survey on device-to-device communication in cellular networks. *IEEE Commun. Surv. Tuts.*, 16(4):1801–1819, Nov. 2014.

[4] J. Kim, J. Lee, J. Kim, and J. Yun. M2M service platforms: Survey, issues, and enabling technologies. *IEEE Commun. Surv. Tuts.*, 16(1):61–76, Feb. 2014.

[5] S.-L. Tsao and C.-H. Huang. Review: a survey of energy efficient MAC protocols for IEEE 802.11 WLAN. *ACM Trans. Computer Communications*, 34(1):54–67, Jan. 2011.

[6] P. Serrano, A. D. L. Oliva, P. Patras, V. Mancuso, and A. Banchs. Greening wireless communications: status and future directions. *ACM Trans. Computer Communications*, 35(14):1651 – 1661, Aug. 2012.

[7] T. Pering, Y. Agarwal, R. Gupta, and R. Want. CoolSpots: reducing the power consumption of wireless mobile devices with multiple radio interfaces. In *Proc. MobiSys'06*, June 2006.

[8] T. Jin, G. Noubir, and B. Sheng. WiZi-Cloud: application-transparent dual ZigBee-WiFi radios for low power Internet access. In *Proc. IEEE INFOCOM'11*, Apr. 2011.

[9] Cisco. Aironet wireless LAN adapters 350 series technical specifications. `http://www.cisco.com/en/US/docs/wireless/wlan_adapter/350_cb20a/user/linux/configuration/guide/icglappA.html`, Sept. 2013.

[10] *IEEE 802.11 WG, Part 11: Wireless LAN Medium Access Control (MAC) and Physical Layer (PHY) Specification, Standard, Aug. 1999.*

[11] B. Chen, K. Jamieson, H. Balakrishnan, and R. Morris. Span: an energy-efficient coordination algorithm for topology maintenance in ad hoc wireless networks. *ACM Trans. Wireless Networks*, 8(5):481–494, Sept. 2002.

[12] V. Rodoplu and T. H. Meng. Minimum energy mobile wireless networks. *IEEE J. Selected Areas Communications*, 17(8):1333–1344, Aug. 1999.

[13] E.-S. Jung and N. H. Vaidya. An energy efficient MAC protocol for wireless LANs. In *Proc. IEEE INFOCOM'02*, Jan. 2002.

[14] S. Ramanathan. A unified framework and algorithm for (T/F/C)DMA channel assignment in wireless networks. In *Proc. IEEE INFOCOM'97*, Apr. 1997.

[15] A. Ephremides and T.V. Truong. Scheduling broadcasts in multihop radio networks. *IEEE Trans. Communications*, 38(4):456–460, Apr. 1990.

[16] J. Zhu, X. Guo, L.L. Yang, and W.S. Conner. Leveraging spatial reuse in 802.11 mesh networks with enhanced physical carrier sensing. In *Proc. IEEE ICC'04*, June 2004.

[17] Z. Abichar and J.M. Chang. Group-based medium access control for IEEE 802.11n wireless LANs. *IEEE Tran. Mobile Computing,*, 12(2):304–317, July 2013.

[18] W. Ye, J. Heidemann, and D. Estrin. Medium access control with coordinated adaptive sleeping for wireless sensor networks. *IEEE/ACM Tran. Networking*, 12(3):493–506, June 2004.

[19] T. van Dam and K. Langendoen. An adaptive energy-efficient MAC protocol for wireless sensor networks. In *Proc. ACM SenSys'03*, Nov. 2003.

[20] L. Bin Jiang and S.-C. Liew. Improving throughput and fairness by reducing exposed and hidden nodes in 802.11 networks. *IEEE Trans. Mobile Computing*, 7(1):34–49, Jan. 2008.

[21] G. Miao, N. Himayat, G.Y. Li, A. T. Koc, and S. Talwar. Interference-aware energy-efficient power optimization. In *Proc. IEEE ICC'09*, June 2009.

[22] G. Miao, N. Himayat, Y. Li, and A. Swami. Cross-layer optimization for energy-efficient wireless communications: a survey. *Wirel. Commun. Mob. Comput.*, 9(4):529–542, Apr. 2009.

[23] V. Kawadia and P. R. Kumar. Principles and protocols for power control in wireless ad hoc networks. *IEEE J. Selected Areas in Communications*, 23(1):76–88, Jan. 2005.

[24] S. Narayanaswamy, V. Kawadia, R. S. Sreenivas, and P. R. Kumar. Power control in ad-hoc networks: Theory, architecture, algorithm and implementation of the COMPOW protocol. In *European Wireless Conference*, pages 156–162, Feb. 2002.

[25] T.-S. Kim, H. Lim, and J. C. Hou. Improving spatial reuse through tuning transmit power, carrier sense threshold, and data rate in multihop wireless networks. In *Proc. MobiCom'06*, Sept. 2006.

[26] T. S. Kim, H. Lim, and J. C. Hou. Understanding and improving the spatial reuse in multihop wireless networks. *IEEE Trans. Mobile Computing*, 7(10):1200–1212, 2008.

[27] E.-S. Jung and N. H. Vaidya. A power control MAC protocol for ad hoc networks. *ACM Tran. Wireless Networks*, 11(1-2):55–66, Jan. 2005.

[28] J. P. Monks, V. Bharghavan, and W.-M. W. Hwu. A power controlled multiple access protocol for wireless packet networks. In *Proc. IEEE INFOCOM'01*, June 2001.

[29] A. Muqattash and M. Krunz. A single-channel solution for transmission power control in wireless ad hoc networks. In *Proc. ACM MobiHoc'04*, May 2004.

[30] P. Li, X. Geng, and Y. Fang. An adaptive power controlled MAC protocol for wireless ad hoc networks. *IEEE Tran. Wireless Communications*, 8(1):226–233, Jan. 2009.

[31] K. Rahimi Malekshan and W. Zhuang. An energy efficient MAC protocol for fully-connected wireless networks. In *Proc. IEEE ICC'13*, June 2013.

[32] K. Rahimi Malekshan, W. Zhuang, and Y. Lostanlen. An energy efficient MAC protocol for fully connected wireless ad hoc networks. *IEEE Trans. Wireless Communications*, 13(10):5729–5740, Oct. 2014.

[33] K. Rahimi Malekshan, W. Zhuang, and Y. Lostanlen. Coordination-based medium access control with space-reservation for wireless ad hoc networks. *IEEE Trans. Wireless Communications*, 15(2):1617–1628, Feb. 2016.

[34] K. Rahimi Malekshan and W. Zhuang. Joint scheduling and transmission power control in wireless ad hoc networks. *submitted to IEEE J. Selected Areas in Wireless Communications*.

[35] S. Choi, J. d. Prado, N. Sai Shankar, and S. Mangold. Ieee 802.11e contention-based channel access (EDCF) performance evaluation. In *Proc. IEEE ICC'03*, May 2003.

[36] D. He and C. Q. Shen. Simulation study of IEEE 802.11e EDCF. In *Proc. IEEE VTC'03*, Oct. 2003.

[37] Y. Gao, X. Sun, and L. Dai. IEEE 802.11e EDCA networks: Modeling, differentiation and optimization. *IEEE Trans. Wireless Communications*, 13(7):3863–3879, July 2014.

[38] Q. Zhao, D.H.K. Tsang, and T. Sakurai. A scalable and accurate nonsaturated ieee 802.11e edca model for an arbitrary buffer size. *IEEE Trans. Mobile Computing*, 12(12):2455–2469, Dec 2013.

[39] Ching-Ling Huang and Wanjiun Liao. Throughput and delay performance of IEEE 802.11e enhanced distributed channel access (EDCA) under saturation condition. *IEEE Trans. Wireless Communications*, 6(1):136–145, Jan 2007.

[40] A. Banchs, P. Serrano, and L. Vollero. Providing service guarantees in 802.11e EDCA WLANs with legacy stations. *IEEE Trans. Mobile Computing*, 9(8):1057–1071, Aug 2010.

[41] L. Zhao, L. Cong, H. Zhang, W. Ding, and J. Zhang. Game-theoretic EDCA in IEEE 802.11e WLANs. In *Proc. IEEE VTC*, pages 1–5, Sept 2008.

[42] C. Huang and S. Shioda. Detailed analysis for ieee 802.11e EDCA in non-saturated conditions - frame-transmission-cycle approach. In *Proc. IEEE WiOpt*, May 2013.

[43] Z. Wang and X. Guo. Priority-based parameter performance optimization for EDCA. In *Proc. IEEE ICCSNT*, Oct 2013.

[44] F. Borgonovo, A. Capone, M. Cesana, and L. Fratta. ADHOC MAC: New MAC architecture for ad hoc networks providing efficient and reliable point-to-point and broadcast services. *Wirel. Netw.*, 10(4):359–366, July 2004.

[45] H. A. Omar, Weihua Zhuang, and Li Li. VeMAC: A TDMA-Based MAC protocol for reliable broadcast in VANETs. *Mobile Computing, IEEE Transactions on*, 12(9):1724–1736, Sept. 2013.

[46] I. Rhee, A. Warrier, M. Aia, J. Min, and M.L. Sichitiu. Z-MAC: A hybrid MAC for wireless sensor networks. *IEEE/ACM Trans. Networking*, 16(3):511–524, June 2008.

[47] H. Woesner, J.-P. Ebert, M. Schlager, and A. Wolisz. Power-saving mechanisms in emerging standards for wireless LANs: the MAC level perspective. *IEEE Personal Communications*, 5(3):40–48, June 1998.

[48] J. Zhang, G. Zhou, C. Huang, S.H. Son, and J. A. Stankovic. TMMAC: An energy efficient multi-channel MAC protocol for ad hoc networks. In *Proc. IEEE ICC'07*, June 2007.

[49] F. R. Dogar, P. Steenkiste, and K. Papagiannaki. Catnap: exploiting high bandwidth wireless interfaces to save energy for mobile devices. In *MobiSys'10*, June 2010.

[50] E. Rozner, V. Navda, R. Ramjee, and S. Rayanchu. NAPman: network-assisted power management for WiFi devices. In *Proc. MobiSys'10*, June 2010.

[51] J. Manweiler and R. Roy Choudhury. Avoiding the rush hours: WiFi energy management via traffic isolation. *IEEE Trans. Mobile Computing*, 11(5):739 –752, May 2012.

[52] Z. Zeng, Y. Gao, and P. R. Kumar. SOFA: A sleep-optimal fair-attention scheduler for the power-saving mode of WLANs. In *Proc. ICDCS'11*, June 2011.

[53] M. Anand, E. B. Nightingale, and J. Flinn. Self-tuning wireless network power management. In *Proc. MobiCom'03*, Sept. 2003.

[54] D. Qiao and K. G. Shin. Smart power-saving mode for IEEE 802.11 wireless LANs. In *Proc. IEEE INFOCOM'05*, March 2005.

[55] V. Namboodiri and L. Gao. Energy-efficient VoIP over wireless LANs. *IEEE Trans. Mobile Computing*, 9(4):566 –581, Apr. 2010.

[56] R. Krashinsky and H. Balakrishnan. Minimizing energy for wireless web access with bounded slowdown. *Wirel. Netw.*, 11(1-2):135–148, Jan. 2005.

[57] M. J. Miller and N. F. Vaidya. A MAC protocol to reduce sensor network energy consumption using a wakeup radio. *IEEE Trans. Mobile Computing*, 4(3):228–242, May 2005.

[58] E. Shih, P. Bahl, and M. J. Sinclair. Wake on wireless: an event driven energy saving strategy for battery operated devices. In *Proc. MobiCom'02*, Sept. 2002.

[59] J. Liu and L. Zhong. Micro power management of active 802.11 interfaces. In *Proc. MobiSys'08*, June 2008.

[60] X. Zhang and K. G. Shin. E-mili: energy-minimizing idle listening in wireless networks. In *Proc. MobiCom'11*, Sept. 2011.

[61] A. S. Hamza, S.S. Khalifa, H. S. Hamza, and K. Elsayed. A survey on inter-Cell interference coordination techniques in OFDMA-Based cellular networks. *IEEE Communications Surveys Tutorials*, 15(4):1642–1670, Nov. 2013.

[62] A. Damnjanovic, J. Montojo, Y. Wei, T. Ji, T. Luo, M. Vajapeyam, T. Yoo, O. Song, and D. Malladi. A survey on 3GPP heterogeneous networks. *IEEE Tran. Wireless Communications*, 18(3):10–21, June 2011.

[63] M. Ismail, A. T. Gamage, W. Zhuang, X. Shen, E. Serpedin, and K. Qaraqe. Uplink decentralized joint bandwidth and power allocation for energy-efficient operation in a heterogeneous wireless medium. *IEEE Trans. Communications*, 63(4):1483–1495, April 2015.

[64] R. Zhang, M. Wang, L. X. Cai, Z. Zheng, and X. Shen. LTE-unlicensed: the future of spectrum aggregation for cellular networks. *IEEE Wireless Communications*, 22(3):150–159, June 2015.

[65] L. B. Jiang and S. C. Liew. Improving throughput and fairness by reducing exposed and hidden nodes in 802.11 networks. *IEEE Transactions on Mobile Computing*, 7(1):34–49, Jan. 2008.

[66] T. ElBatt and A. Ephremides. Joint scheduling and power control for wireless ad hoc networks. *IEEE Trans. Wireless Communications*, 3(1):74–85, Jan. 2004.

[67] Y. Li and A. Ephremides. A joint scheduling, power control, and routing algorithm for ad hoc wireless networks. *Ad Hoc Networks*, 5(7):959 – 973, Sept. 2007.

[68] A. Gjendemsjo, D. Gesbert, G. E. Oien, and S. G. Kiani. Optimal power allocation and scheduling for two-cell capacity maximization. In *Proc. WIOPT'06*, Apr. 2006.

[69] A. Gjendemsj, D. Gesbert, G. E. Oien, and S. G. Kiani. Binary power control for sum rate maximization over multiple interfering links. *IEEE Trans. Wireless Communications*, 7(8):3164–3173, August 2008.

[70] J. Zander. Performance of optimum transmitter power control in cellular radio systems. *IEEE Trans. Vehicular Technology*, 41(1):57–62, Feb. 1992.

[71] P. Hande, S. Rangan, M. Chiang, and X. Wu. Distributed uplink power control for optimal sir assignment in cellular data networks. *IEEE/ACM Transactions on Networking*, 16(6):1420–1433, Dec. 2008.

[72] H. Xing and S. Hakola. The investigation of power control schemes for a device-to-device communication integrated into OFDMA cellular system. In *Proc. IEEE PIMRC'10*, Sept. 2010.

[73] M. Lauridsen, A. R. Jensen, and P. Mogensen. Reducing lte uplink transmission energy by allocating resources. In *Proc. IEEE VTC Fall'11*, Sept 2011.

[74] S.-L. Wu, Y.-C. Tseng, and J.-P. Sheu. Intelligent medium access for mobile ad hoc networks with busy tones and power control. *IEEE J. Selected Areas in Communications*, 18(9):1647–1657, Sept. 2000.

[75] A. Muqattash and M. Krunz. Power controlled dual channel (PCDC) medium access protocol for wireless ad hoc networks. In *Proc. IEEE INFOCOM'03*, Apr. 2003.

[76] G. Miao, N. Himayat, G.Y. Li, and S. Talwar. Distributed interference-aware energy-efficient power optimization. *IEEE Trans. Wireless Communications*, 10(4):1323–1333, Apr. 2011.

[77] R. Zheng and R. Kravets. On-demand power management for ad hoc networks. In *Proc. IEEE INFOCOM'03*, March 2003.

[78] ITU-T recommendation G.114: One-way transmission time, 2003.

[79] Cisco. The minimum SINR required to support the corresponding data rate in IEEE 802.11a/g. `http://www.cisco.com/en/US/docs/wireless/controller/7.0MR1/configuration/guide/cg_mesh.html`, Dec. 2013.

[80] P. Gupta and P. R. Kumar. The capacity of wireless networks. *IEEE Transactions on Information Theory*, 46(2):388–404, March 2000.